



D.1.1 Analysed historical climate data and projections for the region

Views and opinions expressed are those of the author(s) only and do not necessarily reflect those of the European Union or HADEA. Neither the European Union nor the granting authority can be held responsible for them.



Funded by the
European Union

Disclaimer

This information and content of this report is the sole responsibility of the GENESIS consortium members and does not necessarily represent the views expressed by the European Commission or its services. Whilst the information contained in the documents and webpages of the project is believed to be accurate, the author(s) or any other participant in the GENESIS consortium makes no warranty of any kind with regard to this material.

Report Information

Grant Agreement / Proposal ID	101157447
Project Title	Geologically Enhanced Nature-based Solutions for climate change resiliency of critical water InfraStructure
Project Acronym	GENESIS
Project Coordinator	IGME-CSIC
Project starting date / end date	1 September 2024 / 1 November 2025
Related Work Package	WP1: Macaronesia Water Climate Risk Observatory
Lead Organisation	Instituto Tecnológico de Canarias
Document title	D.1.1 Analysed historical climate data and projections for the region
Submission Date	1 November 2025
Dissemination level	Public
DOI	https://doi.org/10.5281/zenodo.17492714

Quality verification

Prepared by	Checked by	Verified by	Approved by
Daniel Reyes Parrilla	Rafael Nebot Medina Alejandro Curbelo Fontelos Megan Expósito Brazier	Gerardo Meixueiro Rios	Alejandro García Gil

Revision History

Revision	Revision Date	Changes	Authorised	Function
1	01/10/2025	Draft	Daniel Reyes Parrilla	WP Leader
2	05/10/2025	Draft	Rafael Nebot Medina	WP Partner
3	11/10/2025	Draft	Alejandro Curbelo Fontelos	WP Partner
4	23/10/2025	Draft	Megan Expósito Brazier	WP Partner
4	31/10/2025	Final Version	Daniel Reyes Parrilla	WP Leader

Executive summary

The study establishes detailed historical climate baselines for the Macaronesian islands. Downscaled global reanalysis data (ERA5) at ~180 m resolution, obtained through the TopoPyScale tool, were combined with satellite-based evapotranspiration estimates (PySEBAL) to produce consistent temperature, precipitation, humidity, and water-flux datasets for the Canary Islands, Azores, Madeira, and Cape Verde. The multi-indicator framework, which includes the SPEI drought index, reveals robust warming across all archipelagos and region-specific changes in atmospheric moisture.

Methodology:

TopoPyScale downscales ERA5 climate fields using a high-resolution digital elevation model, capturing fine-scale topographic effects. PySEBAL (SEBAL) integrates Landsat imagery with meteorological inputs to estimate actual evapotranspiration and vegetation productivity. This hybrid approach addresses the scarcity of in-situ observations on small islands by combining spatially complete reanalysis and satellite data, resulting in a high-resolution, temporally consistent climate record suitable for trend analysis.

Regional Climate Trends:

All archipelagos exhibit significant warming. In La Palma, high-elevation areas warmed by approximately +1.9 °C per decade, while Gran Canaria's interior experienced an increase of around +2.2 °C per decade. Nighttime temperatures rose nearly as rapidly as daytime ones, reducing the diurnal temperature range. Relative humidity decreased during the day and at low-humidity hours, leading to drier conditions during hot afternoons, although slight nocturnal increases were detected. Precipitation changes are modest but regionally important: drier islands (Cape Verde and parts of the Canaries and Madeira) show mild rainfall declines, while the Azores record small increases in annual totals.

Evapotranspiration and Drought:

Rising temperatures increased evaporative demand. Potential evapotranspiration (PET) rose across wet and dry periods, and drought indices (SPEI) indicate more frequent water deficits. In La Palma's summit zones, the number of days with significant water deficits has grown. In Gran Canaria's interior, a transition from wet to moisture-limited conditions has occurred, with early-century evapotranspiration increases giving way to recent drought intensification. In Cape Verde, total rainfall remains largely unchanged, but a slight rise in atmospheric moisture content may modestly alleviate extreme aridity.

Archipelago Summaries:

- **Canary Islands:** Steep warming, declining humidity, and reduced groundwater recharge characterize the wet highlands (e.g. Tenerife, La Palma), while the dry

lowlands (Lanzarote, Fuerteventura) show further aridification. Drought severity has intensified across the archipelago.

- **Azores:** All island groups warmed by roughly +0.6–0.75 °C per decade, with stronger nighttime warming enhancing nocturnal humidity. The overall climate remains wet, with minimal rainfall change but growing storm intensity.
- **Madeira:** Warming is pronounced, particularly along the south coast (~1.0 °C/decade). Absolute humidity increased, whereas relative humidity declined, indicating drier valley conditions. Rainfall trends are near zero.
- **Cape Verde:** Rising temperatures and a slight increase in absolute humidity were observed. Despite enhanced moisture capacity, the archipelago remains extremely dry.

Policy Relevance:

The identified trends quantify growing water stress and heat-related risks in Macaronesia. The results provide a robust evidence base for adaptation planning consistent with EU climate strategies, which emphasize enhanced information systems and nature-based solutions in outermost regions. Findings support measures such as reforestation of laurel forests to improve fog interception, modernization of irrigation practices, and climate-resilient infrastructure design. The high-resolution datasets generated within the GENESIS project enhance regional and European planning for sustainable water and land management under a changing climate.

Table of Contents

Executive summary	1
Table of Contents	3
List of Tables	5
List of Figures.....	6
List of Equations	9
List of Abbreviations	10
1. Introduction.....	11
1.1 Climate Change and Freshwater Resources on Oceanic Islands.....	11
1.2 State of the art methods and studies.....	15
2. GENESIS Methodolgy	19
2.1 TopoPyScale.....	19
2.2 PySEBAL	20
2.3 Standardized Precipitation Evapotranspiration Index (34).....	23
2.4 Consideration of WaPOR Reference Evapotranspiration as a Surrogate for Potential Evapotranspiration	24
2.4 Climate Trend Calculation.....	25
2.5 Weighted and Normalized Slope Aggregation.....	26
2.6 Precipitation Error Rates.....	28
3. Results.....	29
3.1 Canary Islands	29
3.1.2 La Palma.....	29
3.1.2 Gran Canaria	45
3.1.3 El Hierro	56
3.1.4 Tenerife	59
3.1.5 La Gomera	68
3.1.6 Lanzarote	71
3.1.7 Fuerteventura	74
3.2 Azores	77
3.2.1 Azores – Western Group	77
3.2.2 Azores – Central Group.....	80
3.2.3 Azores - Eastern Group.....	82
3.3 Madeira.....	84
3.3.1 Madeira Island.....	84

3.3.2 Porto Santo.....	92
3.4 Cape Verde	95
3.4.1 Santiago	95
3.4.2 Boa Vista.....	98
3.4.3 Brava.....	100
3.4.4 Fogo	103
3.4.5 Maio.....	105
3.4.6 Sal.....	108
3.4.7 Santo Antão.....	110
3.4.8 São Nicolau	113
3.4.9 São Vicente.....	115
4. Conclusion.....	118
References.....	119

List of Tables

Table 1: Precipitation Error Rates 28

List of Figures

Figure 1: Potential Evapotranspiration Trend – Gran Canaria Highlands.....	24
Figure 2: Reference Evapotranspiration Trend – Gran Canaria Highlands.....	25
Figure 3: La Palma Highlands – Normalized Trends.....	29
Figure 4: Maximum Temperature Trend – La Palma Highlands	31
Figure 5: Minimum Relative Humidity Trend – La Palma Highlands	32
Figure 6: Precipitation Trend – La Palma Highlands.....	32
Figure 7: Eastern La Palma – Normalized Trends.....	35
Figure 8: Maximum Temperature Trend – Eastern La Palma.....	36
Figure 9: Minimum Relative Humidity Trend – La Palma Highlands	37
Figure 10: Western La Palma – Normalized Trends.....	40
Figure 11: Maximum Temperature Trend – Western La Palma.....	41
Figure 12: Minimum Relative Humidity Trend – La Palma Highlands	42
Figure 13: Gran Canaria Highlands – Normalized Trends.....	45
Figure 14: Maximum Temperature Trend – Gran Canaria Highlands	46
Figure 15: Minimum Relative Humidity Trend – Gran Canaria Highlands	47
Figure 16: Northern Gran Canaria – Normalized Trends	48
Figure 17: Maximum Temperature Trend – Northern Gran Canaria	49
Figure 18: Relative Humidity Trend – Northern Gran Canaria.....	50
Figure 19: East, South and West of Gran Canaria – Normalized Trends.....	52
Figure 20: Maximum Temperature Trend – East, south and west of Gran Canaria.....	53
Figure 21: Minimum Relative Humidity Trend – East, south and west of Gran Canaria	54
Figure 22: El Hierro – Normalized Trends	56
Figure 23: Maximum Temperature Trend – El Hierro	57
Figure 24: Minimum Relative Humidity Trend – El Hierro.....	58
Figure 25: East, South and West of Tenerife – Normalized Trends	59
Figure 26: Maximum Temperature Trend – East, South and West of Tenerife	60
Figure 27: Minimum Relative Humidity Trend – East, South and West of Tenerife	61
Figure 28: Northern Tenerife – Normalized Trends.....	62
Figure 29: Maximum Temperature Trend – Northern Tenerife.....	63
Figure 30: Minimum Relative Humidity Trend – Northern Tenerife	64
Figure 31: Tenerife Metropolitan Area – Normalized Trends.....	65
Figure 32: Maximum Temperature Trend – Tenerife Metropolitan Area	66

Figure 33: Minimum Relative Humidity Trend – Tenerife Metropolitan Area.....	67
Figure 34: La Gomera – Normalized Trends.....	68
Figure 35: Maximum Temperature Trend – La Gomera.....	69
Figure 36: Minimum Relative Humidity Trend – La Gomera	70
Figure 37: Lanzarote – Normalized Trends.....	71
Figure 38: Maximum Temperature Trend – Lanzarote.....	72
Figure 39: Minimum Relative Humidity Trend – Lanzarote	73
Figure 40: Fuerteventura – Normalized Trends	74
Figure 41: Maximum Temperature Trend – Fuerteventura	75
Figure 42: Minimum Relative Humidity - Fuerteventura.....	76
Figure 43: Western Group of Azores – Normalized Trends	77
Figure 44: Minimum Longwave Radiation – Azores Western Group.....	78
Figure 45: Minimum Specific Humidity – Azores Western Group.....	79
Figure 46: Central Group of Azores – Normalized Trends	80
Figure 47: Minimum Longwave Radiation – Azores Central Group	81
Figure 48: Minimum Specific Humidity – Azores Central Group.....	81
Figure 49: Eastern Group of Azores – Normalized Trends	82
Figure 50: Minimum Longwave Radiation – Azores Eastern Group.....	83
Figure 51: South Coast of Madeira – Normalized Trends	84
Figure 52: Minimum Longwave Radiation Trend – Madeira South Coast.....	85
Figure 53: Maximum Vapour Pressure Trend – Madeira South Coast	86
Figure 54: North Coast of Madeira – Normalized Trends	87
Figure 55: Minimum Longwave Radiation Trend – North Coast of Madeira	88
Figure 56: Maximum Vapour Pressure Trend – North Coast of Madeira.....	88
Figure 57: Mountainous Region of Madeira – Normalized Trends.....	89
Figure 58: Minimum Temperature Trend - Mountainous Region of Madeira	90
Figure 59: Maximum Vapour Pressure Trend - Mountainous Region of Madeira.....	91
Figure 60: Porto Santo – Normalized Trends.....	92
Figure 61: Minimum Longwave Radiation Trend – Porto Santo.....	93
Figure 62: Maximum Vapour Pressure Trend – Porto Santo	94
Figure 63: Santiago – Normalized Trends.....	95
Figure 64: Minimum Longwave Radiation Trend - Santiago	96
Figure 65: Maximum Specific Humidity Trend - Santiago	97
Figure 66: Boa Vista – Normalized Trends.....	98

Figure 67: Minimum Longwave Radiation Trend – Boa Vista	99
Figure 68: Maximum Specific Humidity Trend – Boa Vista.....	99
Figure 69: Brava – Normalized Trends	100
Figure 70: Minimum Longwave Radiation Trend - Brava.....	101
Figure 71: Maximum Specific Humidity Trend - Brava.....	102
Figure 72: Fogo – Normalized Trends.....	103
Figure 73: Minimum Longwave Radiation Trend - Fogo	104
Figure 74: Maximum Specific Humidity Trend - Fogo	104
Figure 75: Maio – Normalized Trends	105
Figure 76: Minimum Longwave Radiation Trend - Maio.....	106
Figure 77: Maximum Specific Humidity Trend - Maio.....	107
Figure 78: Sal – Normalized Trends	108
Figure 79: Minimum Longwave Radiation Trend - Sal	109
Figure 80: Maximum Specific Humidity Trend - Sal.....	109
Figure 81: Santo Antão – Normalized Trends.....	110
Figure 82: Minimum Longwave Radiation Trend – Santo Antão	111
Figure 83: Maximum Specific Humidity Trend – Santo Antão.....	112
Figure 84: São Nicolau – Normalized Trends	113
Figure 85: Minimum Longwave Radiation Trend – São Nicolau.....	114
Figure 86: Maximum Specific Humidity Trend – São Nicolau	114
Figure 87: São Vicente – Normalized Trends	115
Figure 88: Minimum Longwave Radiation Trend – São Vicente	116
Figure 89: Maximum Specific Humidity Trend – São Vicente.....	117

List of Equations

Equation 1: Water Balance	23
Equation 2: Multi-Scale Water Balance Accumulation.....	23
Equation 3: SPEI	23
Equation 4: Recency Factor.....	26
Equation 5: Combined Weight with Recency and Duration.....	27
Equation 6: Weighted Slope.....	27
Equation 7: Normalized Weighted Slope.....	27

List of Abbreviations

- AEMET – Agencia Estatal de Meteorología (Spanish State Meteorological Agency).
- AET – Actual Evapotranspiration.
- BWP – Biomass Water Productivity.
- CDS – Copernicus Data Store.
- DEM – Digital Elevation Model.
- ECMWF – European Centre for Medium-Range Weather Forecasts.
- ERA5 – Fifth-generation ECMWF atmospheric reanalysis dataset.
- ET – Evapotranspiration.
- EU – European Union.
- GCP – Google Cloud Platform.
- GRASS – Geographic Resources Analysis Support System.
- HADEA – European Health and Digital Executive Agency.
- IEEP – Institute for European Environmental Policy.
- IGME-CSIC – Instituto Geológico y Minero de España – Consejo Superior de Investigaciones Científicas (Spanish Geological and Mining Institute, Spanish National Research Council).
- MAPE – Mean Absolute Percentage Error (no explicit definition in text, but used as a metric in analysis).
- NbS – Nature-based Solutions.
- PET – Potential Evapotranspiration.
- PySEBAL – Python implementation of the Surface Energy Balance Model.
- Psurf – Surface pressure.
- Q_{air} – Specific humidity (air water vapor content).
- RDA – NCAR Research Data Archive.
- RCMs – Regional Climate Models.
- RET – Reference Evapotranspiration (as in WaPOR Reference Evapotranspiration).
- SDGs – Sustainable Development Goals.
- SEBAL – Surface Energy Balance Model.
- SPEI – Standardized Precipitation Evapotranspiration Index.
- SRTM – Shuttle Radar Topography Mission.
- WP – Work Package (e.g. WP1 – Work Package 1).
- WMO – World Meteorological Organization.
- WaPOR – Water Productivity through Open access of Remotely sensed derived data.

1. Introduction

1.1 Climate Change and Freshwater Resources on Oceanic Islands

Islands are widely recognized as some of the most vulnerable regions to climate change impacts. In Macaronesian archipelagos – which includes the Canary Islands, Azores, Madeira, and Cape Verde – the small land area and unique ecosystems mean that climate hazards like sea-level rise, extreme rainfall events, droughts and high winds can have outsized effects (1). Water resources are a particular concern, the naturally limited freshwater (mostly groundwater fed by rainfall) on islands is easily compromised under changing climate conditions (2).

Observational records already show a clear warming trend across the Macaronesian islands in recent decades, especially since the late 1970s, consistent with global anthropogenic climate change. Future projections indicate continued warming (on the order of 1–3 °C by the late 21st century) and suggest a decrease in overall precipitation for the Canary Islands with progressive salinization of aquifers, combined with growing demand, are creating precarious water shortages in many island communities (3).

Ecosystems across Macaronesia are exceptionally vulnerable to climate change, with profound implications for water regulation. The cloud-shrouded laurel forests (laurisilva) and other endemic vegetation zones perform critical ecosystem services by capturing moisture, regulating hydrology, and stabilizing soils. For instance, studies in the Canary Islands have shown that fog interception by dense laurel canopy can contribute as much as 20–45% of total precipitation, directly enhancing groundwater (4). These forests and upland habitats also promote infiltration and prevent soil erosion, buffering the islands against droughts, floods and landslides. However, shifting climate patterns are already stressing these ecosystems. Rising temperatures and irregular rainfall are making laurel forests one of the most climate-threatened habitats in the region (5). The degradation of these natural systems weakens their water-regulating functions, reducing aquifer recharge and increasing surface runoff. In contrast, the restoration of such landscapes enhances infiltration and supports groundwater replenishment. Nature-based Solutions (NbS) offer a pathway to recover both hydrological regulation and coastal protection that are otherwise lost through ecosystem degradation (6), more on NbS is discussed below.

In fact, ensuring a reliable freshwater supply under drought conditions has become a central concern. Multi-country initiatives like the ADAPTaRES project have underscored this by coordinating water management actions across Madeira, the Canary Islands and Cape Verde – promoting efficient water use, reuse, and irrigation to strengthen drought resilience (7).

In addition to water issues, island infrastructure is also at high risk and heavily exposed to extreme weather events. Infrastructures such as roads, ports, power and water facilities lies near coasts or flood-prone valleys, making them highly vulnerable to intense storms and heavy rainfall. A single extreme event can inflict outsized damages: for example, torrential rains and flooding in Madeira (February 2010) caused losses exceeding €1 billion (8). In Macaronesia, frequent Atlantic storm surges and coastal floods have led to losses of approximately €250 million over the past decade, impacting tourism hubs and settlements alike (9).

Furthermore, long-term climatic shifts are making these problems worse. Warming is unequivocally underway in Macaronesia's climate, as observational records show significant temperature increases, especially in elevated terrains. For instance, nighttime minimum temperatures in the Canaries have risen by over +0.2 °C per decade at summit locations, and the frequency of "tropical nights" (nighttime $T_{\min} \geq 20$ °C) has climbed markedly in many areas (10).

While tourism is often the focus, climate change also threatens a wide spectrum of livelihoods across Macaronesia. Rural economies that depend on subsistence farming and local natural resources are increasingly at risk from water scarcity and declining crop yields as drought frequency rises. Fisheries and coastal communities are likewise imperiled by ocean warming and extreme weather events. For example, more frequent marine heat extremes and coastal storms are damaging fish stocks and infrastructure, with intensified erosion threatening harbours and shore-based livelihoods (8). Warming seas are also encouraging a tropicalization of marine ecosystems. Around the Canary Islands, the poleward spread of harmful tropical algae is expected to increase cases of ciguatera fish poisoning, a food-borne illness new to these latitudes (11). Public health vulnerabilities are compounding: heatwaves are becoming more intense, posing direct risks to human health, especially for the elderly and outdoor workers, and heavy precipitation events raise the odds of water-borne disease outbreaks as water and sanitation systems get stressed. Indeed, climate change impacts on small islands are profoundly multi-sectoral, already affecting water and food security, health, and local economies and these compound risks threaten the well-being of communities across the archipelagos. Precipitation patterns are expected to diverge across the region, a drying trend is projected for the Canary Islands and Madeira, whereas the Azores may paradoxically face more frequent extreme rainfall events (3).

Even where total rainfall declines, the prospect of more erratic, heavy downpours raises concerns for flash floods, soil erosion and water management. These evolving climate pressures threaten not only natural ecosystems but also key economic sectors (from agriculture to tourism) that underpin island livelihoods. Such vulnerabilities imbue urgent significance to climate adaptation planning in Macaronesia. The very characteristics that make these islands unique, their small size, isolation, and concentrated coastal development, also amplify their sensitivity to climate hazards and limit their response options. Policymakers now recognize that preparing island territories for climate impacts is an immediate priority, not a distant goal. The European Union's climate resilience strategies explicitly highlight the need for swift adaptation in high-risk regions. The EU Adaptation Strategy (updated 2021) stresses "faster and more systemic adaptation" since climate effects are "already being felt" (12). In particular, Europe's outermost regions, which include Macaronesian islands, are singled out for dedicated support. The EU's 2013 Adaptation Strategy had already called for bolstering preparedness in outermost islands against extreme weather and coastal threats (9), and upcoming EU initiatives (e.g. the Coastal Communities Resilience Strategy due 2026) are expected to channel greater resources into island adaptation (13).

This policy focus reflects a clear reality: small islands require tailored, proactive climate resilience measures. High exposure (e.g. dense tourism infrastructure along coastlines) and limited adaptive capacity (e.g. constrained freshwater and land resources) mean that following the same development path is not sustainable in a changing climate. Strengthening flood defenses, diversifying water supply (desalination, reuse), climate-proofing roads and ports, and protecting ecosystems are all urgent adaptation needs. The Horizon Europe Project GENESIS, in line with these priorities, is undertaking a climatic study to inform evidence-based adaptation. By characterizing recent climate trends and future

risks in Macaronesia, the project aims to provide the knowledge base that policy-makers and local stakeholders require for resilient planning. There is strong alignment with EU strategy: improving climate-risk knowledge and data is the first step to “smarter adaptation”, one of the core objectives of the 2021 EU strategy (12).

Local governance and community-based adaptation initiatives are increasingly complementing top-down strategies in Macaronesia. In addition to European Union climate adaptation programs, island-level governments and municipalities have begun implementing their own measures, often in collaboration across archipelagos and with active community participation. A notable example is the LIFE Garachico project in Tenerife (Canary Islands), led by the town’s local authorities to develop affordable flood defenses and preparedness in a coastal community (9). This initiative introduced an early warning system for storm surges alongside participatory planning – residents helped devise self-protection protocols for neighborhood humidity goods at risk. The project’s partnership spanned multiple islands (including links to Azorean partners), enabling inter-island knowledge transfer and cooperation on adaptation solutions. Such efforts demonstrate the value of governance at the local scale: by engaging citizens and tailoring actions to island-specific needs, Macaronesian communities are enhancing their resilience in ways that top-down policies alone might not achieve. These grassroots and inter-island collaborations effectively bolster the broader EU climate adaptation framework with on-the-ground action and shared learning.

Ultimately, effective climate adaptation for these island regions is not only an environmental imperative but also a socio-economic one – safeguarding communities, economies and cultural heritage in Macaronesia hinges on our capacity to anticipate and adapt to the climatic shifts already in motion. A final challenge confronting this effort is the issue of data availability and spatial heterogeneity in volcanic island terrains. Macaronesian islands are known for their dramatic topography – from soaring volcanic peaks to rugged coastlines – which creates a patchwork of microclimates over short distances. Steep elevation gradients, orographic cloud effects, and complex land-sea interactions produce highly localized climate variations. However, the meteorological observation networks on these islands are relatively sparse and uneven, often clustered near populated areas or lower elevations. As a result, important facets of the climate can go under-sampled. On volcanic islands, a single ridge can divide a lush, rain-soaked slope from a dry valley just a few kilometers away. When weather station networks are too sparse, or when their data are not accessible it is very difficult to capture the full variability of local microclimates and weather patterns (14).

Groundwater resources constitute a critical lifeline for the Macaronesian islands, and climate change is altering their recharge and quality dynamics. Most islands rely heavily on groundwater aquifers for drinking water and agriculture, yet changing rainfall regimes and rising sea levels are disrupting the balance of these fragile water systems. In mountainous islands like Madeira, a projected decrease in precipitation directly threatens not only upland ecosystems but also the small streams and aquifer systems that depend on rainwater captured in the cloud-covered highlands (8). Reduced rainfall and faster runoff mean less natural recharge to refill groundwater reservoirs. At the same time, in lower-lying and drier islands, prolonged droughts and continued groundwater over-exploitation are leading to saline intrusion of coastal aquifers. On Santiago Island in Cape Verde, for example, intensive pumping combined with rainfall deficits has resulted in seawater infiltrating the aquifers, degrading water quality and leaving some communities with only brackish water supplies (14). Such salinization and depletion of groundwater not only endanger drinking water security but also harm groundwater-dependent ecosystems (such as oasis-like habitats and spring-fed valleys). In the long term, the contraction of

fresh groundwater lenses under climate pressure poses one of the most serious threats to Macaronesian water security, underscoring the need for adaptive water management that includes aquifer recharge enhancement and careful demand management.

Nature-based Solutions (NbS) are increasingly recognized as vital adaptation tools for the Macaronesian archipelagos. NbS involve the sustainable management and restoration of ecosystems to address climatic threats while providing co-benefits for biodiversity and human well-being. For these islands, investing in ecosystem restoration has proven to enhance natural resilience. For instance, reforestation programs are underway to expand native laurel forests in parts of the Canaries, once mature, these restored woodlands improve cloud water interception and infiltration to aquifers, reduce soil erosion on slopes, and sequester carbon (5). Similarly, protecting and rehabilitating wetlands and riparian zones helps regulate floods and water storage, which is particularly valuable in seasonally dry landscapes. In coastal areas, conserving dune systems, mangroves (where present), and seagrass beds can help dissipate wave energy and guard against storm surges, thereby complementing or substituting hard infrastructure. Indeed, healthy ecosystems often function as natural defense infrastructure: coastal wetlands can defend communities from storm surge and sea-level rise, and well-managed forests safeguard water supplies and stabilize soils (15). By implementing NbS, such as sustainable land-use practices, forest and watershed restoration, and marine protected areas, Macaronesian islands are not only adapting to climate impacts but also enhancing their ecological integrity and the services that local communities depend upon.

Despite being grouped under Macaronesia, each archipelago faces distinct climate profiles and vulnerabilities, which necessitates differentiated adaptation approaches. The Azores, Madeira, the Canary Islands, and Cape Verde vary markedly in their climates – from the humid mild conditions of the Azores to the hyper-arid environments of parts of Cape Verde. These differences shape the risks each island group confronts. Cape Verde, lying closest to the African Sahel, endures chronic aridity and water scarcity; its limited native vegetation was largely depleted over centuries, and today the islands are prone to drought, soil erosion, and desertification. At present, they are adapting there focuses on water conservation, drought-resistant agriculture, and reforestation to restore soils. The Azores, by contrast, have an oceanic climate with abundant rainfall and no dry season (17). They are less threatened by drought or heat extremes than the other islands, but they are increasingly exposed to powerful Atlantic storms and even the occasional hurricane remnant, which infrastructure must be prepared to withstand (18). Madeira and the Canary Islands occupy intermediate positions: they have both wet highlands and dry lowlands and thus face a mix of threats, from heatwaves and wildfires in drier areas to intense rainfall events and landslides in mountainous terrain.

Finally, the climate adaptation needs of Macaronesia are closely tied to broader global frameworks and findings. International assessments like the IPCC have repeatedly identified small islands as particularly at risk, emphasizing the urgency of accelerating adaptation in such regions (11). The experience of Macaronesian islands – from water stress and biodiversity loss to extreme weather damages – aligns with these global observations and adds weight to calls for ambitious climate action to limit warming (as per the Paris Agreement goals). Moreover, the adaptation efforts in these archipelagos contribute to and benefit from worldwide initiatives like the Sendai Framework for Disaster Risk Reduction (2015–2030) and the United Nations Sustainable Development Goals (SDGs). The Sendai Framework's emphasis on reducing vulnerability to natural hazards and improving early warning systems is reflected in Macaronesia's community-level actions (for example, the flood alert systems and preparedness plans in the Canaries fulfill Sendai-aligned goals of disaster risk reduction). At the same time, building climate resilience locally supports

progress towards the SDGs – notably SDG 13 (Climate Action), but also goals on clean water, sustainable cities, and the protection of life on land and below water. Indeed, the SDGs explicitly recognize that combating climate change is integral to sustainable development, highlighting targets for safeguarding water resources, ecosystems, and livelihoods (19). By situating their adaptation strategies within these global frameworks, the Macaronesian archipelagos not only gain guidance and impetus from international research and funding, but also serve as living laboratories for sustainable adaptation in island settings – demonstrating how climate resilience can be pursued in tandem with biodiversity conservation and socio-economic development.

1.2 State of the art methods and studies

Assessing historical climate trends in data-sparse regions – such as small islands and remote archipelagos – is a recognized challenge, and a number of approaches have emerged to address it. Researchers have long attempted to compensate for limited station observations by developing gridded climate datasets that integrate multiple sources and interpolate values across space. Global initiatives have produced century-long datasets like CRUTEM and GISTEMP for temperature, or GPCC and CRU-TS for precipitation, which blend station records into continuous fields (20). These products extend back to the 19th or early 20th century, providing broad-scale trend estimates even over oceans and isolated lands. However, their resolution is typically coarse (e.g. 0.5° latitude/longitude), and their accuracy in island regions depends entirely on the scant local data available. As a recent data assessment noted, “the existing climatic information is still unrepresentative in many territories” with low station density – meaning even the best global datasets can struggle to reflect fine-grained island climates (20).

Recognizing this, climate scientists have increasingly turned to high-resolution reanalysis and downscaling techniques to better characterize local trends. Reanalysis datasets have been a game-changer for data-sparse areas. Reanalyses (such as ECMWF’s ERA5 and its land-focused derivative ERA5-Land) use data assimilation to merge available observations (from stations, satellites, ships, etc.) with a weather model, producing a spatially complete, physically consistent record of past climate. Modern reanalyses offer hourly data at resolutions of ~30 km or finer globally, and ~9 km for land variables in ERA5-Land (21).

Importantly, they inherently cover small islands and remote grids by inferring conditions based on surrounding data and atmospheric dynamics. For instance, ERA5 explicitly includes grid cells for many tiny islands (using a ≥50% land mask criterion) and thus can provide 2 m temperature, rainfall, wind, etc., for those locations even in the absence of direct measurements (22).

While reanalysis cannot replace ground truth, it serves as a powerful surrogate where observations are missing or discontinuous. Studies focusing on island climates have leveraged reanalysis outputs to discern trends that were previously hard to detect. A notable example comes from the Caribbean: (23) analyzed climate trends over the Lesser Antilles using a satellite-blended reanalysis dataset, which incorporated satellite rainfall estimates to better capture island precipitation patterns. The high-resolution data allowed the identification of changes in rainfall distribution and intensity over Guadeloupe, Dominica, Martinique and surrounding islands – insights that would have been elusive with sparse rain gauge records alone. As this case illustrates, the fusion of satellite remote sensing with reanalysis is especially valuable for islands, enabling researchers to “study rainfall patterns with greater detail” than ever before.

Similarly, in Pacific islands, reanalysis-driven analyses have supplanted earlier data gaps; for example, in Vanuatu and Fiji, atmospheric reanalyses combined with satellite sea surface temperatures have been used to document warming trends and shifting drought frequency where station data were fragmentary. In summary, reanalysis products represent a state-of-the-art foundation for trend analysis in data-sparse regions – one that GENESIS can exploit by extracting Macaronesian climate signals (e.g. long-term temperature and moisture changes) from global reanalysis archives. Another key approach is climate downscaling, both statistical and dynamical, to achieve finer spatial detail. Downscaling is crucial for small islands that are often just a few grid cells wide in global models. Dynamical downscaling uses regional climate models (RCMs) or high-resolution global models to simulate climate at scales of a few kilometers, explicitly resolving island topography and coastlines. Recent work emphasizes that only with such high resolution can certain island climate processes be accurately captured – for instance, sea-breeze circulations, mountain-induced cloud/rainfall patterns, or the sharp climate contrasts across an island’s terrain (24). In one study focusing on Guadeloupe (French Antilles), researchers found that using a convection-permitting RCM (~2 km grid) was necessary to reproduce the island’s observed rainfall extremes and orographic effects; the study concluded that dynamical downscaling is indispensable to study the climate on small islands (24).

Statistical downscaling, on the other hand, involves developing empirical relationships between large-scale climate variables and local observations, which can then be used to interpolate or bias-correct coarse data. In Macaronesia and similar volcanic regions, a common statistical approach has been to incorporate topographic predictors (elevation, slope orientation, etc.) to refine temperature and precipitation fields. For example, a case study from Jeju Island (Korea) – another mid-latitude volcanic island – demonstrated a simple yet effective method: researchers calculated localized temperature lapse rates separately for the drier northern and wetter southern flanks of the island’s central volcano, and used these elevation-based adjustments to downscale temperatures across the island (14). This tailored lapse-rate approach substantially improved the representation of temperature gradients compared to assuming a constant lapse rate.

The Interactive Digital Climate Atlas of the Canary Islands provides a practical example of statistical downscaling and interpolation applied in our region of interest. This project, led by Spanish scientists, compiled all available climate station data in the Canaries and employed geospatial modeling to generate high-resolution (100 m) maps of climatic variables (25). The resulting atlas – delivered through a GIS web portal – reveals the fine-scale temperature and precipitation patterns across the archipelago’s complex terrain and tracks their trends over recent decades.

Such tools effectively bridge the gap between point observations and the real spatial diversity of island climates, aiding local planners in visualizing micro-scale climate risks (for instance, identifying hotspots of declining rainfall or increasing heat in specific valleys or slopes). In addition to data-centric methods, several peer projects and studies have tackled climate trend assessment in Macaronesia or comparable island regions, providing valuable context and techniques for GENESIS. A cornerstone in the scientific literature is a study that conducted a comprehensive analysis of Macaronesia’s climate history (3). Long-term records dating back to the 19th century were assembled for each major island group—beginning in 1865 for the Azores and Madeira, and 1885 for the Canaries—through careful homogenization of archival observations. The results revealed coherent patterns of variability across the islands and, notably, identified a significant warming phase after 1976, which stands out as the clearest signal of anthropogenic climate change in the

record. In terms of precipitation, the trends appeared less uniform; one striking result was observed for Cape Verde, which endured severe drought conditions through the mid-20th century, followed by a slight recovery in rainfall during the early 21st century.

These findings underscore the value of extending island climatological series as far back as possible – allowing current changes to be viewed in the context of multi-decadal fluctuations and historical extremes. The GENESIS project builds upon such baselines by updating them with the latest data and higher-resolution analysis. Another relevant effort is the EU Horizon 2020 SOCLIMPACT project, which, while future-oriented, laid important groundwork in downscaling and impact assessment for European islands. SOCLIMPACT developed tailored high-resolution climate projections for islands in various regions (including the Canary Islands and Madeira) for the 2030–2100 period (26).

In doing so, the project highlighted the inadequacy of coarse global models for island planning – “the coarse spatial resolution of available projections makes it difficult to derive valid statements for islands” – and demonstrated how finer-scale modeling can yield more actionable insights (26).

Although GENESIS is focused on observed trends and recent past, the methodologies from SOCLIMPACT (such as bias-correcting global models with island data, or coupling climate and economic impact models) inform our approach to linking climate signals with sectoral vulnerabilities. On the adaptation front, EU-funded initiatives in Macaronesia and other island regions illustrate how climate information feeds into risk management. The LIFE Garachico project in Tenerife, for example, combined climate scenario analysis with local topographic data to map coastal flood hazard under rising sea levels and more frequent storms (9). They produced dynamic GIS maps of vulnerability and risk for various time horizons, which are being used to design an adaptation strategy (a “Flexible Adaptation Pathways” framework) for the town of Garachico. This exemplifies a state-of-the-art use of climate trend and projection data at the community level – translating climate science outputs into practical tools like early warning systems, flood zoning, and an innovative resilience fund.

Likewise, in the Mediterranean, the LIFE ADAPT2CLIMA project developed a decision-support platform for Crete, Sicily and Cyprus that integrates climate projections with crop models to evaluate agriculture vulnerabilities (27). While ADAPT2CLIMA is outside Macaronesia, it shares a common objective with GENESIS: providing user-friendly, policy-relevant climate insight for island decision-makers

In summary, the state-of-the-art practice for characterizing past climate trends in Macaronesia and similarly data-sparse regions relies on a hybrid toolkit. It combines enhanced observations (via gridded datasets and homogenized long-term records), model-based reconstruction (via reanalyses and downscaling to resolve local detail), and thematic studies linking climate to impacts (via integrated assessments and mapping of risks). By surveying successful examples – from the construction of historical climate series, to the use of ERA5 and satellite data in island trend detection, to the deployment of high-resolution climate atlases and sectoral impact models – we ensure that the GENESIS deliverable draws on cutting-edge knowledge.

This review also highlights the importance of continued data improvement: expanding climate monitoring networks in volcanic islands, further developing remote-sensing techniques for fine-scale climate observation, and fostering open data portals (like the Canary Islands climate atlas) will all enhance our ability to detect changes in these vulnerable regions. The GENESIS project, aligned with Horizon Europe’s goals and the EU Adaptation Strategy, contributes to this advancing frontier by not only analyzing Macaronesia’s past and present climate, but also by demonstrating methodologies that

can be replicated in other island contexts. Through rigorous trend analysis informed by the best available methods, our deliverable will support evidence-based adaptation planning – helping Macaronesian territories navigate the uncertain climate future with robust information at hand.

2. GENESIS Methodology

Within the scope of the GENESIS project, a significant effort was undertaken to produce high-resolution climate datasets for the four target archipelagos: the Canary Islands, Madeira, Azores, and Cape Verde. The primary objective was to dynamically downscale climate data, encompassing both historical reanalysis and future projections, to a fine spatial resolution. After an initial assessment revealed that downscaling the available climate change projections was not feasible, the focus was concentrated on historical records.

2.1 TopoPyScale

TopoPyScale uses the ERA5 (22) reanalysis product, that is the most suitable option for creating a detailed historical climate dataset. This process was accomplished by leveraging a 90-meter Shuttle Radar Topography Mission (SRTM) Digital Elevation Model (DEM), which was resampled to the target 180-meter resolution to serve as the topographical basis for the downscaling.

The core of this work was performed using TopoPyScale, a Python library designed for climatological and cryosphere studies. Due to the specific requirements of the GENESIS project, the standard version of the tool was insufficient. Consequently, a dedicated fork of the software was developed, incorporating substantial improvements and new functionalities, with a pull request for integration into the main repository currently pending. The relevance of these contributions is highlighted by the inclusion of the GENESIS project as a use case in the official TopoPyScale documentation¹.

A major challenge encountered was the acquisition of the extensive ERA5 dataset. Initial attempts using the standard Copernicus Data Store (CDS) proved unfeasible due to severe limitations on request sizes and progressively lower job priorities. To overcome this bottleneck, a robust data retrieval strategy was implemented, combining downloads from the NCAR Research Data Archive (RDA) and Google Cloud Platform (GCP), which hosts ERA5 data in the efficient Zarr format. This multi-source approach entirely replaced the use of CDS.

Substantial modifications and enhancements were contributed to the TopoPyScale software to meet the project's demands and improve its overall performance. These contributions include:

- The development and integration of a new module to handle data retrieval directly from the RDA repository.
- Significant improvements to the processing of Zarr-formatted data, enhancing efficiency.
- Optimization of the final remapping step, which projects results from processed clusters back onto the original DEM grid.
- The addition of a new cluster category to explicitly exclude points from processing, such as sea areas or locations with no data.

¹ https://topopyscale.readthedocs.io/latest/00_use_cases/

- Implementation of a condition to refine the interpolation of height-dependent variables.
- The capability to calculate relative humidity from the downscaled variables.
- Inclusion of a simple DEM resampling utility to halve spatial resolution when needed.
- Preparatory work to enable parallel processing for future scalability.

In addition to these software enhancements, a convenience utility was also developed to monitor the status of large-scale RDA and Zarr downloads by reporting progress to a shared Google Sheet.

To support the primary downscaling workflow, a suite of auxiliary scripts and tools was developed. These included a preprocessing script for the DEM to adjust near-zero elevation values for numerical stability, and a tool to precisely define the optimal geographical boundaries for each study region.

Additionally, an extensive evaluation of other potential climate data sources was conducted, including historical and future projection datasets like WorldClim, IFS, ROCIOCAN (AEMET), and various ESGF reanalyses, before ultimately selecting ERA5 for its suitability. Furthermore, 2D and 3D visualization scripts were created to verify the correctness and quality of the DEM datasets. Finally, a master script was engineered to orchestrate the entire downscaling process, capable of reading distinct configuration files for each region, managing parallel downloads, and accepting command-line parameters for flexible execution. The meticulous preparation of these configuration files was in itself a critical task that ensured the successful and consistent application of the methodology across all target areas.

The resulting downscaled data can be found in (28), (29), (30), (31) and (32)

2.2 PySEBAL

The estimation of monthly actual evapotranspiration (AET) and biomass production across the Macaronesian archipelagos (data was only available for La Palma and Gran Canaria) was done by using PySEBAL (28), a Python implementation of the Surface Energy Balance Model (SEBAL) (29). This method closes the land-surface energy balance at the time of each satellite overpass and derives the latent heat flux as a residual of net radiation, soil heat flux, and sensible heat flux. Instantaneous AET and evaporative fraction are then scaled to daily and, from there, aggregated to monthly values. PySEBAL also computes vegetation indicators and biomass/water productivity from the same inputs.

During the GENESIS project a fully automated workflow was established to integrate data acquisition, preprocessing, and model execution. Custom scripts were developed to manage the systematic downloading and preparation of input datasets, thereby reducing manual intervention and ensuring timely updates. A dedicated containerised environment was created to ensure the workflow could run consistently on different computing systems, while also providing better control over how computing tasks are run in parallel, making the overall process faster and more efficient. In addition, the original PySEBAL methodology was adapted to the conditions of Macaronesia, where the lower frequency of Landsat overpasses compared to the reference study area required a more flexible

temporal processing strategy. These adaptations collectively strengthened the robustness and applicability of the workflow in insular regions.

Input data

The following datasets were used as inputs to PySEBAL:

- **Satellite imagery:** Landsat (30) versions 7 and 8 were used as described in the PySEBAL documentation. Preprocessing includes cloud masking and mosaicking where needed.
- **Meteorology:** Following the PySEBAL workflow, GLDAS NOAH v2.1 (31) was used. From this dataset, specific humidity (Q_{air}), surface pressure (P_{surf}), air temperature, wind speed, and downward shortwave radiation were extracted. Relative humidity was then computed from Q_{air} and P_{surf} . These layers were averaged to daily values and resampled to the project grid using GRASS (32) before being used by PySEBAL.
- **Topography:** The Copernicus DEM GLO-30 (32) was used. This DEM represents the surface distributions. Elevation and derived slope/aspect inform PySEBAL's radiation and aerodynamic calculations.

Core Modelling (SEBAL in PySEBAL)

The method is based on a simple energy balance: all the energy arriving at the land surface is either stored in the ground, used to heat the air, or used to evaporate water. PySEBAL calculates each of these parts from satellite and meteorological data:

- **Net radiation:** how much solar and thermal energy reaches and leaves the surface (from Landsat and GLDAS, adjusted for terrain using the DEM).
- **Soil heat flux:** the small portion that goes into warming the soil, estimated from surface temperature and vegetation cover.
- **Sensible heat flux:** the portion that warms the air, estimated by comparing “hot” and “cold” reference pixels in each image (a very dry bare area versus a well-watered vegetated area).
- **Latent heat flux:** whatever is left over, is the energy actually used to evaporate water and drive transpiration by plants.

That last term is converted into evapotranspiration (ET). By repeating the calculation for every pixel in an image, we get a spatial map of water use. Instantaneous values from the satellite overpass are then scaled to daily totals using meteorological data, and these daily ET values are summed up to get monthly total.

Gap Filling and Monthly Maps

Because Landsat satellite don't pass every day, and clouds often block the view, not all days or pixels have data. To build complete monthly maps, PySEBAL applies two simple filling steps:

- Time filling: when a pixel was missing for a few days, we estimated it by looking at nearby dates and fitting a smooth curve over time.
- Space filling: if a pixel was still missing after that, we filled it by looking at the values of neighbouring pixels in the same image.

This way, every monthly map covers the full islands, even if some Landsat scenes were cloudy. The filling method estimate many values, but it helps ensure the final dataset is complete and consistent across all archipelagos.

Outputs

For each island of the Macaronesian archipelago (Azores, Madeira, Canary Islands, and Cape Verde), we delivered monthly maps of the following outputs:

- Actual Evapotranspiration (AET): The measured or estimated amount of water actually transferred from the land surface to the atmosphere through evaporation from soil and water bodies and transpiration by vegetation under existing moisture conditions.
- Potential Evapotranspiration (PET): The maximum possible amount of water that could be transferred from the land surface to the atmosphere through evaporation and transpiration if sufficient water were available to fully meet atmospheric demand.
- Biomass Water Productivity (BWP): the ratio of biomass produced to the amount of water consumed, indicating the efficiency of water use in biomass generation.

These outputs provide the spatially distributed water-use information needed for analysis. They can be found in (39).

2.3 Standardized Precipitation Evapotranspiration Index (34)

The Standardized Precipitation Evapotranspiration Index (SPEI) provides a drought metric that integrates water supply (precipitation) and atmospheric demand (PET). It expresses anomalies as standard-normal scores so different climates and time scales are comparable. These are the steps to calculate this index:

1. Climatic water balance

$$D_t = \text{Precipitation}_t - \text{PET}_t$$

Equation 1: Water Balance

t is the time step, in the GENESIS project will be monthly.

2. Multi-scale accumulation

To target different drought types, sum the water balance over a window of k months:

$$X_{t,k} = \sum_{i=0}^{k-1} D_{t-i}, k \in \{3, 6, 12, 24\}$$

Equation 2: Multi-Scale Water Balance Accumulation

3. Standardization

For each accumulation period k and for each calendar month (to account for seasonality), the series of accumulated climatic water balance values $X_{t,k}$ is analyzed over a chosen reference period (e.g., 2000–2020). These values are fitted to a three-parameter log-logistic probability distribution, which describes how water balance values are statistically distributed for that month and time scale.

From this fitted distribution, the cumulative probability p of each observed $X_{t,k}$ value is obtained, this represents the likelihood of observing a water balance equal to or lower than that value. The probability p then transformed into a standard normal deviate (Z-score) using the inverse of the standard normal cumulative distribution function:

$$\text{SPEI}_{t,k} = \Phi^{-1}(p)$$

Equation 3: SPEI

This transformation expresses the results in standard deviation units (mean = 0, standard deviation = 1), producing the SPEI, which allows direct comparison of wetness and dryness intensity across different climates and time scales.

Positive values of SPEI indicate wetter-than-normal conditions, whereas negative values reflect drier than normal conditions. The magnitude of negative departures is used to classify drought severity, following thresholds adapted from the SPEI (36):

- 0 to -0.99: mildly dry
- -1.00 to -1.49: moderately dry
- -1.50 to -1.99: severely dry
- ≤ -2.00 : extremely dry

Symmetrically, positive values classify wet conditions (moderate, severe, extreme). These thresholds provide a consistent interpretation framework across different time scales.

2.4 Consideration of WaPOR Reference Evapotranspiration as a Surrogate for Potential Evapotranspiration

An initial strategy contemplated the use of the FAO-style reference evapotranspiration (RET) provided by WaPOR (36) as a surrogate for potential evapotranspiration (PET) as in (37), given that PET derived with PySEBAL was, at this stage, only available for Gran Canaria and La Palma. The intention was to extend comparability across islands by adopting a single, widely used atmospheric demand metric where direct PET was missing. The only region where even in this source no data was available was Azores.

A consistency check was conducted over the two islands for which both series existed. When trends were evaluated at the sub-regional scale, it was observed that in several areas PET exhibited an increasing tendency while RET displayed a decreasing tendency over the same period. This systematic sign divergence indicates that RET and PET were not evolving coherently in space and time within the study domain.

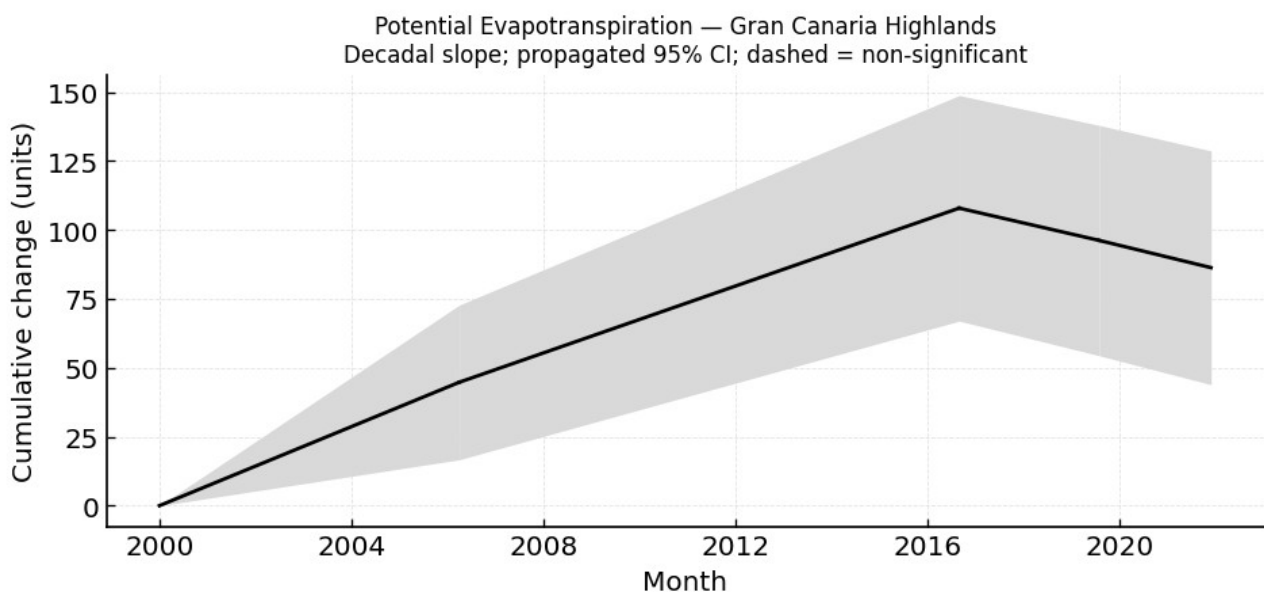


Figure 1: Potential Evapotranspiration Trend – Gran Canaria Highlands

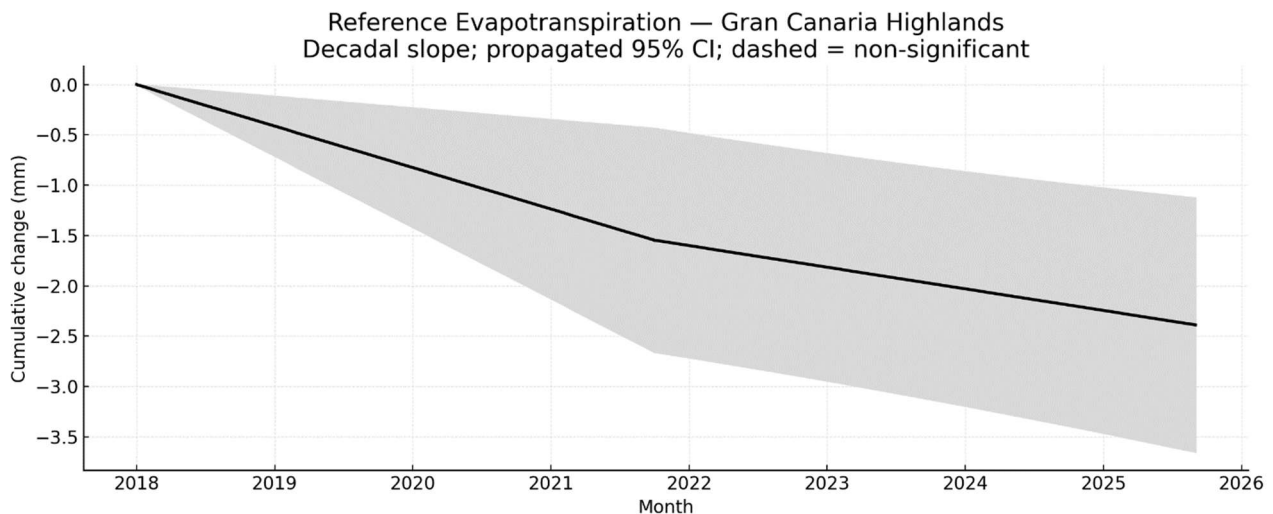


Figure 2: Reference Evapotranspiration Trend – Gran Canaria Highlands

The discrepancy is plausibly attributable to the differing sensitivity of each metric to radiation, humidity, wind, and surface resistances. Regardless of cause, mixing these two constructs would introduce methodological artifacts into trend inference.

For example in the highlands of Gran Canaria, the divergence between PET and RET trends can be attributed to the contrasting sensitivity of both metrics to the local climatic drivers. The area shows a pronounced increase in shortwave and longwave radiation together with rising maximum temperatures, conditions that enhance the energy available for evaporation and therefore raise PET derived from surface energy balance. However, simultaneous increases in humidity and reductions in minimum wind speed reduce the aerodynamic demand of the atmosphere, which are key factors that strongly influence RET in the Penman–Monteith formulation.

In light of these findings, the use of WaPOR RET as a surrogate for PET was discarded. Subsequent analyses of SPEI will be only available for Gran Canaria and La Palma.

The WaPOR data used in the project can be found in (44), (46) and (47).

2.4 Climate Trend Calculation

1. Define zones

Grid cells are grouped into climate-relevant zones (preferably defined by meteorological institutions). Variables are aggregated monthly within each zone: fluxes are summed and state variables averaged.

2. Seasonal adjustment

Seasonal adjustment is performed by STL decomposition (37) to separate each zone’s time series into seasonal, trend, and residual components. The extracted trend component is retained for subsequent analysis.

3. Trend estimation

The slope is estimated by the Theil–Sen estimator (38) and expressed as change per decade. This trend is assessed by the Mann–Kendall test with trend-free pre-whitening (39) to correct for autocorrelation.

4. Uncertainty

Confidence intervals for the trend slope are obtained by a moving-block bootstrap (40) that resamples contiguous blocks of months to preserve temporal autocorrelation.

5. Break detection

Structural breaks in the trend component are detected using the PELT algorithm (41). When change-points are found, the trend analysis (Steps 1–3) is repeated for each segment.

2.5 Weighted and Normalized Slope Aggregation

To obtain a representative trend for each variable and subregion, the decadal slopes (monthly slopes x 120) estimated for all homogeneous segments defined by structural breakpoints were aggregated using a recency–duration weighting scheme. Each segment s was characterized by its start and end dates, from which the segment duration (d_s) was calculated as the number of days between both limits.

To account for the temporal relevance of recent trends, a recency factor (r_s) was also computed for each segment, representing its relative proximity to the most recent period in the record:

$$r_s = \frac{end_s - end_{min}}{end_{max} - end_{min}}$$

Equation 4: Recency Factor

Where end_s is the segment’s end date, end_{min} the earliest, and end_{max} the most recent end date among all segments.

The combined weight was obtained as the product of duration and recency, normalized so that all segment weights sum to one:

$$w_s = \frac{d_s \times r_s}{\sum_j d_j \times r_j}$$

Equation 5: Combined Weight with Recency and Duration

This weighting ensures that longer and more recent segments have greater influence on the aggregated trend.

The overall weighted slope was calculated as the weighted mean of individual segment slopes, and the weighted p-value as the corresponding weighted mean of the segment-level p-values:

$$slope_{weighted} = \sum_s w_s \times slope_s ; pvalue_{weighted} = \sum_s w_s \times pvalue_s$$

Equation 6: Weighted Slope

Finally, the weighted slope was normalized by the interannual standard deviation (σ_{annual}) of the same variable and area to express it in units of natural variability:

$$slope_{normalized} = \frac{slope_{weighted}}{\sigma_{annual}}$$

Equation 7: Normalized Weighted Slope

This normalization expresses the trend magnitude in units of the variable's natural variability, allowing for direct comparison among variables with different physical units or variability ranges (e.g. temperature in °C, radiation in $W \cdot m^{-2}$, precipitation in mm).

Without normalization, variables with larger numeric scales or higher intrinsic variability would dominate the interpretation of trend magnitudes.

By standardizing relative to their annual variability, the normalized slope provides a dimensionless measure of trend strength, indicating how large the observed change is compared to typical year to decade fluctuations, thus enabling meaningful cross-variable and cross-region comparisons.

2.6 Precipitation Error Rates

In this assessment, rainfall totals from reference station records were compared with the gridded rainfall product resulting of the TopoPyScale execution for Santiago, Fogo, and La Palma to quantify average percentage differences using the Mean Absolute Percentage Error (MAPE). The analysis periods were aligned: annual totals for Santiago and Fogo, monthly totals for La Palma later aggregated to annual, with years prior to 1995 excluded where applicable. For each reference point, the nearest valid grid cell in the gridded dataset was selected. Daily values were summed to match the corresponding monthly or annual periods. For every overlapping period, the absolute difference between the gridded estimate and the reference was divided by the reference value and expressed as a percentage. Monthly periods with a zero reference value were excluded to avoid division by zero, for solving this the monthly data was aggregated to annual data. The reported MAPE is the average of these percentages, where lower values indicate closer agreement and higher values indicate larger average percentage differences, subject to the extent of temporal overlap and the representativeness of the nearest grid cell.

Station	Island	MAPE
Caldera de Taburiente	La Palma	70.4 %
Atalaia	Fogo	58.83 %
Achad Furna	Fogo	91.05 %
Ponte Ferro	Santiago	81.33 %
São Francisco	Santiago	159.04 %
Ribeirão Chiqueiro	Santiago	174.24 %
São Jorge dos Órgãos	Santiago	402.8%
Aeroporto (Praia)	Santiago	519.09%

Table 1: Precipitation Error Rates

The stations data and error rates results can be found in (52).

3. Results

This section presents the climate trends observed across the four Macaronesian archipelagos (Canary Islands, Azores, Madeira, and Cape Verde) using monthly downscaled ERA5 reanalysis data (via TopoPyScale) covering the period January 1995 to December 2024. Additionally, monthly satellite-based evapotranspiration estimates (from PySEBAL) were analyzed for Gran Canaria and La Palma, the only islands with available data, spanning January 2000 to December 2020. The section examines the regional and local evolution of temperature, radiation, humidity, precipitation, and drought indicators (SPEI) across the study area.

All the trends files and plots can be found in (49).

3.1 Canary Islands

3.1.2 La Palma

La Palma Highlands

Comparison of the trend between climate variables:

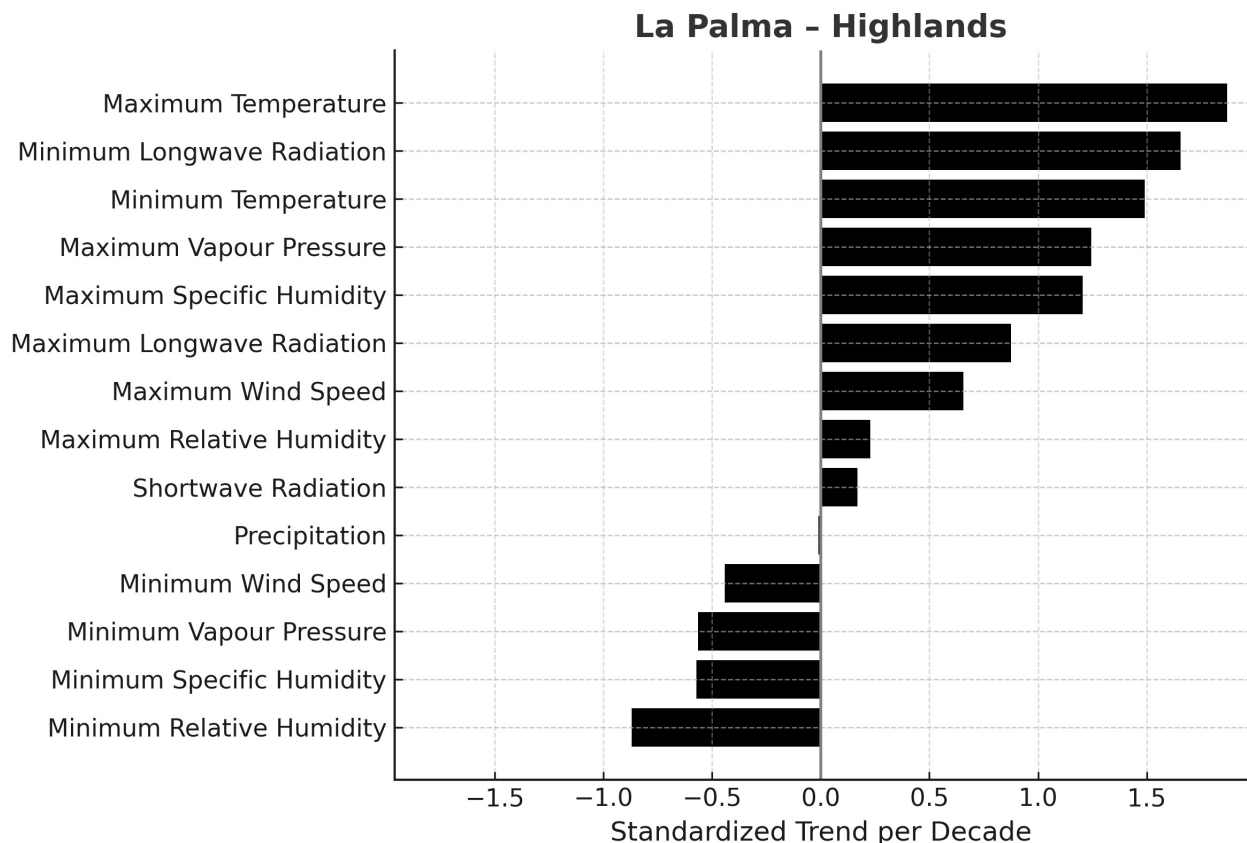


Figure 3: La Palma Highlands – Normalized Trends

In the Highlands of La Palma, the most dramatic changes relative to historical variability have been in temperature and in dryness indicators. After normalizing trends by their typical variability, maximum temperature emerges with one of the highest relative trend magnitudes (normalized trend ~ 1.87 , the largest positive change). In other words, warming of daytime highs is the most significant climate shift in this subregion. Minimum temperatures also show a large normalized increase (~ 1.49), albeit not as extreme as the maximum. Consistent with the warming, moisture-related variables like maximum specific humidity and maximum vapour pressure have high normalized increases (> 1). By contrast, precipitation has changed the least – its normalized trend (~ -0.01) is essentially negligible, highlighting that rainfall hasn't shifted much compared to its large year-to-decade swings. The largest relative decline is seen in minimum relative humidity, which has a normalized trend around -0.87 . This signifies that the drop in midday relative humidity is a notably large change in the context of its variability (i.e. the air's driest humidity levels are markedly lower now relative to past norms). In summary, the interior summits have become much warmer and drier at minimum humidity times, with those two aspects being the most significant shifts relative to other climate variables.

Temperature and Radiation:

The high-altitude interior of La Palma has experienced a pronounced warming. Maximum daily temperatures in the Cumbres de La Palma region have increased by approximately $+1.9^\circ\text{C}$ per decade (weighted trend, $p < 0.05$). Minimum temperatures have risen as well (about $+0.68^\circ\text{C}/\text{decade}$) but at roughly half the rate of daytime highs. This widening gap indicates a growing diurnal range. The warming is corroborated by significant increases in longwave radiation fluxes, consistent with a warmer surface and atmosphere. Daily maximum longwave radiation has trended upward by $\sim 4.1 \text{ W/m}^2$ (per decade), and nighttime minimum longwave flux by $\sim 4.9 \text{ W/m}^2$ – a substantial rise likely linked to enhanced thermal emission and possibly reduced cloud cover at night. Shortwave radiation has increased slightly (on the order of $+0.09 \text{ W/m}^2$ per decade, a minor positive trend). The net effect is a warmer, somewhat sunnier summit climate. All these trends are statistically significant (p -value < 0.05). Notably, the longwave radiation increase (especially at night) suggests clearer or drier nights. Daytime shortwave gains are modest, implying only slight decreases in cloudiness or dust during the day.

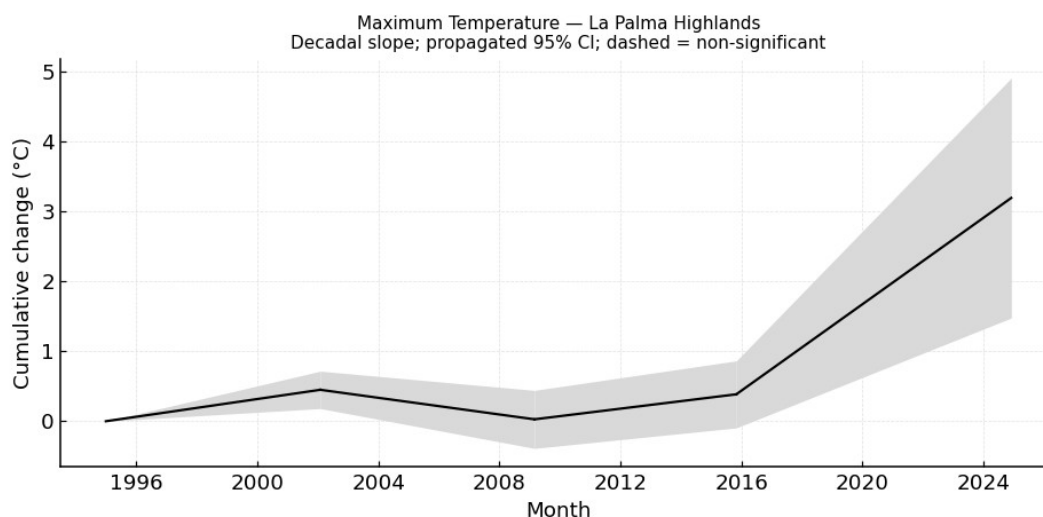


Figure 4: Maximum Temperature Trend – La Palma Highlands

Humidity and Precipitation:

Atmospheric moisture trends in the Highlands region reveal a contrast between absolute humidity and relative humidity. Specific humidity has increased in step with temperature: at the time of daily humidity maxima (typically early morning), specific humidity rose by ~ 0.00046 kg/kg per decade (~ 0.46 g/kg). This indicates that warmer air is holding more moisture at saturation times. By contrast, during the driest part of the day, specific humidity has slightly decreased (~ -0.00014 kg/kg per decade), meaning the absolute moisture content of the air at low-humidity hours has declined. In terms of relative humidity, the minimum (often mid-afternoon when air is warmest) shows a sharp downward trend of about -2.0% per decade (from $\sim 16\text{--}17\%$ in the 1990s to considerably drier values now, $p\text{-value} < 0.05$). Thus, the driest daytime conditions are becoming even drier in a relative sense. In contrast, the maximum daily relative humidity (often at night or morning) has a slight upward trend ($\sim 0.24\%$ per decade, not large but statistically significant), suggesting that near-saturated conditions at night have been maintained or even enhanced (likely because nights are warmer, closer to dew point, allowing relative humidity to stay high). These combined humidity changes imply a more arid feeling during the day (lower relative humidity_min) even as absolute moisture increases: the air holds more water overall, but it is further from saturation in the heat of the day. Precipitation in the summit region shows a mild declining trend, but the magnitude is small. The weighted trend is on the order of -0.92 mm per decade in monthly rainfall (negative, $p < 0.05$). This equates to only a small percent decrease over years; indeed, the normalized change is near zero (-0.01), indicating that rainfall variability dominates any slight downward trend. In other words, total rainfall has not changed drastically – the long-term trend is slightly downward but subtle. However, rainfall patterns have varied over time (see breakpoints below). All climate trends noted (temperature, humidity, precipitation) are statistically significant at the 95% confidence level unless stated otherwise.

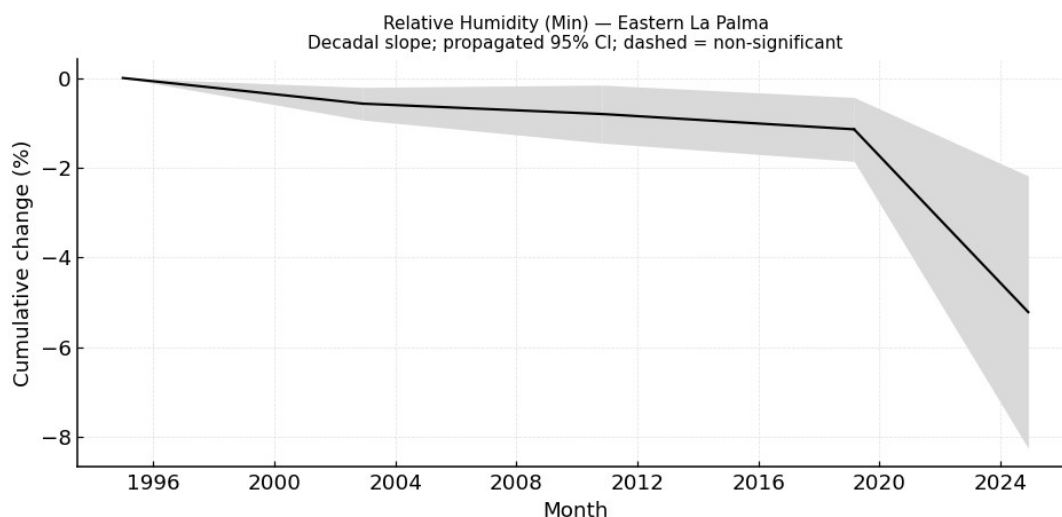


Figure 5: Minimum Relative Humidity Trend – La Palma Highlands

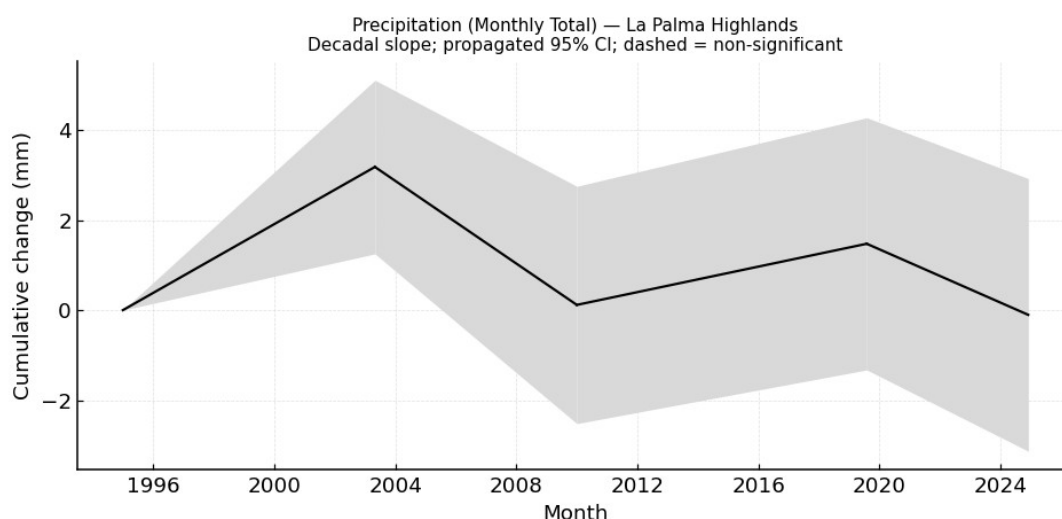


Figure 6: Precipitation Trend – La Palma Highlands

Wind and Vapour Pressure:

Wind patterns at the Highlands have shifted towards stronger peak winds and calmer lows. The daily maximum wind speed has increased by about +0.44 m/s per decade ($p < 0.05$). This suggests more frequent or intense wind events. Meanwhile, the minimum wind speeds have slightly decreased (~ -0.05 m/s per decade), implying slightly calmer conditions during typically still periods. These changes point to a greater range in wind activity – stronger daytime upslope winds, yet very little change (a slight decline) in nighttime downslope or calm conditions. Consistent with the temperature and humidity changes, vapour pressure trends diverge between moist and dry times. The partial pressure of water vapour at saturation has risen by roughly +66 Pa per decade (~ 0.66 hPa). This is a direct consequence of warmer temperatures, the air’s capacity for moisture increased, and indeed more water vapour is present at humid times. On the other hand, the minimum

vapour pressure, during very dry air periods, has decreased by about -20 Pa/decade, reflecting the fact that when the air is dry, it's even drier in absolute. In practical terms, the summit air can reach higher absolute humidity when moist, but also lower absolute humidity when dry, reinforcing the notion of more extreme humidity swings.

Temporal Breakpoints:

The climate evolution at La Palma Highlands has not been linear; several breakpoints in the trends are evident. Segmented trend analysis identifies meaningful change-points around the early 2000s, late 2000s, and mid-2010s.

For instance, temperature shows a notable inflection circa 2015: prior to 2015, the warming rate of maximum temperature was on the order of only ~ 0.5 – 0.6 °C/decade, but after ~ 2015 the rate steepened to ~ 3.1 °C/decade. This recent accelerated warming aligns with the period of record-breaking global temperatures in the late 2010s. Earlier, a modest cooling or plateau was observed in the mid-2000s (there is a slight negative trend segment around 2002–2009 before the sharp upswing) – likely reflecting a pause in warming or natural variability during that interval.

Precipitation:

Precipitation likewise exhibits breakpoints. The late 1990s into early 2000s was relatively wet, even the segment from 1995–2003 shows increasing rainfall. From ~ 2003 to 2010 the Highlands saw a significant decrease in rainfall (negative precipitation trend segment). Another breakpoint around 2010 shows a partial rebound until 2019. Most recently, after 2019, the trend turns downward again, suggesting that the last few years have been drier. These segmented trends indicate climate variability on longer trends.

Wind:

Wind and other variables also show breakpoints consistent with these periods (e.g. wind speeds rising more in the post-2010 era), but the most salient changes are seen in temperature and precipitation around the noted years. In summary, around 2002–2003 and 2009–2010 are key pivot points (transition to drier phases), and 2015 marks a dramatic pivot to faster warming in the summit climate.

Evapotranspiration and Drought:

The combined effect of warming and slight drying is reflected in evapotranspiration behavior and drought indices. PET has been increasing as temperatures rise and radiation is ample. Concurrently, AET depends on water availability from rainfall. In wet periods, AET can meet this atmospheric demand, but in dry periods a gap grows between PET and AET.

For instance, during a wet spring month (March–May) of 2016, the Cumbres region had abundant moisture: actual evapotranspiration reached ~ 302 mm in May 2016, nearly

matching the potential evapotranspiration of ~305 mm for that month. This implies the land had enough water for vegetation and soils to evaporate at the atmosphere's full demand rate. By contrast, in a dry period such as late 2020, AET fell well below PET. In December 2020, AET was only about 54 mm, whereas PET was ~80 mm. In other words, only ~67% of the potential evaporation actually occurred, indicating significant water stress.

This unmet demand is a hallmark of drought conditions. The Standardized Precipitation-Evapotranspiration Index (SPEI) captures these water deficits over various timescales. The SPEI for La Palma Highlands reveals that drought episodes have become more pronounced in recent years. A severe multi-year drought occurred around 2019–2020: by July 2020, the 24-month accumulated SPEI had dropped to approximately -1.3 , indicating a significant moderate-to-severe drought over the preceding two years. Shorter-term index at that time was even lower (SPEI-3 ~ -1.3 in mid-2020, reflecting an acute seasonal drought). This drought was one of the worst on record, comparable to or exceeding earlier events. For example, the data show a notable drought in late 2003–2004: by early 2004, SPEI-3 had plummeted to about -1.9 , and SPEI-6 was below -1.5 , signifying an intense dry spell that developed rapidly. That 2003–2004 event also pushed the 12-month SPEI near -1.0 , though the longer 24-month conditions were nearer normal, the drought was sharp but not yet two years long at that point.

In summary, the interior summits have seen increased evaporative demand (rising PET with warming) and slightly reduced rainfall, which together yield more frequent water deficits. Actual evapotranspiration still reaches high values in wet, but during prolonged dry spells AET is curtailed well below PET. Drought indices confirm more frequent moderate droughts, with multi-decade drought severity around SPEI ~ -1 to -1.5 in recent decades. The period around 2019–2021 stands out as especially dry (SPEI-24 ~ -1.5 in late 2020). These evolving hydro-climatic conditions point to growing challenges for water availability and ecosystems in the highlands of La Palma, as warmer temperatures drive up demand and even slight declines in moisture result in significant drought stress.

Eastern La Palma

Comparison of the trend between climate variables:

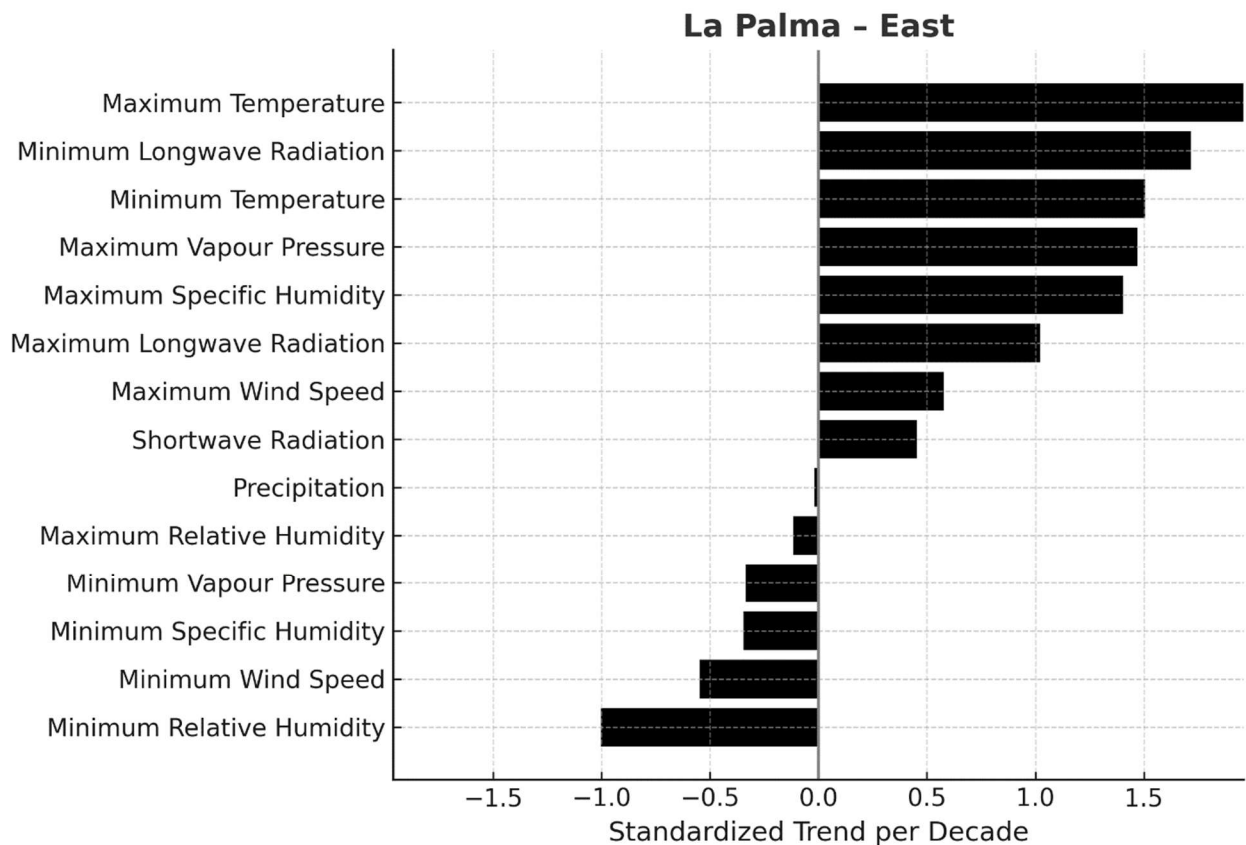


Figure 7: Eastern La Palma – Normalized Trends

The normalized trends in East of La Palma highlight temperature as the dominant change, much like at the summit. The maximum temperature trend is the most significant in relative terms (normalized ~ 1.96 – the highest among variables). This underscores that the warming of daytime temperatures on the east slope is a standout change. The minimum temperature trend (normalized ~ 1.51) is also large but not as extreme as the maximum. Among moisture variables, maximum specific humidity and maximum vapour pressure have high normalized increases (around 1.4–1.5), reflecting that even a small absolute increase is large compared to their variability.

Conversely, precipitation has one of the smallest normalized trends (~ -0.019), indicating essentially no substantial change relative to typical fluctuations. A very notable relative decline is in minimum relative humidity, which has a normalized change around -1.00 . This suggests that the drop in afternoon relative humidity is highly significant compared to historical variability – midday dryness on the east side is a much more pronounced phenomenon now. The wind changes have moderate normalized values, indicating smaller significance relative to variability.

Summarizing, the east interior’s climate has been most altered by heat and aridity. The strongest signals are the rise in temperature and the decline in relative humidity at minimum, both of which can exacerbate evapotranspiration and drying.

Temperature and Radiation:

The East of La Palma show climate trends similar in direction to the summits, with strong warming evident. The maximum daily temperature has been rising at roughly $+1.99\text{ }^{\circ}\text{C}$ per decade ($p < 0.05$). This nearly $2\text{ }^{\circ}\text{C}/\text{decade}$ rate of increase is comparable to the summit warming and is highly significant. Minimum temperatures have increased by about $+0.61\text{ }^{\circ}\text{C}/\text{decade}$, indicating warmer nights but a smaller trend than daytime highs.

Consequently, the diurnal temperature range on the eastern slopes has expanded. The warming is accompanied by changes in radiation: longwave radiation has increased consistently (on the order of $+4.1\text{ W}/\text{m}^2$ in daily maximum, $+4.6\text{ W}/\text{m}^2$ in minimum, per decade), reflecting higher temperatures and possibly a decrease in cloud cover. Shortwave solar radiation has a more noticeable positive trend here than at the summit, approximately $+0.33\text{ W}/\text{m}^2$ per decade increase in integrated shortwave flux. This suggests a modest reduction in cloudiness or dust on the east side, leading to greater sunshine over time. All these trends are significant at $p\text{-value} < 0.05$.

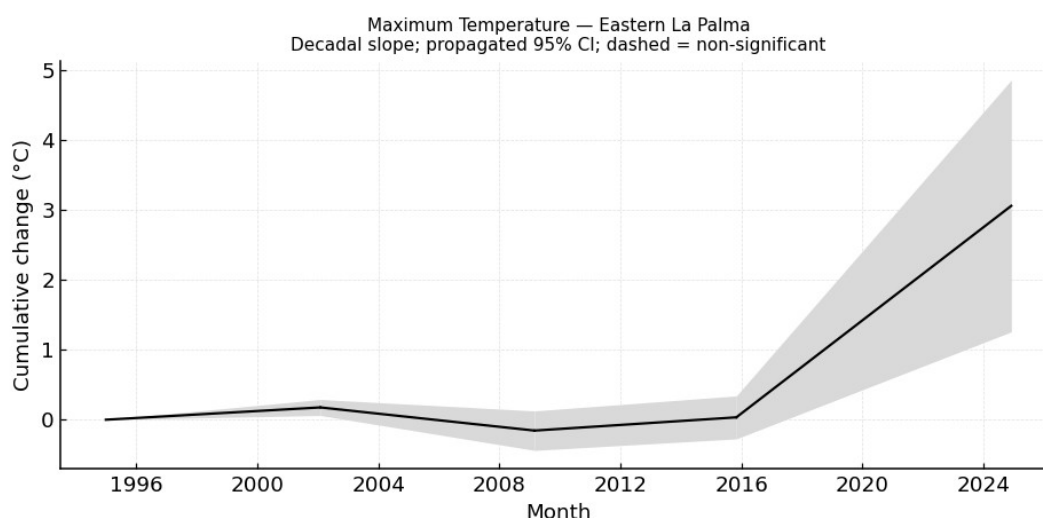


Figure 8: Maximum Temperature Trend – Eastern La Palma

Humidity and Precipitation:

Warming on the east side is likewise altering humidity. The trend in monthly maximum specific humidity is about $+0.000462\text{ kg}/\text{kg}$ per decade ($\sim 0.46\text{ g}/\text{kg}$ per decade). This indicates that the air is carrying more water vapour when it's near saturation. However, specific humidity at the driest time of day shows a slight decline (approximately $-0.000086\text{ kg}/\text{kg}$ per decade). Thus, as with the summit, the absolute humidity is up in moist periods and down during the driest periods.

The effect on relative humidity is more pronounced because of the warming. The minimum relative humidity on the eastern area has dropped significantly by roughly -2.9% per decade ($p < 0.05$). In contrast, maximum relative humidity has a very slight negative trend of about -0.08% /decade. This small decline suggests that even the most humid periods have become just a touch less humid in relative terms, unlike the highlands. Taken together, the eastern interior atmosphere is absolutely moister with higher specific humidity when warm, but relatively during the heat of the day due to the larger capacity of warmer air to hold moisture.

Meanwhile, the total precipitation in Eastern La Palma has a slight downward trend. The weighted trend indicates a decrease of about -1.10 mm per decade in monthly rainfall. This

is a negligible change relative to normal rainfall variability (normalized trend ~ -0.019). In practical terms, annual rainfall on the eastern slopes has not dramatically changed, there is no strong long-term loss of rainfall, only a hint of a decline. Indeed, the east side remains one of the wetter parts of the island, but it appears slightly drier on average than a few decades ago. Importantly, rainfall variability dominates, the region still experiences very wet years and dry years, and the minor negative trend does not override that natural variability. Nonetheless, subtle shifts in rainfall timing or intensity could be occurring, even if the total amount hasn't changed much.

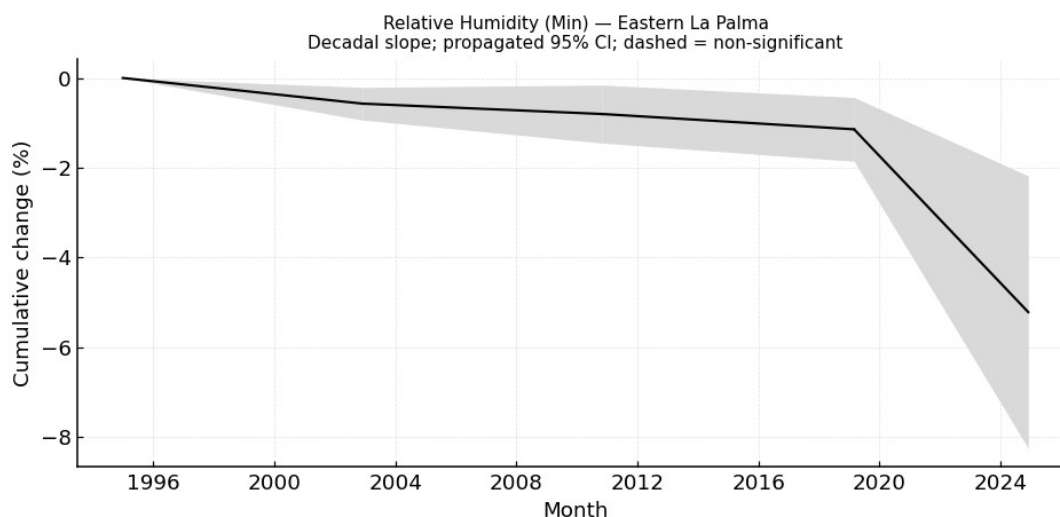


Figure 9: Minimum Relative Humidity Trend - La Palma Highlands

Wind and Vapour Pressure:

The east shows moderate changes in wind behavior. Peak wind speeds have increased on average (~ 0.31 m/s per decade for daily maximum wind speed, p -value < 0.05). Strong daytime upslope winds or trade-wind bursts may be a bit stronger now than in the past. On the other hand, minimum wind speeds have decreased by about -0.11 m/s per decade, indicating that the calmest periods (often nighttime when winds slacken on slopes) are even calmer. This could reflect reduced nighttime thermal contrasts leading to weaker downslope flows, or simply that while daytime winds intensified, nights remained unchanged, effectively lowering the minimum. The result is an increased daily wind range: breezier highs and very low lows (almost stagnant air at times in the night/morning). The trends in wind are relatively small in absolute terms but consistent with a regime of stronger diurnal circulation under warming. In terms of atmospheric moisture, vapour pressure changes mirror those in temperature and specific humidity. The maximum vapour pressure (proxy for water vapour content at saturation times) has risen by ~ 70 Pa per decade (~ 0.70 hPa). With warmer air, the partial pressure of water vapour in morning air has climbed (indicative of higher dew points and more humid air masses when clouds/fog form). Meanwhile, the minimum vapour pressure (during the driest, hottest period each day) has fallen by about -12.8 Pa/decade. This absolute drop in low-end moisture further confirms that the driest air is drier now than before. So, despite overall more water vapour in the atmosphere, the driest conditions strip out more of that moisture by afternoon. In summary, the east interior's air has a higher moisture capacity and achieves higher vapour

pressures at night, but warm afternoons yield very low humidity and vapour pressure, contributing to a drying stress on vegetation during those hours.

Temporal Breakpoints:

The eastern interior climate history also shows distinct phases. Around the early 2000s, there was a pivot in temperature and precipitation trends. In fact, segmented analysis for East of La Palma indicates a slight cooling or stable period in the 2000s before the recent sharp warming. Specifically, from about 2002 to 2009, the trend in maximum temperature was actually slightly negative (on the order of $-0.47\text{ }^{\circ}\text{C/decade}$), suggesting a lull or cooling during that interval. However, after 2009 the trend turned positive, and after 2015 it surged. The most dramatic breakpoint is again around 2015: post-2015, the warming rate of maximum temperature jumps to $\sim 3.33\text{ }^{\circ}\text{C/decade}$. In other words, nearly all the net warming in the record has occurred since about 2010, with an especially steep climb in the last decade. This mirrors the Cumbres region and likely relates to large-scale climate warming and possibly local feedbacks (e.g. reduced cloud cover amplifying heating on the east slopes after 2015). For precipitation, the breakpoints align with shifts between wet and dry spells. From 1995 to 2003, the eastern interior actually experienced a wetting trend (segment shows $+1.05\text{ mm/decade}$ in monthly rainfall) – this was a relatively wet period culminating in the early 2000s. A break in 2003 ushered in a drying trend: roughly 2003–2010 saw a substantial decrease in precipitation (segment $\sim -3.61\text{ mm/decade}$). This corresponds to the well-known mid-2000s drought period. Another breakpoint around 2010 then marks a recovery – from 2010 to 2019, precipitation trended up again ($+0.67\text{ mm/decade}$, indicating some wetter years in the 2010s). Finally, after 2019, the trend turns downward once more (estimated $\sim -2.65\text{ mm/decade}$ in 2019–2024 segment), consistent with a return to drier conditions in the very recent years. These alternating segments reveal that eastern La Palma's rainfall is characterized by multi-decade oscillations – a wet late-90s, dry mid-2000s, moderately wet mid-2010s, then a dry turn by the end of the 2010s. Relative humidity and wind show breakpoints that coincide with these periods (for instance, relative humidity_{min} drop accelerated after ~ 2010 , and wind speeds increased more post-2010), suggesting that the climate regime shifts (wet vs dry periods) also affect cloud cover and circulation. In summary, key breakpoints for East of La Palma occur around 2003, 2010, and 2015. The decade ~ 2003 marks the end of a wet era and the start of a drying one, ~ 2010 marks a transition towards wetter conditions (and the beginning of accelerated warming), and ~ 2015 marks a dramatic jump in warming rate and a swing back towards drier conditions.

Evapotranspiration and Drought:

The water balance on the east side is heavily influenced by its higher rainfall and cloud drip, but even here, warming has increased evaporative demand. Potential evapotranspiration has risen with temperature, meaning the atmosphere tends to evaporate more water. The actual water loss, AET, depends on moisture supply. The east generally receives more rainfall and moisture than other subregions, so it often has abundant AET. In fact, there are times when AET equals or even exceeds PET on the east side, indicating very wet conditions where soils are saturated. For example, in July 2020, an anomalously wet month for the east, the data suggest AET $\sim 300.8\text{ mm}$ and PET $\sim 285.5\text{ mm}$. This can happen in short periods if rainfall is high. Nonetheless, during prolonged dry periods, the east side also

experiences deficits. The SPEI drought indices show that in the east the long-term drought indices are a bit less extreme than drier areas, but it still undergoes drought cycles.

During the severe 2019–2020 episode, SPEI-3 dropped to around -1.1 in mid-2020, indicating a sharp short-term drought. The 24-month SPEI on the east at that same time was about -0.8 , which signifies a moderate long-term drought but notably less severe than the summit or west side. This suggests that while 2019–2020 was dry, the eastern slopes might have retained some moisture, mitigating the two-decade cumulative drought impact to some degree. Still, earlier droughts have hit hard, the 2003–2004 drought, for instance, was island-wide. In early 2004, eastern SPEI would likewise have been strongly negative (records show island-wide SPEI-12 near -1 in 2004). Similarly, the 2011–2012 period and 2016–2017 saw below-normal rainfall and negative SPEI on the east, with SPEI-12 dipping below -1 at times, indicating moderate drought.

Thus, drought evolution on the east side reflects its pattern of wet and dry phases – after 2003, a multi-decade drought persisted until ~ 2008 , then relief, then another dry period late 2010s. Despite higher average moisture, warming has increased PET demand here as well, which means that even normal rainfall now more quickly translates into water stress. The result is that forests and crops on the east face higher evaporative losses. The overall SPEI trend might be slightly downward, towards more frequent mild drought, but mostly the record shows oscillations.

In conclusion, Eastern La Palma remains the more humid interior region, and can often satisfy evaporative demand. Yet, during major droughts like 2020, it is not spared: SPEI indices confirm significant drought occurrences, though the long-term severity (SPEI-24 ~ -0.8 in 2020) was a bit less extreme than in the summit or west (which hit ~ -1.3). This resilience is likely due to the climatological surplus moisture on the windward side, but as climate warms, even this surplus can be depleted in extended dry spells, signaling a need for continued monitoring of water resources and ecosystem health on La Palma's east flank.

Western La Palma

Comparison of the trend between climate variables:

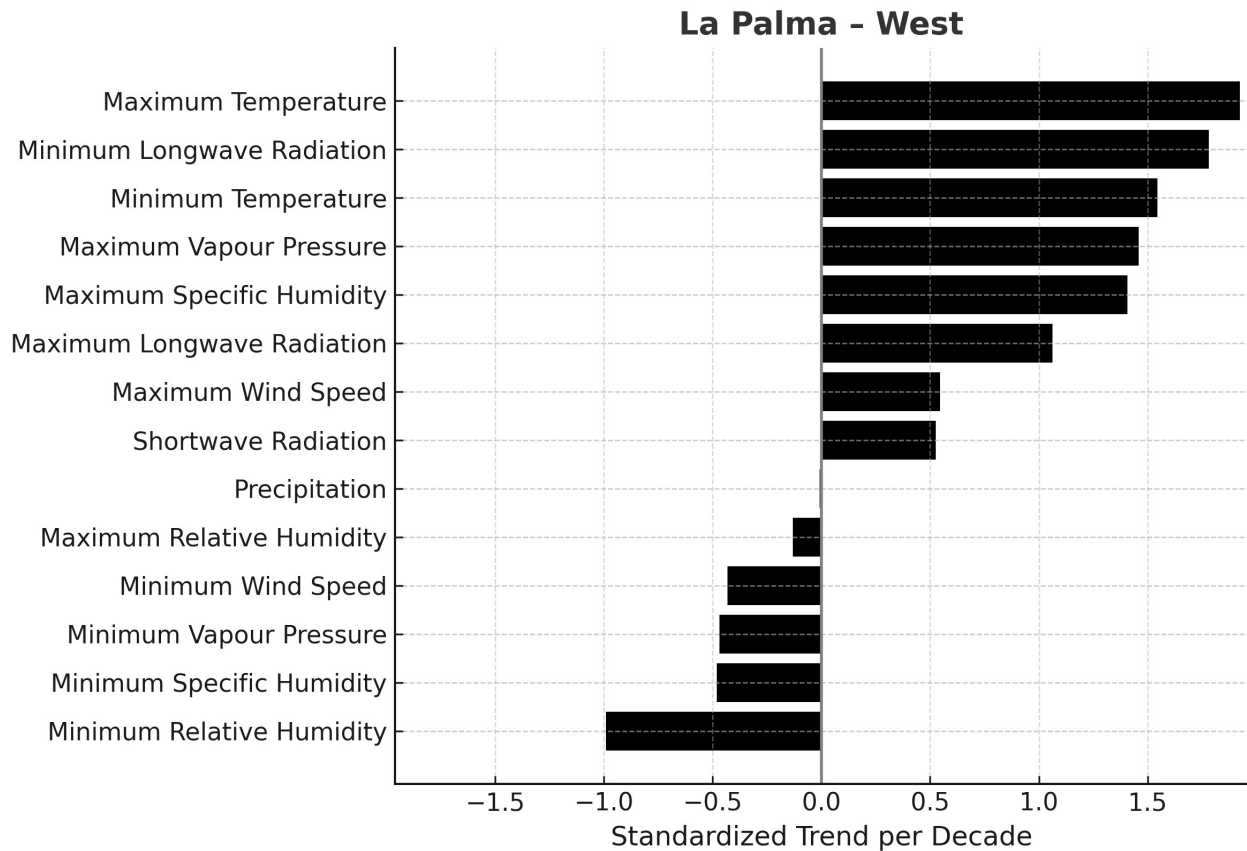


Figure 10: Western La Palma – Normalized Trends

The west interior’s normalized trends underscore the dominance of warming. The maximum temperature trend has a normalized magnitude of ~ 1.92 , which is the highest positive change among variables. This indicates the warming of daytime high temperatures is a very significant change, outpacing the variability of that metric historically. The minimum temperature is also high (~ 1.55), showing nights warming considerably relative to their past variability.

On the moisture front, maximum specific humidity and maximum vapour pressure have normalized trends around 1.4–1.46, again highlighting increased moisture capacity, though note that in absolute terms the west is still drier than the east. Minimum relative humidity on the west has one of the largest negative normalized shifts (approximately -0.99 to -1.0). This means the proportional drop is about as extreme, relative to variability, as the warming of temperatures. Indeed, midday relative humidity was already low and has become markedly lower, a big relative change for the west’s microclimate.

Precipitation’s normalized trend (~ -0.0096) is negligible, reiterating that rainfall changes are minimal in context. Maximum wind has a moderate normalized increase (~ 0.545) and minimum wind exhibits a similar magnitude decrease (~ -0.432), indicating these are smaller signals. The clear takeaway is that heat and aridity have surged: the western interior is considerably hotter and relatively drier, with those two variables showing the strongest normalized departures. These shifts likely exacerbate the west side’s naturally water-limited environment, making it even more extreme compared to historical norms.

Temperature and Radiation:

The west of La Palma has undergone a warming trajectory much like the rest of the island's highlands. Maximum temperatures have risen by about $+2.0\text{ }^{\circ}\text{C}$ per decade ($p\text{-value} < 0.05$), essentially indistinguishable from the rates seen in the east and summit regions. This robust warming of daytime highs is a dominant feature of the western interior climate trend. Minimum temperatures are up roughly $+0.64\text{ }^{\circ}\text{C}/\text{decade}$, indicating significantly warmer nights as well, though again, less than the daytime increase.

This warming is associated with changes in radiative fluxes: the longwave radiation reaching the surface and emitted from it has increased (daily maximum longwave by $\sim 4.76\text{ W}/\text{m}^2$ per decade, minimum longwave by $\sim 5.03\text{ W}/\text{m}^2$ per decade). The western slopes, being leeward, typically have clear skies. The observed longwave gains likely reflect rising surface temperatures and possibly slightly reduced cloud cover at night. Shortwave radiation has increased notably on the west side, about $+0.34\text{ W}/\text{m}^2$ per decade in integrated incoming solar flux. This is a relatively large increase in sun exposure, consistent with a trend towards fewer clouds or dust on the west, the already sunnier side of the island. In fact, the normalized shortwave trend on the west is one of the highest among radiative variables (shortwave flux normalized trend ~ 0.53). Together, these indicate the west side is getting hotter and somewhat drier. All temperature and radiation trends are significant at $p\text{-value} < 0.05$, underscoring a confidently detected change.

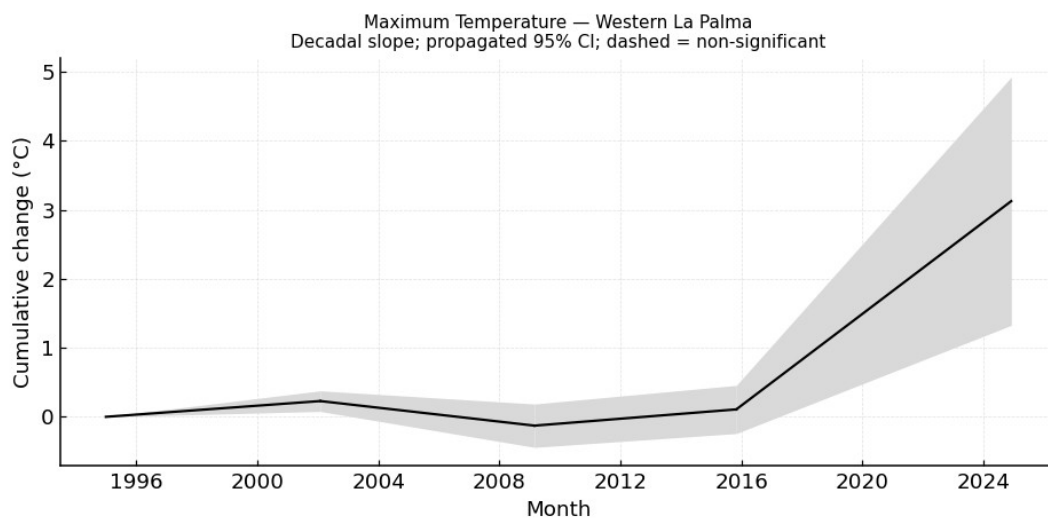


Figure 11: Maximum Temperature Trend – Western La Palma

Humidity and Precipitation:

The west, historically the drier side, shows a pronounced drying in relative terms under the warming climate. Maximum specific humidity has increased by $\sim 0.000460\text{ kg}/\text{kg}$ per decade ($\sim 0.46\text{ g}/\text{kg}$), nearly identical to the rises seen elsewhere – a warmer atmosphere holding more vapour at saturation times. Meanwhile minimum specific humidity has decreased $\sim -0.000112\text{ kg}/\text{kg}$ per decade. Thus, as on the other slopes, absolute humidity is up during humid periods and down during the driest periods. For the west side, which is

generally drier, this translates to very low absolute humidity at midday in recent years. Relative humidity changes are stark, its minimum has been dropping by about -3.0% per decade, and this is a slightly larger decline than on the east, reflecting that already dry afternoons are becoming even drier. This means if typical minimum was $\sim 20\%$ some decades ago, it is on the order of $14\text{--}15\%$ now. The maximum relative humidity on the west has a small negative trend ($\sim -0.09\%/decade$), similar to the east in sign and magnitude. In essence, the west's daily now ranges from slightly lower highs to much lower lows. The much drier days could influence wildfire risk and plant stress, given how low it can get.

Precipitation on the west is relatively scarce climatologically, and the trend indicates a minor further reduction. The weighted trend is around -0.60 mm per decade in monthly precipitation, which is very small in absolute terms (on an annual basis, perhaps ~ 7 mm less per decade). Normalized, this is ~ -0.0096 , effectively no significant change relative to variability with $p\text{-value} < 0.05$. Thus, the total rainfall hasn't significantly changed. Western La Palma still gets roughly the same low amounts of rain, with high interannual variability. All said, the west interior remains the driest subregion, and trends show it becoming even drier in terms of humidity and rainfall.

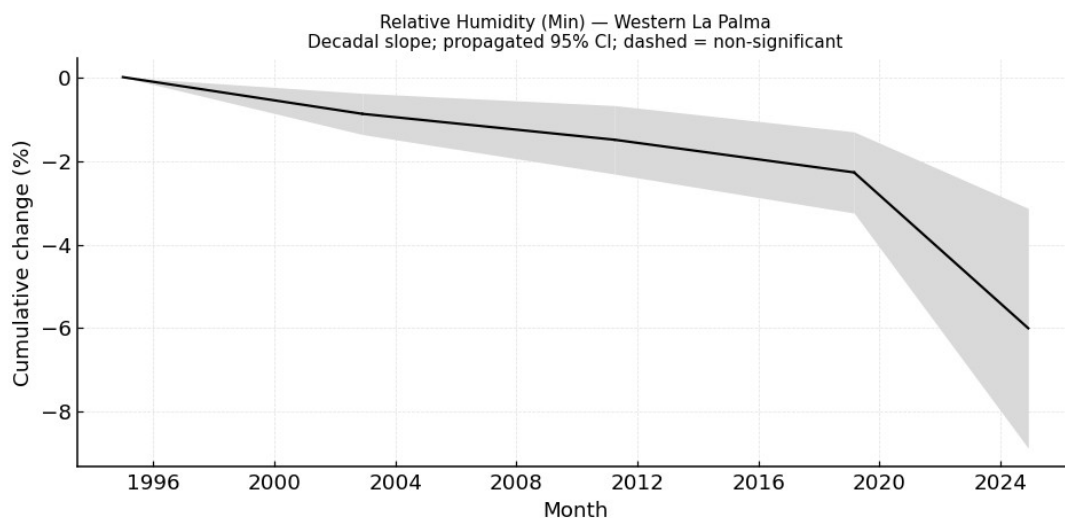


Figure 12: Minimum Relative Humidity Trend – La Palma Highlands

Wind and Vapour Pressure:

Wind trends on the west side show enhanced windiness in peak periods. The maximum wind speed has risen by approximately $+0.29$ m/s per decade. The minimum wind speeds have decreased (~ -0.084 m/s per decade), meaning very calm conditions are a bit more frequent. In the west's valleys and lee slopes, nights can be extremely still, this trend implies nights might be slightly more stagnant now.

The water vapour dynamics align with the warming and drying: maximum vapour pressure has increased by about $+69$ Pa per decade (~ 0.69 hPa), in line with warming-induced moisture capacity gains. This is the extra vapour in the air during humid periods (e.g. early morning). On the flip side, minimum vapour pressure has dropped by roughly -16.7 Pa/decade. That corresponds to ~ 0.167 hPa less at the driest times, which is significant given how low those values already are. Thus, the west interior is seeing conditions that

favor more intense drying: stronger sun and wind by day, lower humidity, and greater atmospheric demand.

Temporal Breakpoints:

The climate timeline of the west interior features similar phase changes to the rest of La Palma, with some nuances due to its aridity. Around 2002–2003, there was a transition from an earlier wet phase to a dry phase, mirroring the island-wide 2000s drought.

Pre-2003, there is evidence the west might have had slightly increasing rainfall or at least no decline. Indeed, one segment from 1995–2003 shows a robust positive precip trend in the west. After 2003, a pronounced drying is observed. Segmented data for Western La Palma show a precipitation decline from 2003 to 2010 on the order of -3.44 mm/decade, similar to the east side. Then about 2010 there is a breakpoint where precipitation trends upward again through 2019 ($+1.06$ mm/decade in 2010–2019 segment), and a subsequent downturn after 2019 (segment ~ -1.69 mm/decade). These align with known drought periods: mid-2000s dry, early-mid 2010s some recovery, late 2010s dry again.

Temperature on the west side followed a comparable pattern of breakpoints. During 2002–2009, the west interior saw a flat or slight cooling trend in temperatures (one segment has ~ -0.50 °C/decade for maximum temperature during 2002–2009). After the 2009–2010 break, warming resumes, and after 2015 it accelerates steeply. In the data, from 2015 onward the maximum temperature trend is ~ 3.32 °C/decade, virtually identical to the east side's post-2015 surge. This indicates a synchronous response across the island, after 2015, all subregions warmed very rapidly.

The west's minimum relative humidity trend became more negative after 2010 as well, consistent with the notion that after the 2009 breakpoint, when warming picked up and rainfall was still recovering, the drying effect on humidity took hold.

In summary, key breakpoints for Western La Palma occur around 2003, 2010, and 2015. Around 2003 the regime shifted to drier and eventually less cloudy, by 2010 things momentarily improved rainfall-wise but warming started to dominate, and by 2015 the warming dominated overwhelmingly, pushing the climate to new extremes. The period since ~ 2019 appears to be a continuation of the high-temperature, low-rainfall regime, essentially a return of severe drought conditions. These changes are consistent with broader shifts observed in the Canary Islands and Northeast Atlantic climate around those times.

Evapotranspiration and Drought:

The western interior is particularly prone to water stress, and the data show increasing evaporative demand exacerbating that stress. Potential ET has risen with the strong increase in solar radiation and temperature on the west side, meaning the already high demand for moisture in this semi-arid region is now even higher. However, actual rainfall has not increased to compensate, so Actual ET is often limited by lack of water. Indeed, unlike the east side, the west interior rarely if ever sees AET meet PET for extended periods, moisture is the limiting factor. During rare wetter episodes, AET will increase, but those are exceptions.

A clear example of drought impact is the period of 2019–2020. By July 2020, SPEI-24 on the west interior had fallen to about -1.3 , a level indicating a substantial cumulative rainfall deficit over two years. At the same time, SPEI-3 was around -1.25 and SPEI-12 ~ -1.03 , revealing that short-term and one-decade drought metrics were also in the moderate to severe range. This quantifies the multi-decade drought that severely affected La Palma in that timeframe. West side vegetation likely experienced significant stress then. Another severe drought in the record for the west was 2008-09 and 2011-12. The segmented analysis already noted post-2019 drying, indeed late 2020 into 2021 SPEI remained very low (SPEI-24 ~ -1.3 to -1.5 through 2021, similar to the summit).

The west AET in such times plummets. For instance, in a dry winter month (Dec 2020), AET was only ~ 30 – 50 mm regionally, whereas PET was much higher ($\sim 80+$ mm), a clear moisture shortfall. Conversely, during a somewhat wetter winter month, AET might rise but is still capped by the modest rainfall. Cloud cover is also pertinent, the west side depends less on horizontal precipitation than the east, so it doesn't have that auxiliary water source. With the observed increase in sunshine, there's even less fog to moisten the west. Consequently, drought indices on the west respond mostly to rain shortages and high PET.

Over the decades, it is possible to infer an overall drift towards more arid conditions, even if rainfall stayed roughly the same, PET increases mean effective aridity is worse. The trend in SPEI would thus be downward, though it's punctuated by variability. Notably, the west interior was one of the areas showing the strongest recent drought signals in the Canary Islands. The period ~ 2012 – 2017 had recurrent rainfall deficits (with SPEI-12 oscillating below zero frequently), culminating in the extreme 2020 drought.

In practical terms, what the data and trends illustrate is that the west side's water balance is increasingly strained. When rains fail, soil moisture depletes faster now due to higher evaporative demand. In the 1990s, a dry winter might have caused moderate stress, but under today's warmer conditions, a similar rainfall deficit produces more severe SPEI drops. Indeed, during late 2020–2021, the combination of persistent low rain and high PET gave one of the worst multi-decade droughts on record for west La Palma (SPEI-24 ~ -1.5).

Looking forward, unless rainfall increases, the west will likely experience more frequent drought conditions because the baseline PET is higher. Overall, the drought indices confirm the increasing drought intensity: where once a 2-decade drought might have been SPEI ~ -1 , now we are seeing ~ -1.3 to -1.5 for comparable rainfall shortages. This places ecosystems and water resources under greater pressure. The west side, being already marginal for agriculture without irrigation, will face heightened challenges as temperatures continue to rise. In conclusion, while the total precipitation hasn't plummeted, the combination of increased heat, slightly less humidity, and unchanged low rainfall means that the western interior of La Palma is more drought-prone now than a few decades ago, with recent SPEI data capturing some of the most severe dry episodes in the observational record.

3.1.2 Gran Canaria

Gran Canaria Highlands

Comparison of the trend between climate variables:

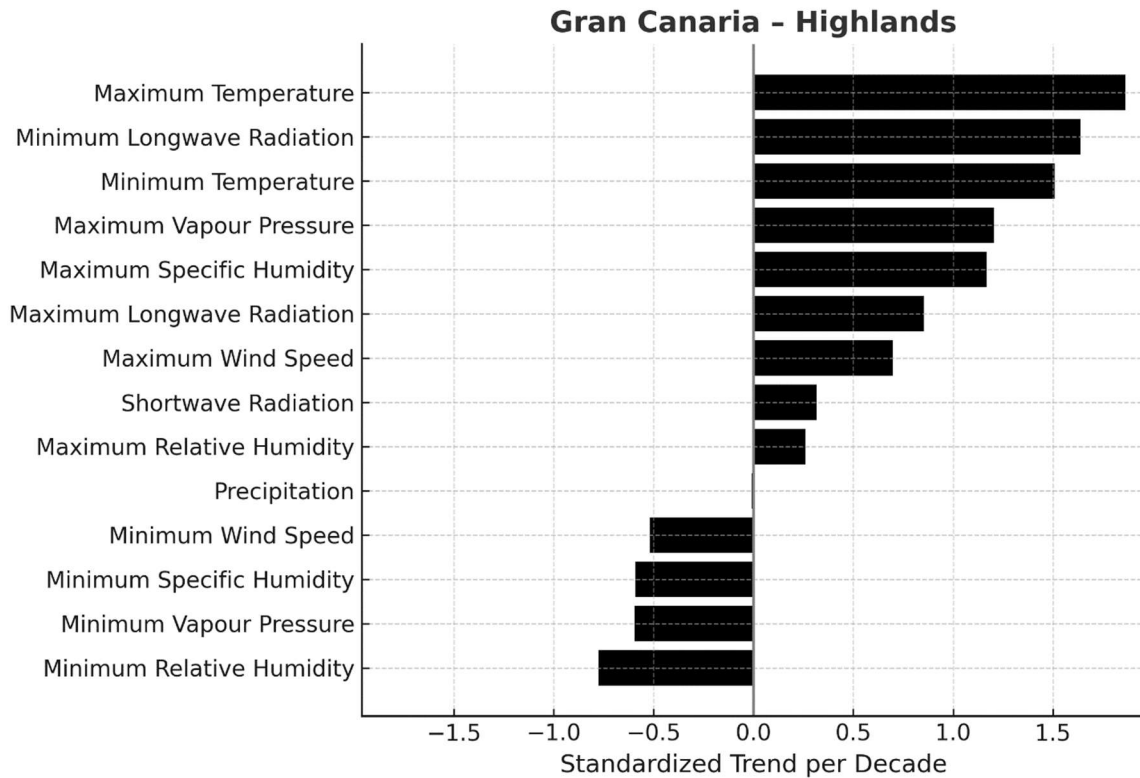


Figure 13: Gran Canaria Highlands – Normalized Trends

Normalized trends in the highlands underscore a clear dominance of warming. Maximum temperature shows one of the strongest positive normalized changes on the island (~1.86), while minimum temperature also exhibits a substantial rise (~1.51). This indicates that both daytime and nighttime temperatures have warmed significantly, although the increase in daytime highs remains more pronounced. Longwave radiation, both maximum and minimum, presents large positive normalized changes (~0.85 to +1.64), confirming a steady rise in the surface energy balance consistent with a warmer atmosphere and enhanced greenhouse trapping.

On the moisture side, Maximum Specific Humidity and Maximum Vapour Pressure show normalized increases of ~1.17 and +1.21, reflecting the greater capacity of warmer air to hold water vapour. Yet, the contrast between humid and dry periods has widened sharply: Minimum Relative humidity presents one of the strongest normalized decreases (~-0.78), accompanied by declines in minimum specific humidity (~-0.59) and minimum vapour pressure (~-0.59). These negative signals indicate that although moist conditions are slightly more humid, dry hours have become markedly drier. Precipitation shows a near-zero normalized change (~-0.008), suggesting that rainfall has not compensated for the increased evaporative demand. Wind speed patterns reveal a mild strengthening of

daytime winds and weaker nocturnal breezes, but these effects are secondary compared with the dominant warming, these are drying signals. Overall, the highlands have transitioned towards hotter, sunnier, and drier conditions, with pronounced atmospheric desiccation during the daytime.

Temperature and radiation:

The high-altitude areas of Gran Canaria has experienced significant warming over the 1995–2024 period. Maximum temperature rose by approximately +1.9 °C in total (~0.6 °C/decade, p-value < 0.05), whereas minimum temperature increased by only +0.7 °C (~0.2 °C/decade) over the same period. This widening day–night temperature gap suggests stronger daytime heating with only modest nocturnal warming. Consistent with this, shortwave radiation has increased slightly (+0.2 W/m² total change, p-value < 0.05), indicating somewhat sunnier days. Downwelling longwave radiation has risen by about +5 W/m² at night and +4 W/m² during the day (p-value < 0.05), consistent with a warmer atmosphere and enhanced greenhouse effect over the highlands.

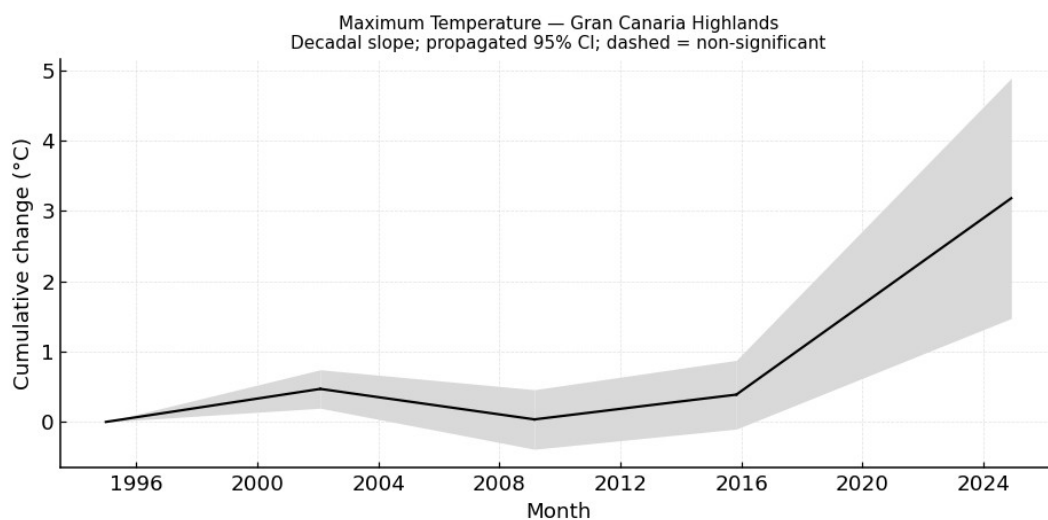


Figure 14: Maximum Temperature Trend – Gran Canaria Highlands

Humidity and vapour pressure:

Marked drying accompanied the warming in this region. Minimum relative humidity declined significantly, decreasing by about –1.7% over 30 years (p < 0.05). Although the absolute drop is modest (from roughly 16% to 14% on average), it reflects increased aridity during peak heating hours. By contrast, maximum relative humidity changed little (+0.3% total) and remains near saturation on many nights. In terms of absolute moisture, specific humidity shows a diverging trend: maximum specific humidity increased slightly (approximately +0.46 g/kg, p-value < 0.05), while minimum specific humidity decreased (~–0.14 g/kg, p < 0.05). This indicates that warmer air is holding more moisture at night/morning, but midday air is even drier than before. Consistently, vapour pressure during humid periods has climbed (maximum +0.66 hPa ~ 0.00066 bar, p < 0.05), whereas

the minimum vapour pressure attained has dropped by roughly -0.20 hPa (~ -0.00020 bar) — drier lows.

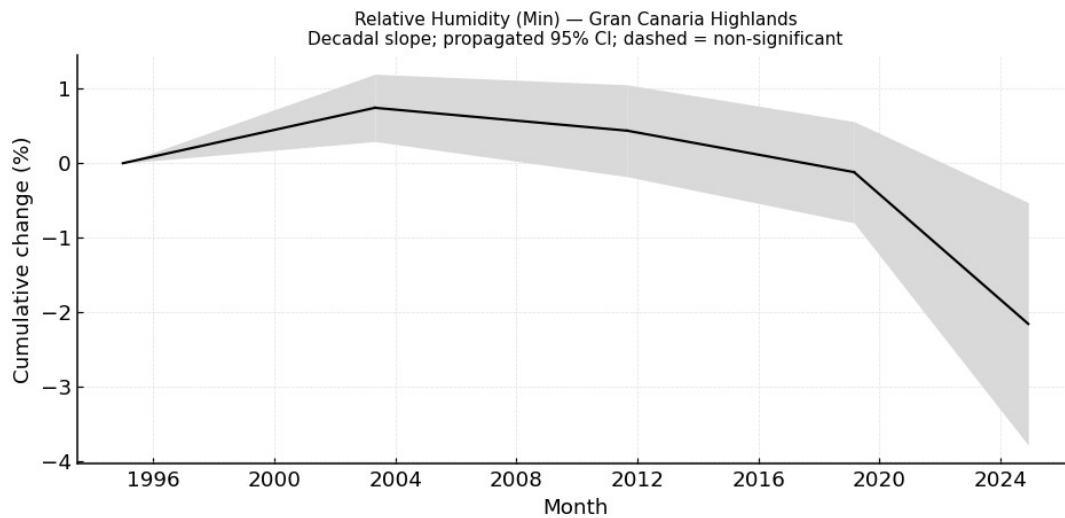


Figure 15: Minimum Relative Humidity Trend – Gran Canaria Highlands

Precipitation and wind:

Total precipitation in Gran Canaria's Highlands shows a slight downward trend. Annual rainfall accumulation has decreased by only on the order of 20 mm over the 30-decade study, a few percent of the long-term mean, a small but statistically significant decline (p -value < 0.05). This suggests marginally drier conditions overall, in line with the observed increase in aridity indices.

Wind patterns have shifted towards greater extremes: maximum wind speed has risen by about $+0.5$ m/s ($p < 0.05$) compared to the mid-1990s, while minimum wind speed has become ~ -0.1 m/s slower. In effect, daytime upslope winds or storm gusts are slightly stronger, whereas nighttime conditions are more stagnant.

Evapotranspiration trends and breakpoints:

Actual evapotranspiration (AET) in the highlands initially increased with warming, then underwent a notable inflection in the mid-2010s. Segmented trend analysis reveals that from 2000 up to around 2012 AET was rising rapidly (approximately $+82$ mm/decade; $p < 0.05$), likely as warmer temperatures and adequate moisture boosted evaporation and plant transpiration. However, a clear breakpoint occurred around 2012–2013, after which AET trends leveled off and eventually reversed. From about 2017 onward, AET fell sharply (down by ~ -56 mm/decade during 2017–2019), indicating that severe moisture limitations in recent years curtailed actual evapotranspiration despite the continued warmth.

Potential evapotranspiration (PET) exhibited a similar regime shift. PET climbed steadily in the early 2000s (on the order of $+60$ – 70 mm/decade increase in evaporative demand through 2000–2010), but the trend flattened in the 2010s. After roughly 2016, PET began to decline (turning to about -40 mm/decade after 2016, based on segmented slopes). This

late-period drop in PET suggests that factors such as increased cloud cover or humidity constraints might have started to counteract the rising temperature effect on atmospheric demand. In summary, the interior highland saw a transition from an increasing- evaporative regime to a water-limited regime in the last decade.

Drought index (SPEI) evolution:

Drought indicators for Cumbres de Gran Canaria confirm a shift towards drier conditions. In the early 2000s, the standardized precipitation–evapotranspiration index (SPEI) was generally positive, reflecting wetter-than-normal conditions (e.g., the 12-month SPEI averaged around +0.8 in 2000–2005). By contrast, in the late 2010s the SPEI values became predominantly negative at all timescales, indicating cumulative moisture deficits. Notably, multi-decade drought has intensified: the 24-month SPEI dropped from consistently positive values in the 1990s–2000s to around –0.8 on average during 2017–2021, signifying an accumulated two-decade drought. The period 2017–2019 stands out as an extreme drought episode – the 12-month SPEI plummeted to about –3.1 in early 2019, one of the most severe anomalies on record for this region. Shorter-term drought indices (SPEI-3 and SPEI-6) fluctuated with seasonal rainfall, but likewise show more frequent deep negatives in 2015–2020 (e.g., SPEI-3 reached –2.0 in late 2015). These SPEI trends illustrate that what used to be intermittently wet conditions have given way to prolonged drought periods in the highlands.

Northern Gran Canaria

Comparison of the trend between climate variables:

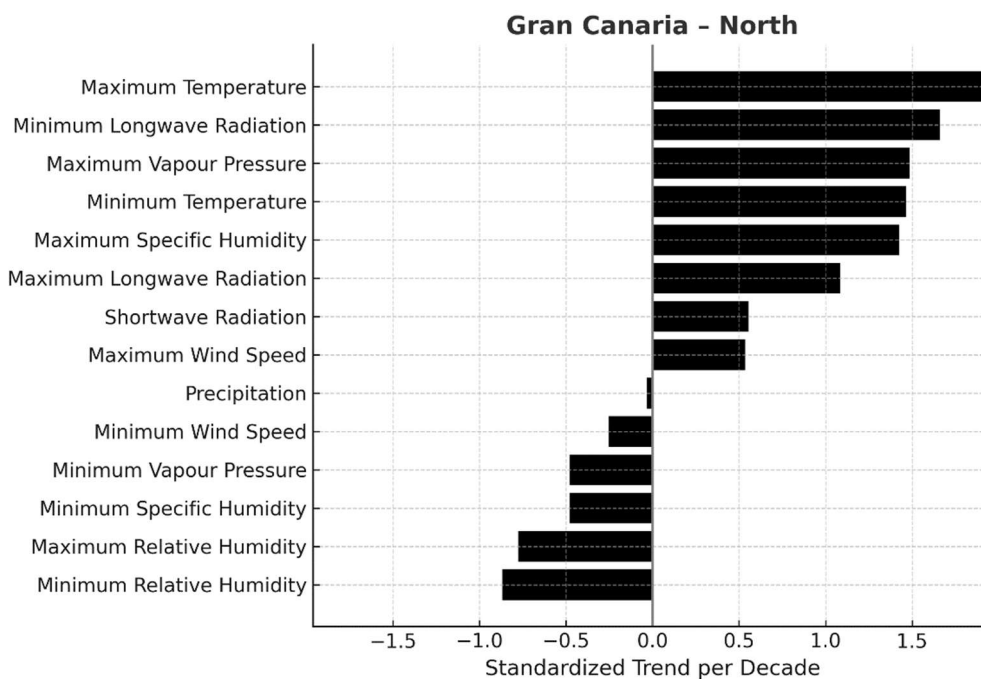


Figure 16: Northern Gran Canaria – Normalized Trends

The northern area exhibits one of the clearest examples of synchronized warming and drying across the island. Maximum temperature presents the highest normalized trend among all variables (~ 1.96), followed closely by minimum temperature (~ 1.48). These magnitudes indicate that the region is warming rapidly both day and night, consistent with increased shortwave and longwave radiation inputs (~ 0.9 to $+1.0$ normalized range).

Moisture-related variables reveal a parallel intensification of aridity. Maximum vapour pressure (~ 1.45) and maximum specific humidity (~ 1.43) both show significant positive changes, pointing to an atmosphere capable of storing more moisture during humid periods. However, minimum relative humidity exhibits the single largest negative normalized shift (-1.00), nearly matching the magnitude of warming in relative terms. Minimum specific humidity (-0.95) and minimum vapour pressure (-0.88) also decline strongly, indicating more pronounced dryness during hot afternoons.

Precipitation shows a normalized change near zero (-0.016), confirming that rainfall reductions are minor compared to interannual variability. Wind extremes show a widening range, slightly stronger maximum winds (~ 0.55 normalized) and calmer minima (-0.55), but these are secondary features. In summary, the north of Gran Canaria has become warmer and considerably drier, with the largest proportional decreases in humidity and the most pronounced increase in daytime heat island-wide. These shifts imply enhanced evaporative stress and recurrent drought risk.

Temperature and radiation:

The northern interior region of Gran Canaria has also undergone significant warming, particularly during daytime. Between 1995 and 2024, the area's maximum temperature rose by roughly $+2.2$ °C (~ 0.7 °C/decade, $p < 0.05$). In contrast, minimum temperature at night increased by only $+0.6$ °C in total (~ 0.2 °C/decade). This disparity indicates an expanding diurnal temperature range, as days get hotter while nights have shown only minor warming. Shortwave radiation increased slightly (on the order of $+0.5$ W/m² over the study period, $p < 0.001$), suggesting a small reduction in cloud cover or haze in the north. Meanwhile, downwelling longwave radiation has risen by around $+3.7$ – 3.8 W/m² ($p < 0.05$), for both daily minima and maxima, consistent with a generally warmer and more radiatively emissive atmosphere over the region.

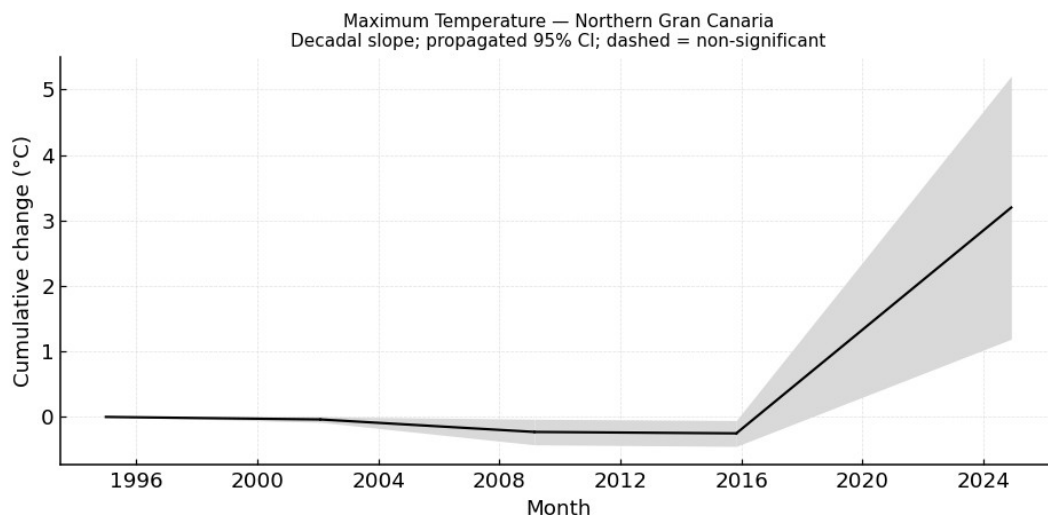


Figure 17: Maximum Temperature Trend – Northern Gran Canaria

Humidity and moisture:

The warming in northern Gran Canaria has been accompanied by a noticeable drying in relative terms. Minimum relative humidity declined significantly – dropping by approximately -3.4 percentage points from 1995 to 2024 ($p < 0.05$). This translates into midday relative humidity falling from roughly the low-30s% to high-20s% on average, indicating drier air during the warmest part of the day. Early morning or nighttime humidity has also slightly decreased (maximum relative humidity trend ~ -0.36 points total, $p < 0.05$), suggesting that even the most humid nights are a bit less humid than before (e.g., reducing from $\sim 85\%$ to $\sim 82\%$ saturation). In terms of absolute moisture, the air's capacity has grown but realized moisture has not kept up during dry times. Specific humidity at saturation (e.g., early morning when humidity peaks) shows a positive but small trend (~ 0.43 g/kg total, though this particular increase was not statistically significant at $p < 0.05$ for this region), whereas specific humidity at the driest time of day has significantly declined (~ -0.16 g/kg, $p < 0.05$). Consequently, vapour pressure has increased slightly at its maximum ($+0.68$ hPa ~ 0.00068 bar, $p < 0.05$), but the lowest daily vapour pressures have fallen (~ -0.24 hPa ~ -0.00024 bar), reinforcing the pattern of drier daytime air despite the warmer climate.

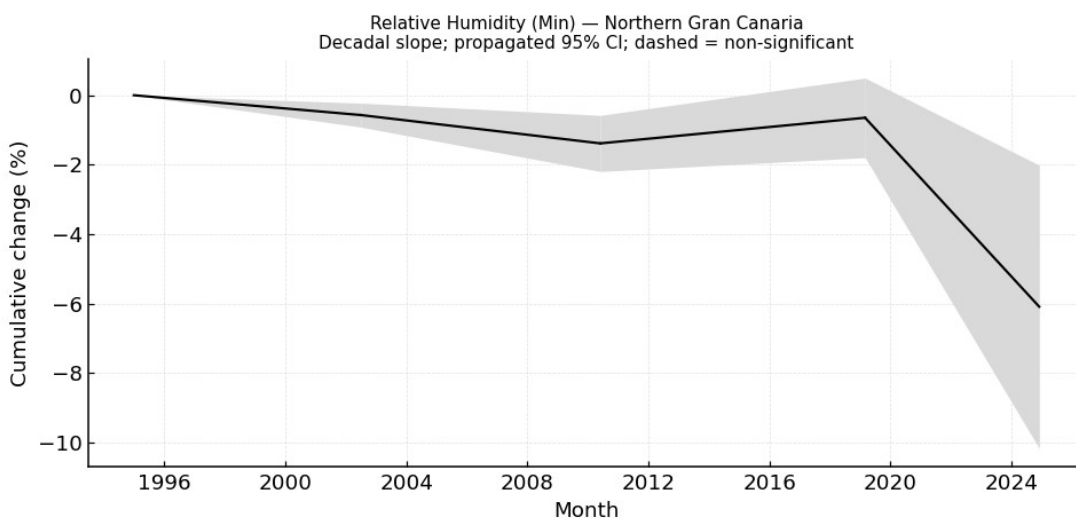


Figure 18: Relative Humidity Trend – Northern Gran Canaria

Precipitation and wind:

Annual precipitation in the north shows a weak downward trend consistent with a drier climate. Cumulative rainfall has diminished by roughly 30–35 mm over the 30-year. While modest in magnitude, this reduction aligns with the decreased humidity and higher evaporative demand observed. Wind speed changes suggest an increase in climate volatility: the highest wind speeds (e.g., during storms or daytime upslope winds) have risen by about $+0.3$ m/s ($p < 0.05$) compared to the 1990s. In contrast, the lowest wind speeds have dropped by roughly -0.07 m/s, indicating slightly calmer minimum conditions. The net effect is a broader range of wind speeds, more intense winds at peak times and very still air at night, which can enhance drying during the day and reduce mixing at night.

Evapotranspiration trends and breakpoints:

Trends in actual and potential evapotranspiration in northern Gran Canaria reflect an early increase in evaporative fluxes followed by a recent downturn associated with drought. From 2000 up to the mid-2010s, AET was generally rising: the first segment of the record (2000–~2005) saw AET increase on the order of +36 mm/decade, and this positive trend persisted at a similar rate through 2016. This implies that, for much of the early 21st century, warmer temperatures and sufficient soil moisture allowed more water to evaporate or transpire. However, a pronounced breakpoint occurred around 2016. After this point, AET trends turned sharply negative, declining at roughly –55 to –60 mm/decade in the late 2010s. In other words, the actual moisture flux from the land surface dropped off steeply as drought set in, despite the continued high potential for evaporation.

PET in this region followed a comparable pattern. During the 2000s, potential evapotranspiration was increasing (initially by ~38 mm/decade early in the decade, then +30 and +18 mm/decade in subsequent segments up to 2018), indicating rising atmospheric demand. But by 2018 a clear reversal is evident: from 2018 onwards PET shows a downward trend (~–36 mm/decade after 2018). This suggests that later in the record, cooler or cloudier conditions associated with drought slightly reduced the potential evaporation rate. Together, these breakpoints signal a shift around 2016–2018 from a warming-driven increasing-evapotranspiration regime to a drought-dominated regime where lack of moisture limits AET and even PET ceases to rise.

Drought index (SPEI) evolution:

The SPEI for the Northern Gran Canaria reinforces the narrative of a trend towards greater drought frequency and severity. In the early 2000s, values at all timescales were mostly positive, for instance, the 12-month SPEI averaged about +0.7 to +0.8, indicative of wetter or normal conditions. Starting in the 2010s, however, the indices display a downward shift. By the late 2010s, the northern interior's SPEI became predominantly negative. The mean 12-month SPEI for 2017–2021 was around –0.6, reflecting a chronic moisture deficit. Notably, the most severe multi-decade drought occurred towards the end of the record: the 24-month SPEI dropped below –1.8 in mid-2019, marking a severe prolonged drought. Shorter-term droughts also became more acute; for example, a sharp summer drought in 2014 pushed the 3-month SPEI down to –2.9 (August 2014), and during the height of the recent drought (early 2019) the 6-month SPEI reached around –3.1, an extreme value. These negative SPEI excursions in the 2010s greatly exceed those earlier in the record, demonstrating that the northern parts of Gran Canaria's interior have entered a period of significantly increased drought risk. The convergence of rising temperature, slightly decreasing rainfall, and high evaporative demand has thus translated into notably drier conditions by the 2020s compared to the relatively wetter baseline of the late 20th century.

East, south and west of Gran Canaria

Comparison of the trend between climate variables:

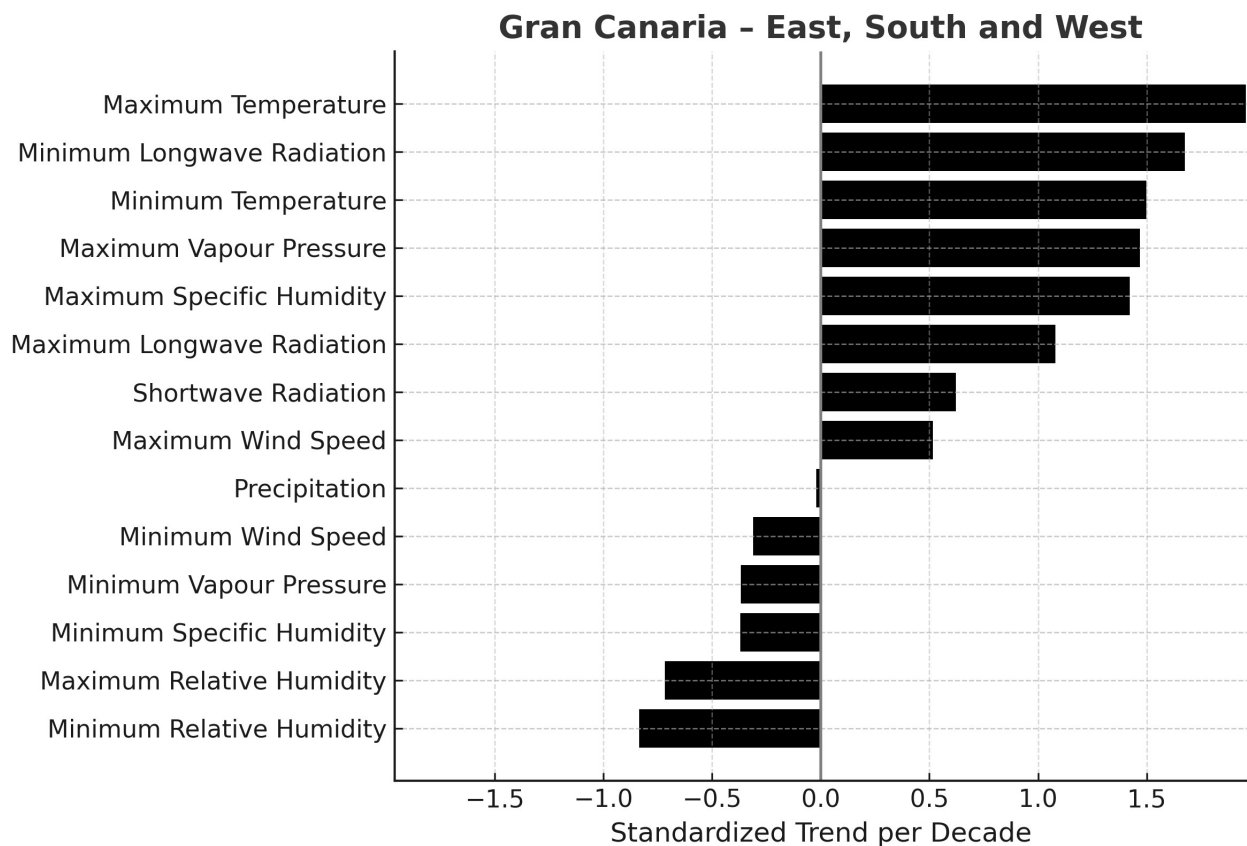


Figure 19: East, South and West of Gran Canaria – Normalized Trends

Across the eastern, southern, and western slopes of Gran Canaria, normalized trends again emphasize the dual rise in temperature and daytime aridity. Maximum temperature shows a normalized increase of ~ 1.92 , the strongest within these lower-elevation interiors, while minimum temperature follows with ~ 1.55 . The thermal signal is reinforced by consistent increases in Longwave Radiation (~ 0.93 to $+0.97$) and moderate gains in shortwave radiation, suggesting a clearer, more irradiated atmosphere.

Moisture indicators mirror the pattern seen elsewhere on the island but with even greater daytime dryness. Maximum Vapour Pressure (~ 1.46) and Maximum Specific Humidity (~ 1.39) both rise, indicating higher potential moisture capacity. However, Minimum Relative humidity records the largest relative decline (~ -1.00), and both Minimum Specific Humidity (~ -0.87) and Minimum Vapour Pressure (~ -0.83) drop sharply. This shows that while the atmosphere can hold more moisture overall, actual air moisture during the driest hours has fallen substantially. Precipitation trends are negligible (~ -0.010 normalized), while wind speed exhibits only minor opposing tendencies (slightly stronger maxima, weaker minima).

Overall, these lowland regions are characterized by intensified heat, lower humidity, and limited rainfall, reflecting the most arid expression of Gran Canaria's climate. The combination of stronger solar input, enhanced potential evaporation, and declining daytime humidity defines a warming-drying transition that is particularly acute in the island's drier flanks.

Temperature and radiation:

This region of Gran Canaria has warmed substantially as well. From 1995 to 2024 the average maximum temperature in this broad interior region climbed by about +2.2 °C (~0.7 °C/decade, $p < 0.05$). Nighttime minimum temperature, however, increased by only roughly +0.6 °C in total, which is a minimal change over 30 years ($p < 0.05$). As a result, diurnal temperature range has grown here, mirroring the pattern in the northern interior: hotter days without much nighttime moderation. Supporting this, there was a slight upward trend in shortwave radiation (~0.4 W/m² overall, $p < 0.05$), consistent with somewhat clearer skies or reduced haze over the east/south interior. Downwelling longwave radiation also increased, by approximately +3.8–3.9 W/m² ($p < 0.05$) for daily minima and maxima, indicating a warmer lower atmosphere across this region.

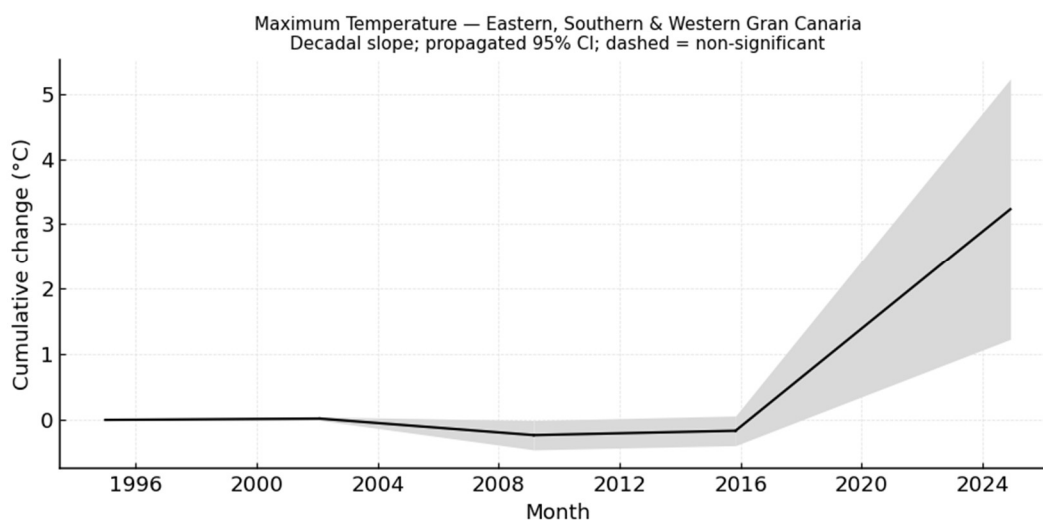


Figure 20: Maximum Temperature Trend – East, south and west of Gran Canaria

Humidity and moisture:

This zone has become drier in tandem with the warming. The driest daytime relative humidity values plummeted significantly — minimum relative humidity declined by around -3.1 percentage points over the study period ($p < 0.01$). Practically, this drop means that midday relative humidity, which averaged in the low 30% range in the 1990s, now more frequently falls into the upper 20% range or lower, enhancing the feeling of aridity during the day. The maximum relative humidity, typically occurring at night or early morning, also shows a slight decrease (~-0.34%, $p < 0.05$). Thus, unlike the highlands where nighttime humidity held steady, even the most humid nights in these lowlands have become a bit drier (e.g., from nearly 90% down to ~85–86% relative humidity at pre-dawn). In absolute terms, specific humidity changes were relatively small and not all were significant. Maximum specific humidity, during moist periods, had a positive but non-significant trend (~0.43 g/kg total increase, but with a not significant p -value ~ 0.11), suggesting a slight rise in the absolute moisture-carrying capacity of the air. Meanwhile, minimum specific humidity saw a significant decline (~-0.12 g/kg, $p < 0.05$), meaning the air's absolute moisture content at the driest time has decreased. Consequently, vapour pressure in high-humidity conditions edged up (~0.67 hPa ~ 0.00067 bar), whereas the lowest vapour

pressures dropped by about -0.18 hPa (~ -0.00018 bar). These changes reinforce a scenario of heightened dryness: the air can hold a bit more moisture in theory due to warmth, but in practice during dry hot afternoons it contains even less moisture than decades ago.

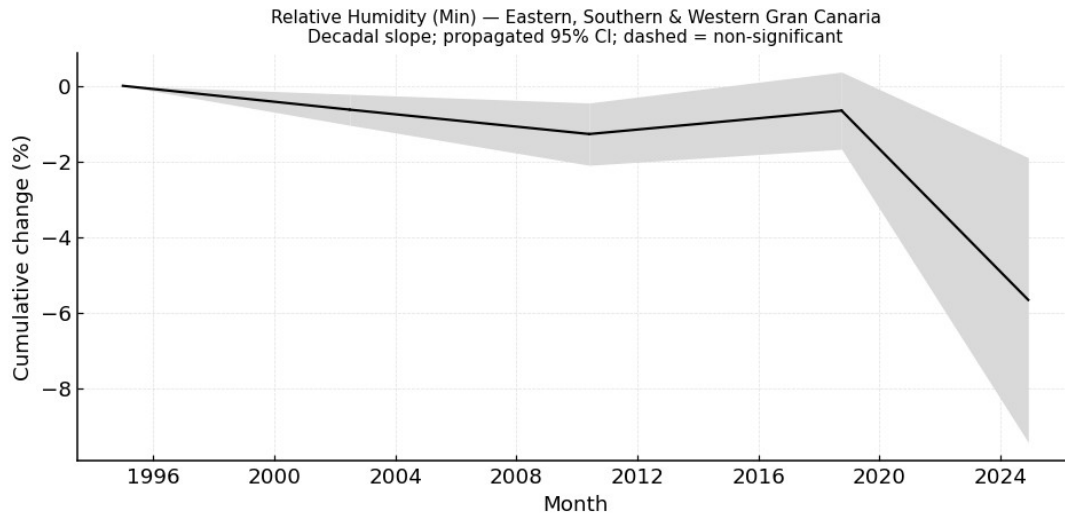


Figure 21: Minimum Relative Humidity Trend – East, south and west of Gran Canaria

Precipitation and wind:

Long-term precipitation in the interior east, south, and west of Gran Canaria has trended downward in line with the archipelago-wide drying. Over 30 years, total annual rainfall in these interior areas decreased by roughly 24 mm ($p < 0.001$), a small but consistent reduction. Given that this region is historically semi-arid (receiving much less rain than the north), even a few tens of millimeters less rainfall may have tangible effects on water availability and ecosystems. Wind speed changes are analogous to those observed elsewhere on the island: the fastest winds have become a bit faster, and the calmest periods even calmer. Specifically, maximum wind speed increased by roughly $+0.25$ m/s ($p < 0.001$) over the period, hinting at stronger daytime sea-breeze or downslope wind events. In contrast, minimum wind speed fell by about -0.08 m/s, indicating slightly more frequent or pronounced still-air conditions at night. This pattern can amplify daytime drying (more wind to evaporate moisture) while potentially allowing cooler, moisture-trapping conditions overnight in low-lying areas.

Evapotranspiration trends and breakpoints:

The interior east/southwest region exhibited dynamic evapotranspiration trends, with clear temporal breakpoints signaling a mid-2010s shift. During the early part of the record (2000–2005), AET was increasing at about $+39$ mm/decade. This upward trend in AET accelerated slightly thereafter, from 2005 to 2017, AET climbed at roughly $+46$ mm/decade. This indicates that warming temperatures and available soil moisture continued to boost evaporation and plant transpiration through the mid-2010s. Around 2017, however, AET behavior changed markedly. From late 2017 to 2020, the trend in AET turned negative ($\sim -$

32 mm/decade), and this drying intensified into 2020–2021 (segmented slope \sim -39 mm/decade in the final segment). In practical terms, after peaking in the mid-2010s, actual evapotranspiration rates began falling, implying that drought conditions and soil moisture depletion started to limit the realized evaporation.

A similar transition is evident in PET. Early in the record, PET rose (e.g., roughly +36 mm/decade up to 2003; $p < 0.05$), though the trend was irregular in the 2000s (a smaller increase of \sim 13 mm/decade during 2003–2007, followed by a larger increase of \sim 48 mm/decade from 2007 to 2018). This indicates that by the late 2000s and early 2010s, climatic demand for evaporation, driven by temperature and radiation was surging. However, a breakpoint around 2018 reversed this course: post-2018 the PET trend is about -35 mm/decade. Therefore, the late 2010s brought a regime shift wherein even the atmospheric thirst for moisture abated slightly, likely due to more frequent cloud cover or lower temperature extremes during the most intense drought years. The overall picture is that the interior east/southwest, which was becoming increasingly evaporative, hit a tipping point around 2017–2018 when intensifying drought reduced both actual and potential evapotranspiration.

Drought index (SPEI) evolution:

Drought conditions in the east, south, and west of Gran Canaria have become more prevalent and severe over the study period, as reflected by SPEI indices. In the early 2000s this region experienced a notable drought episode, for example, by early 2003 the 12-month SPEI had fallen to approximately -2.0, and the short-term 3-month SPEI dropped to -2.5, indicating a sharp but short-lived drought. After that early-2000s dry spell, SPEI values rebounded to near-neutral or positive during the mid-2000s through early 2010s, implying periods of adequate rainfall. However, starting in the mid-2010s, a sustained drying trend emerges. By 2017–2020, all SPEI timescales trend negative, reflecting accumulating drought stress. The mean 24-month SPEI for 2017–2021 was roughly -1.0, a stark contrast to the early-period average of +0.6, signaling a shift to long-term drought conditions. The culmination was the late-2010s drought: by mid-2019 the 24-month SPEI hit a low near -1.6, and the 6-month SPEI fell below -2 in several instances during 2018–2019, denoting severe to extreme drought intensity. Although late 2020 into 2021 saw some recovery (SPEI values rising back towards zero with occasional wet months), the overall frequency of negative SPEI occurrences in the last decade was much higher than in the 1990s or 2000s. This indicates a heightened volatility and a tendency towards drought in the interior east, south, and west of Gran Canaria. In summary, the interior subregions of Gran Canaria's drier sides have undergone pronounced warming and drying, with escalating evapotranspiration early on giving way to moisture-limited conditions and recurrent drought in recent years.

3.1.3 El Hierro

Comparison of the trend between climate variables:

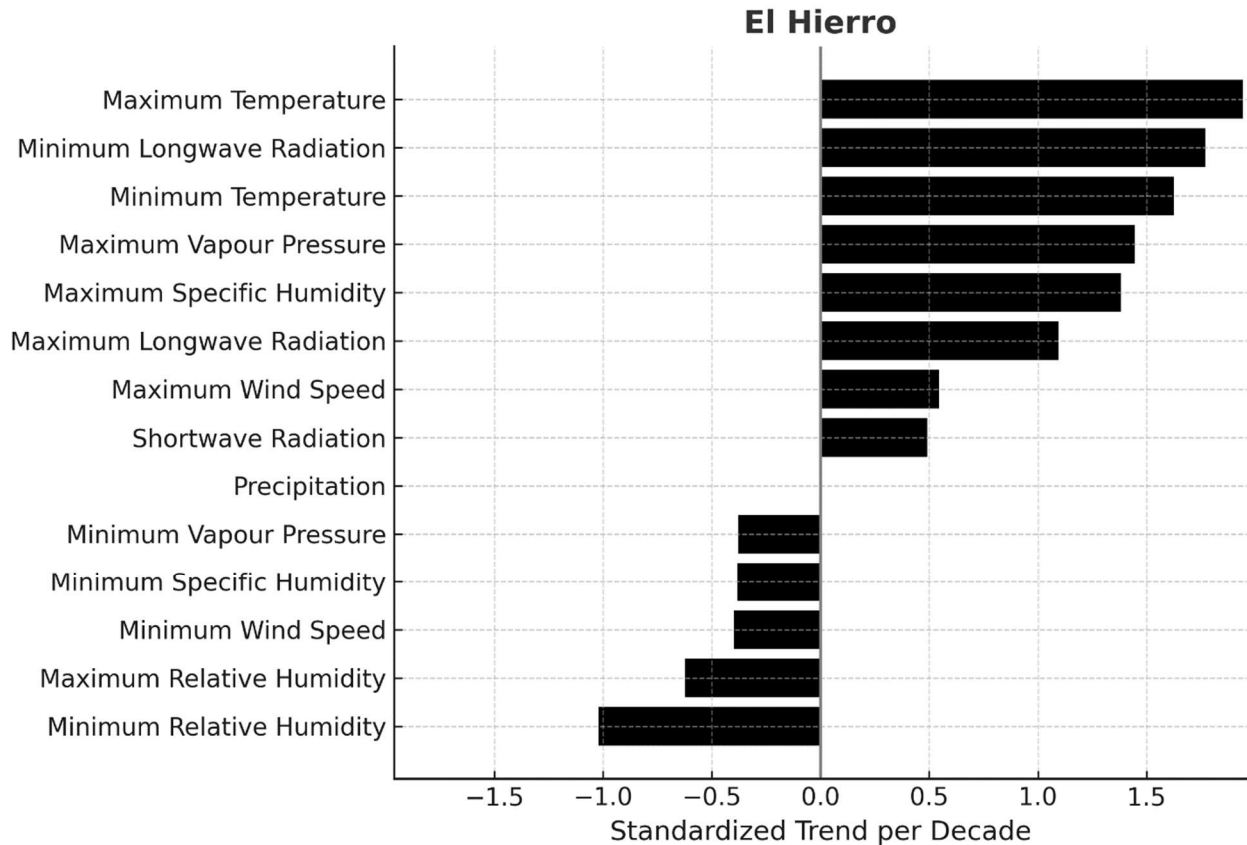


Figure 22: El Hierro - Normalized Trends

El Hierro shows a clear dominance of warming in the normalized trends. Maximum temperature has the strongest positive relative change (~1.94), indicating that daytime highs have increased well beyond their historical variability. Minimum temperature is also large (~1.63), confirming substantially warmer nights, albeit with a smaller amplitude than daytime. These thermal shifts are supported by strong gains in minimum longwave radiation (~1.77) and a notable rise in maximum longwave radiation (~1.10), together with a smaller but consistent increase in shortwave radiation (~0.49), pointing to a more energetic surface-atmosphere system.

On the moisture front, maximum specific humidity (~1.38) and maximum vapour pressure (~1.45) both rise, highlighting greater moisture-holding capacity during humid periods as temperatures climb. In sharp contrast, the driest conditions have become markedly drier: Minimum relative humidity shows the largest negative normalized shift (~-1.02), while minimum specific humidity (~-0.38) and minimum vapour pressure (~-0.38) also decline. This divergenc, more moisture at humid times but less at the driest hours, signals a widening diurnal humidity contrast and intensifying daytime aridity.

Wind changes are secondary: maximum wind speed increases moderately (~0.55) and minimum wind speed decreases slightly (~-0.40), implying a broader daily wind range but with smaller climatic impact than temperature and humidity. Precipitation is effectively

unchanged in relative terms (~ -0.006 normalized), reiterating that rainfall trends are negligible compared with the dominant warming–drying signal. Overall, El Hierro is hotter and relatively drier, with daytime aridity intensifying at a scale comparable to the warming of temperatures.

Temperature and Radiation:

El Hierro has experienced significant warming in recent decades. Mean maximum air temperatures have risen by roughly $+2.1^\circ\text{C}$ per decade ($p < 0.05$), with an especially sharp uptick in the warming rate after 2015–2016. Minimum temperatures increased more modestly (about $+0.64^\circ\text{C}/\text{decade}$), suggesting a widening diurnal temperature range. Consistent with the warming, surface longwave radiation has increased by $\sim 4.7\text{W}/\text{m}^2$ per decade, for both daily minimum and maximum longwave flux, indicating enhanced thermal emission from the surface and atmosphere. Shortwave solar radiation shows a slight upward trend ($\sim 0.37\text{W}/\text{m}^2$ per decade), which may reflect a minor reduction in cloud cover or other changes in insolation. These changes in the radiative budget align with the observed temperature rise. All trends are statistically significant ($p < 0.05$).

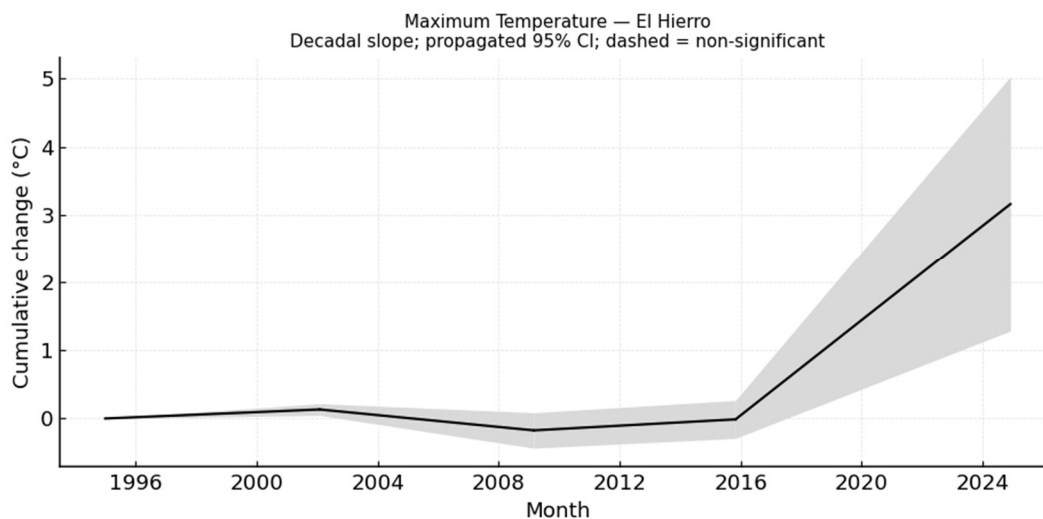


Figure 23: Maximum Temperature Trend – El Hierro

Humidity and Vapour Pressure:

Despite the warming, relative humidity in El Hierro’s interior has been declining, particularly during the driest conditions. The minimum monthly relative humidity has dropped by about -3.3 percentage points per decade ($p < 0.05$), indicating that the air’s driest periods are becoming even drier. Notably, a breakpoint around 2018 marks an accelerated decline in minimum relative humidity, pointing to more extreme low-humidity events in recent years. By contrast, humidity during the moistest periods (relative humidity max) has only decreased slightly (on the order of $-0.3\%/decade$). In absolute terms, however, warmer air has led to higher moisture content. Specific humidity at the upper range (indicator of moisture content on humid days) has increased by about $+0.43\text{g}/\text{kg}$ per decade, and the corresponding vapour pressure maximum has risen by approximately $+0.68\text{hPa}/decade$.

These upward trends in absolute humidity (also significant at $p < 0.05$) imply that the atmosphere can hold and does contain more water vapour now than in the past – even as relative humidity percentages drop – consistent with a warming-driven increase in capacity. Meanwhile, the minimum vapour pressure (during very dry air periods) has fallen slightly (on the order of -0.15 hPa per decade), reinforcing that the driest air masses are getting drier in absolute terms as well. In summary, El Hierro’s interior is warmer and more moisture-laden overall, yet relatively drier at the extremes, compared to a few decades ago.

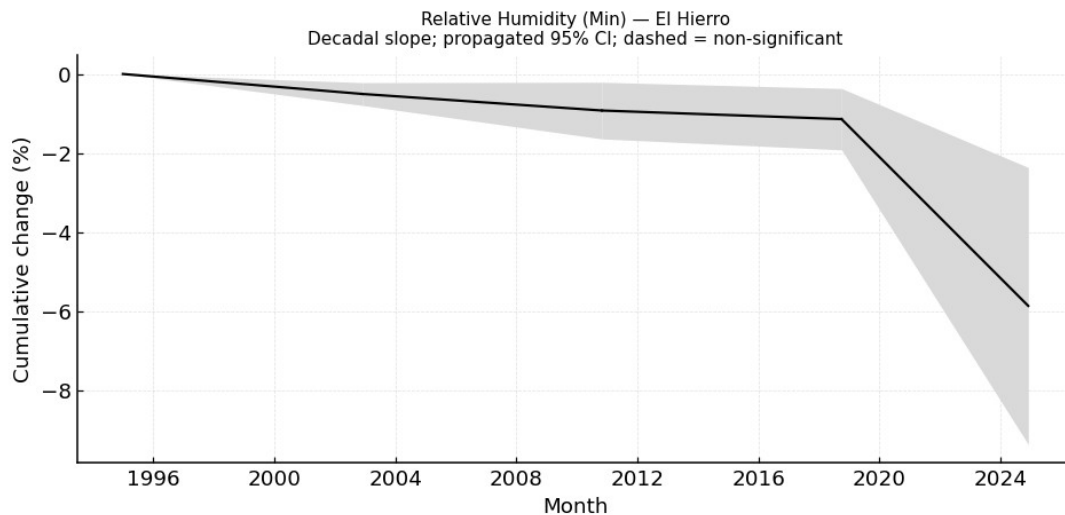


Figure 24: Minimum Relative Humidity Trend – El Hierro

Precipitation:

Annual precipitation in interior El Hierro has not shown any pronounced long-term trend over the 1995–2024 period. The overall slope is a slight decline of ~ -0.26 mm per decade, which is negligible relative to the large year-to-decade rainfall variability. Rather than a steady trend, precipitation has fluctuated decadal: an initial wetting trend in the late 1990s (through ~ 2003) gave way to a drying period in the 2000s, followed by a partial rebound (increased rainfall) in the early 2010s. The late 2010s into the 2020s again show a modest decrease. These shifts produce breakpoints around 2003, 2010, and 2019 corresponding to inflection points between alternating wet and dry spells. However, the net effect is that total rainfall has remained near historical norms, with no statistically significant change in mean annual totals. The slight downward overall trend is not practically significant, and all segments of the record indicate high variability but no clear directional change in precipitation climate.

Wind:

Wind speed in the interior has changed subtly. Maximum wind speeds (e.g. monthly peak gusts or strongest daily winds) show a gentle increasing trend of about $+0.26$ m/s per decade ($p < 0.05$). This suggests that the strongest wind events have become marginally more intense over the 30-decade period. In fact, a trend segmentation indicates a slight

acceleration of wind speed increases after 2017, coinciding with recent years that saw some of the highest gusts. In contrast, minimum wind speeds (calmest conditions, such as nighttime lulls) have slightly decreased by roughly -0.09 m/s per decade ($p < 0.05$). The small drop in minimum winds could imply slightly longer or more frequent calm periods. Taken together, these changes point to a widening of the wind speed range: the strongest winds are a bit stronger, while calm conditions remain prevalent during low-wind periods. All wind trends are statistically significant, but their magnitudes are modest, so the overall wind climate is still characterized by similar typical breezes as in past decades, with a slight tendency towards more extreme gusts.

3.1.4 Tenerife

East, South and West Tenerife

Comparison of the trend between climate variables:

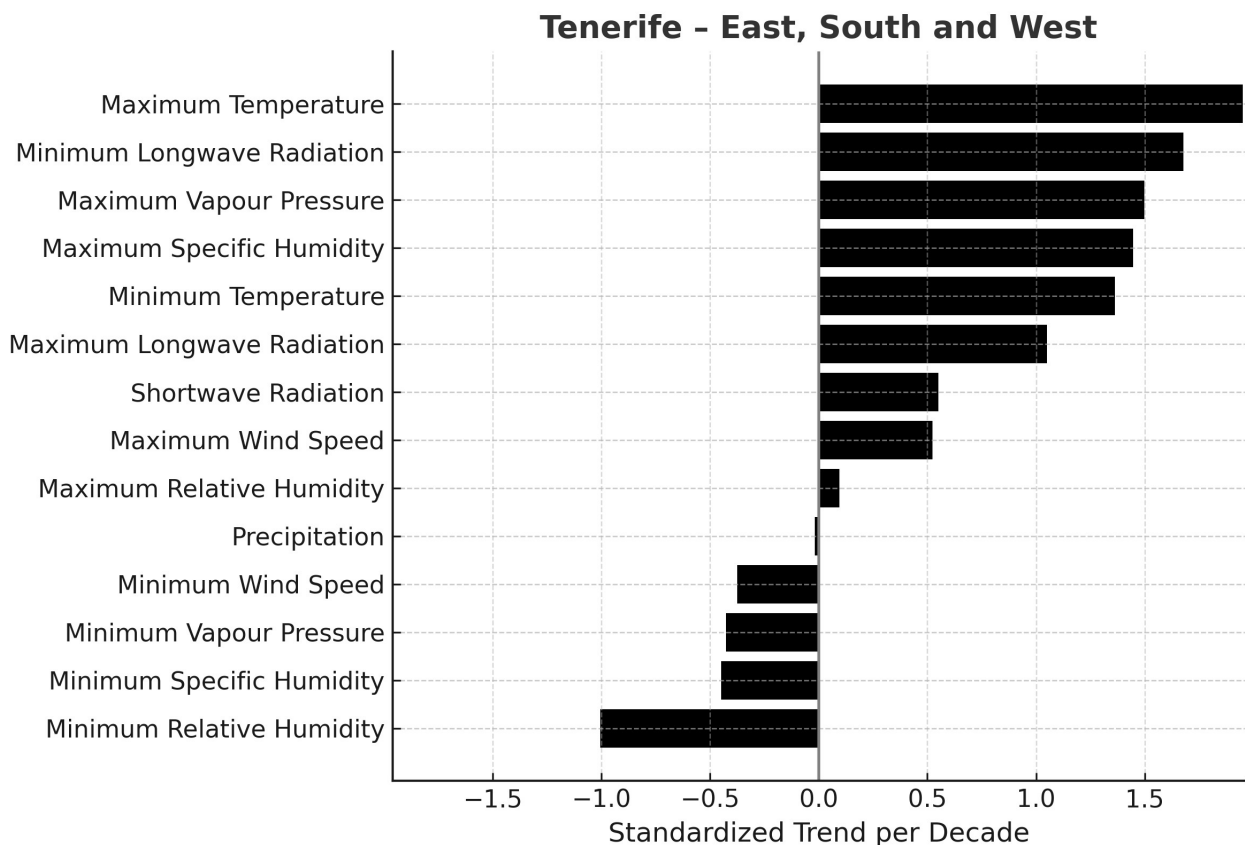


Figure 25: East, South and West of Tenerife – Normalized Trends

Normalized trends underscore the dominance of warming. The maximum temperature shows the strongest positive relative change (~ 1.95), with minimum temperature also high (~ 1.36), indicating substantially warmer days and noticeably warmer nights relative to past variability. The thermal signal is reinforced by large gains in minimum longwave radiation

(~1.68) and a clear rise in maximum longwave radiation (~1.05), while shortwave radiation increases more modestly. On the moisture side, maximum specific humidity (~1.45) and maximum vapour pressure (~1.50) both rise, highlighting enhanced moisture-holding capacity during humid periods. In sharp contrast, minimum relative humidity shows the largest negative shift (~-1.01), and both minimum specific humidity (~-0.45) and minimum vapour pressure (~-0.43) decline, confirming that the driest hours have become markedly drier. Precipitation is negligible in relative terms (~-0.018), and minimum wind speed shows a secondary-scale decrease (~-0.38). Overall, the interior eastern, southern, and western slopes are hotter and relatively drier, with daytime aridity intensifying at a scale comparable to the warming itself.

Temperature and Radiation:

The areas of eastern, southern, and western Tenerife have experienced a significant warming trend over the past ~30 years. The daily maximum temperatures increased by roughly 0.6–0.7 °C per decade ($p < 0.05$), while minimum temperatures rose by about 0.2 °C per decade ($p < 0.05$). This indicates a pronounced daytime warming, with nights warming to a lesser degree. Correspondingly, atmospheric longwave shows a clear increase of approximately 1–2 W/m² per decade ($p < 0.05$). This rise in longwave radiation is consistent with a warmer, more moisture-rich atmosphere trapping more heat. In contrast, incoming shortwave solar radiation changed only slightly (on the order of 0.1 W/m² per decade, $p < 0.05$), suggesting little change in overall cloud cover or sunshine duration in this region. Notably, the warming of daily high temperatures is one of the most pronounced climate changes in this subregion, indicating that heat conditions have shifted substantially compared to other variables.

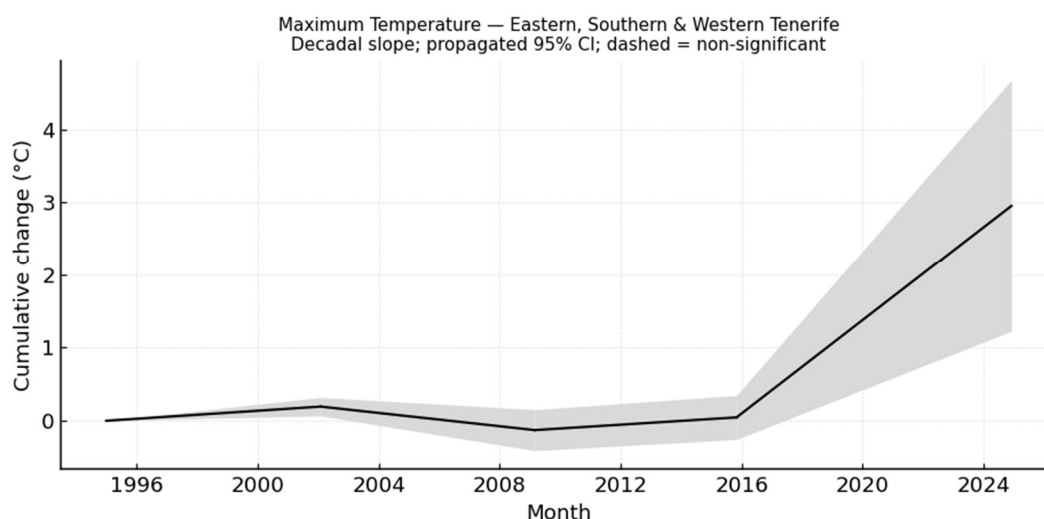


Figure 26: Maximum Temperature Trend – East, South and West of Tenerife

Humidity and Moisture:

Absolute humidity has risen in this region of Tenerife. The maximum daily vapour pressure has increased by about 0.7 hPa in total since 1995 (approximately 0.2–0.3 hPa per decade, $p < 0.05$). Likewise, the peak specific humidity climbed by roughly 6% relative to its mid-1990s value ($p < 0.05$). These changes indicate that the warmer air is holding more moisture at its most humid times of day. Despite higher absolute moisture, relative humidity trends suggest a drier atmosphere in a relative sense during the warmest hours. The minimum daily relative humidity, typically occurring in the afternoon, decreased by ~2–3% over the period (~1% decline per decade, $p < 0.05$). This means that even though there is more water vapour in absolute terms, the interior air is relatively drier at midday because temperatures have risen. By contrast, the maximum daily relative humidity, often reached at night or early morning, showed little change, a slight uptick of <1% overall, not a major or significant change. This stability in relative humidity maxima implies that nighttime near-saturation conditions (e.g. dew formation) remain about as humid as before, even as daytime dryness increases. The rise in absolute humidity metrics is among the larger changes (normalized trends ~1.4–1.5), second only to temperature, whereas changes in relative humidity are moderate in comparison.

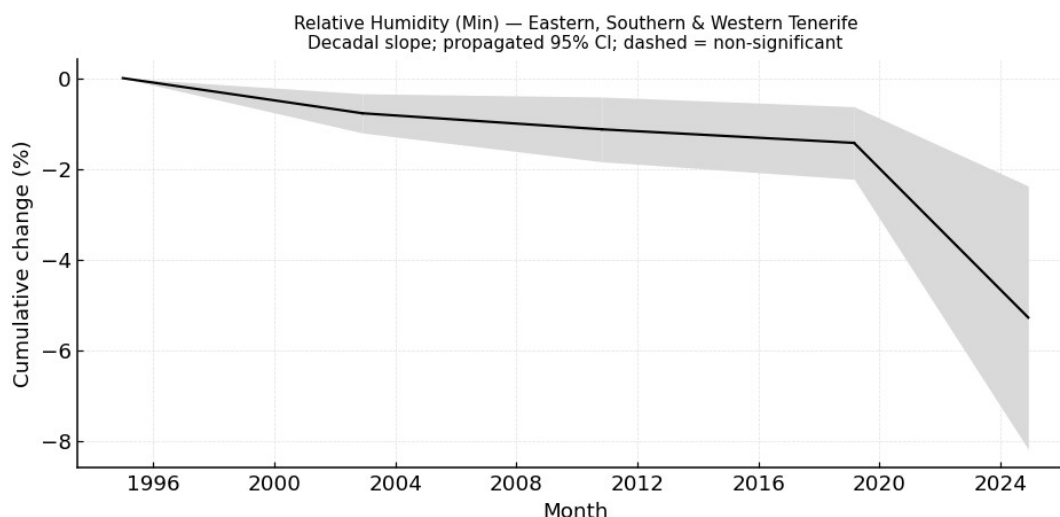


Figure 27: Minimum Relative Humidity Trend – East, South and West of Tenerife

Precipitation:

Total precipitation in the east/south/west Tenerife shows a slight downward trend, though with a very small magnitude relative to natural variability. Rainfall has declined on the order of only 1–3 mm per decade ($p < 0.05$ for the trend), amounting to a few tens of millimeters less rain in total now compared to the mid-1990s. In percentage terms, this decline is minor and the normalized trend is near zero, indicating precipitation has not changed as dramatically as temperature or humidity. Interannual rainfall variability remains much larger than any long-term linear trend. Importantly, no clear temporal breakpoints or step changes were detected in the precipitation time series, the slight drying trend appears to have been a gradual, steady change rather than an abrupt shift. This means there were no statistically significant change-points in rainfall around which the trend behavior altered. The region did not exhibit a sudden regime change in precipitation over 1995–2024.

Wind:

Wind patterns in this area have changed modestly. The daily maximum wind speeds have increased by roughly 0.3 m/s overall since the mid-1990s ($p < 0.05$), translating to a small (~ 0.1 m/s per decade) upward trend in peak winds. This suggests a slight intensification of the strongest wind events in the interior, although the change is relatively minor. Meanwhile, daily minimum wind speeds have not changed substantially. The wind speed trends are small in a climatological sense meaning that wind has been one of the more stable climate variables. No significant breakpoints were identified in the wind time series either, so the observed gentle increase in peak wind has been a smooth trend over time.

North Tenerife

Comparison of the trend between climate variables:

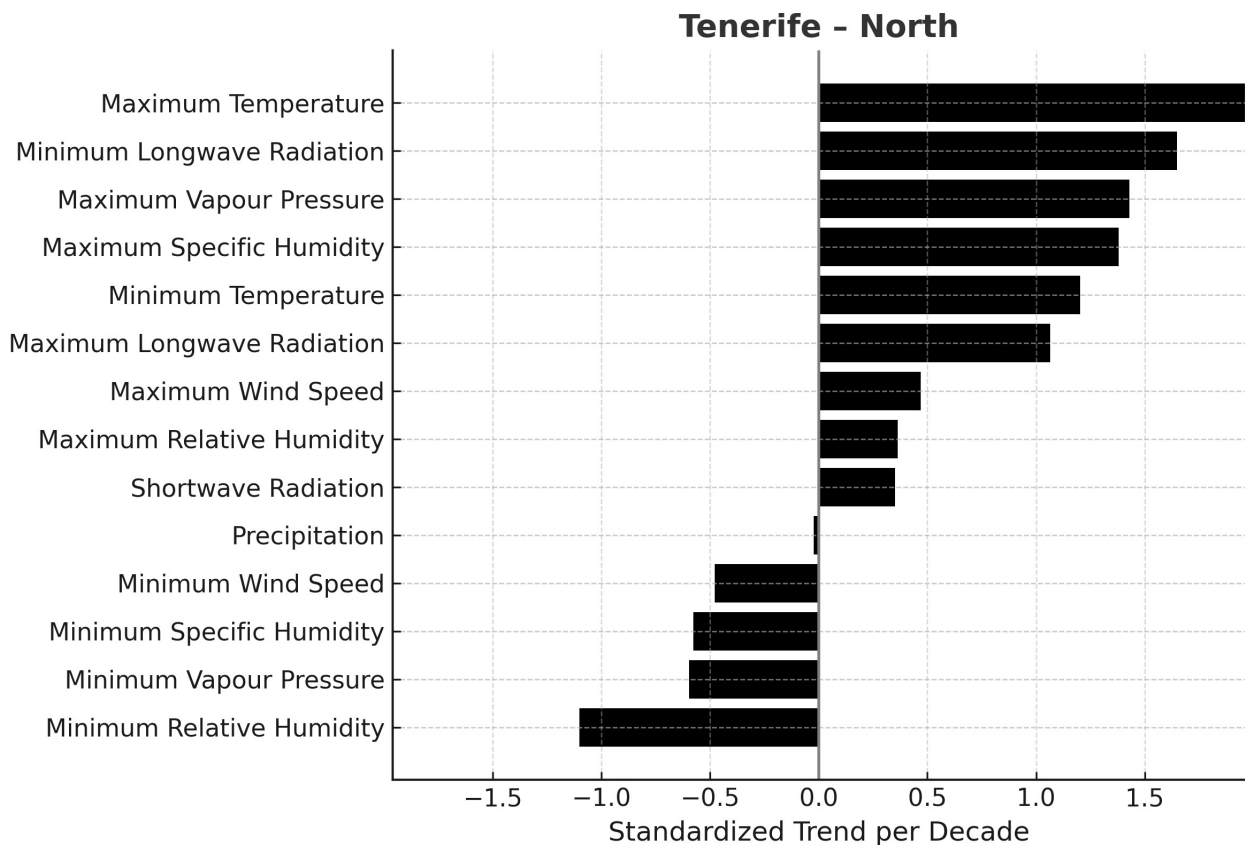


Figure 28: Northern Tenerife – Normalized Trends

The northern interior presents one of the clearest warming–drying patterns on the island. The maximum temperature records the highest positive normalized change (~ 1.96), with minimum temperature also elevated (~ 1.20), pointing to strong daytime warming and appreciable nighttime warming. Longwave radiation increases substantially (~ 1.65 for minimum; ~ 1.07 for maximum), consistent with a more energetic surface–atmosphere system. Moisture indicators split: maximum specific humidity (~ 1.38) and maximum vapour pressure (~ 1.43) rise, yet minimum relative humidity shows the most negative normalized shift (~ -1.10), accompanied by declines in minimum vapour pressure (~ -0.60) and minimum specific humidity (~ -0.58). This divergence signals a widening diurnal humidity contrast

and intensifying daytime dryness. Precipitation changes are minimal in relative terms (~ -0.022). Wind signals are secondary; minimum wind speed weakens (~ -0.48) but remains small compared with the dominant thermal-humidity shifts. In sum, the north interior is warmer and considerably drier, with the largest proportional decrease in daytime humidity closely mirroring the magnitude of warming.

Temperature and Radiation:

The interior of northern Tenerife, which encompasses the more mountainous, typically wetter side of the island, has also warmed markedly. The long-term increase in daily maximum temperature is on the order of $0.5\text{--}0.6\text{ }^\circ\text{C}$ per decade ($p < 0.05$), while minimum temperatures rose by around $0.2\text{ }^\circ\text{C}$ per decade ($p < 0.05$). As in other areas, daytime highs are climbing faster than nighttime lows, indicating a widening of the diurnal temperature range. The enhanced warming is reflected in downwelling longwave radiation, which has grown by about $1.5\text{--}2\text{ W/m}^2$ per decade ($p < 0.05$) over the period – a significant rise consistent with increased greenhouse heat retention in the atmosphere above North Tenerife. Changes in shortwave radiation are minor, there is a slight positive trend ($\sim 0.1\text{--}0.2\text{ W/m}^2$ per decade, $p < 0.05$) in incoming solar radiation, hinting at marginally reduced cloud cover or clearer skies, but the effect is very small. In terms of relative magnitude, the warming of the climate stands out as the dominant change (the highest normalized trend ~ 2.0 for maximum temperature). The increase in longwave radiation is next in significance (normalized ~ 1.6), underlining that thermal energy near the surface has increased substantially. By contrast, changes in sunlight and other variables are comparatively modest.

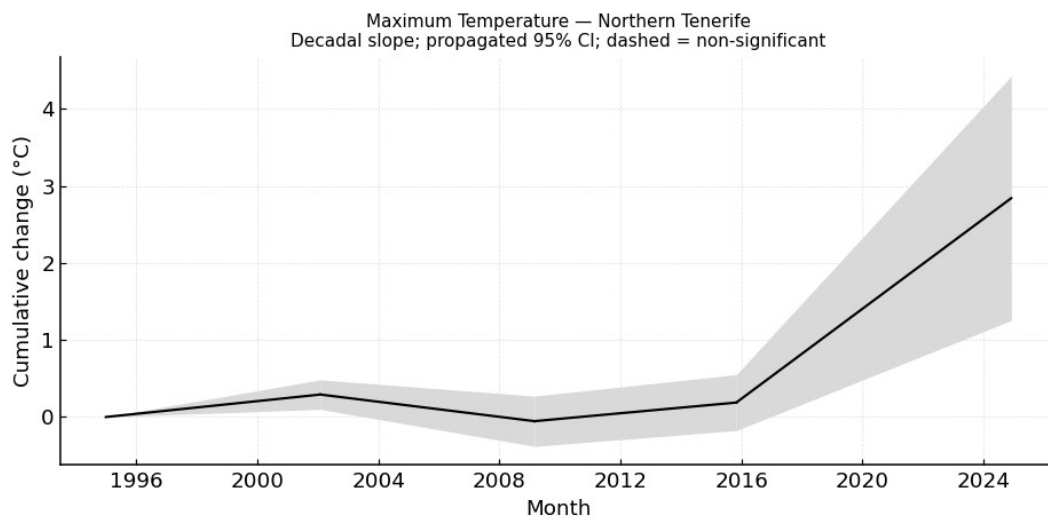


Figure 29: Maximum Temperature Trend – Northern Tenerife

Humidity and Moisture:

The northern interior's atmosphere has become moister in absolute terms but slightly drier in relative terms during the hottest part of the day. The specific humidity of the air has risen: for example, daily maximum specific humidity increased by roughly 0.0005 kg/kg

since 1995 (about a 5–7% gain, $p < 0.05$). Similarly, the vapour pressure at daily humidity maxima went up by on the order of 0.07–0.08 kPa (~0.7–0.8 hPa, $p < 0.05$) over the period, confirming that the air now holds more water vapour at peak times than it did 30 years ago. Meanwhile, relative humidity measures indicate a drying in relative terms when temperatures peak. The minimum relative humidity dropped by about 2–3% from 1995 to 2024 ($p < 0.05$), equivalent to roughly a 1% decline per decade. This significant drop implies that even though there is more moisture in absolute terms, the capacity of warmer air to hold moisture has outpaced the actual increase in moisture, leading to drier relative conditions during the day. Interestingly, the maximum relative humidity (typically reached at night or morning) in North Tenerife shows a slight increase, on the order of +1% over the study period. This minor rise suggests that nighttime humidity may have become a bit higher or closer to saturation, potentially due to more moisture available in cooler overnight air.

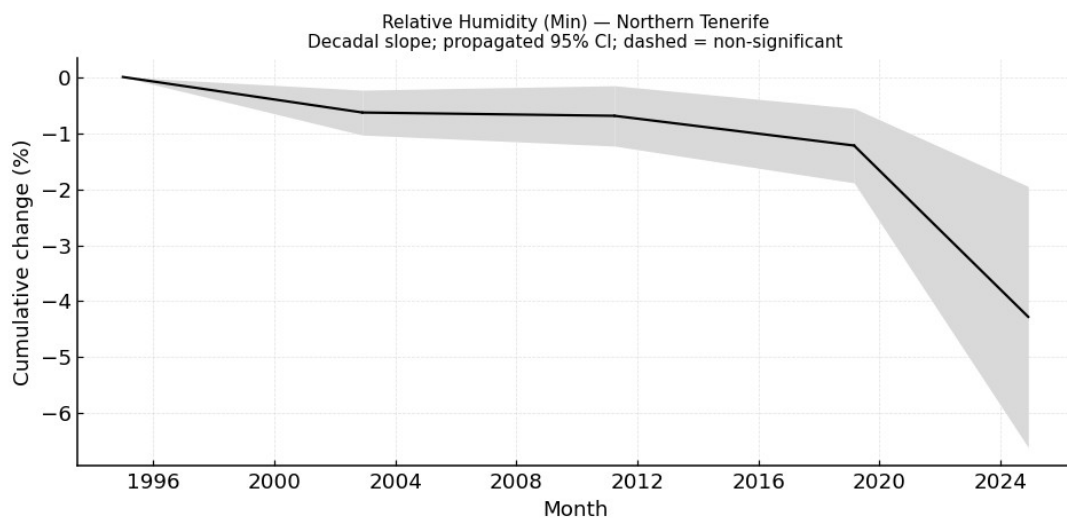


Figure 30: Minimum Relative Humidity Trend – Northern Tenerife

Precipitation:

Interior North Tenerife is traditionally one of the wetter parts of the island, but even here a mild drying tendency is evident. Annual precipitation totals have trended downward, with an overall decrease of roughly 2–3 mm per decade on average ($p < 0.05$). Cumulatively, this suggests perhaps ~50–80 mm less rain per decade, although year-to-decade variability is high. In relative terms this is a small change, and indeed the normalized precipitation trend is very close to zero, indicating that the long-term signal is weak compared to natural fluctuations. There is no clear breakpoint or sudden shift in the precipitation record for North Tenerife’s interior, the data do not show any abrupt change in rainfall regime within 1995–2024. Rather, the slight decline in rainfall appears to have been gradual and steady. This means there were no identifiable years where the precipitation pattern shifted dramatically – instead, any drying has unfolded slowly over the decades.

Wind:

Changes in wind characteristics in North Tenerife's interior are minor but observable. The maximum daily wind speeds have increased by approximately 0.3 m/s overall since the mid-1990s ($p < 0.05$). This is a subtle rise (on the order of +0.1 m/s per decade) indicating that the strongest gusts or daily peak winds are a bit stronger now than before. On the other hand, minimum daily wind speeds have shown little to no change. If anything, a negligible downward trend was detected on the order of -0.1 m/s over the entire period, not climatologically significant. The wind changes carry a low normalized trend (~ 0.4 - 0.5 for wind_max), highlighting that wind is one of the least changed climate variables in this region. As with other variables, no meaningful breakpoints were found in the wind time series, the slight uptick in peak wind has been a gradual trend rather than a sudden change. Overall, the interior north exhibits climate shifts characterized most strongly by warming and increased atmospheric moisture, while precipitation and wind have remained relatively stable in the long run.

Tenerife Metropolitan Area

Comparison of the trend between climate variables:

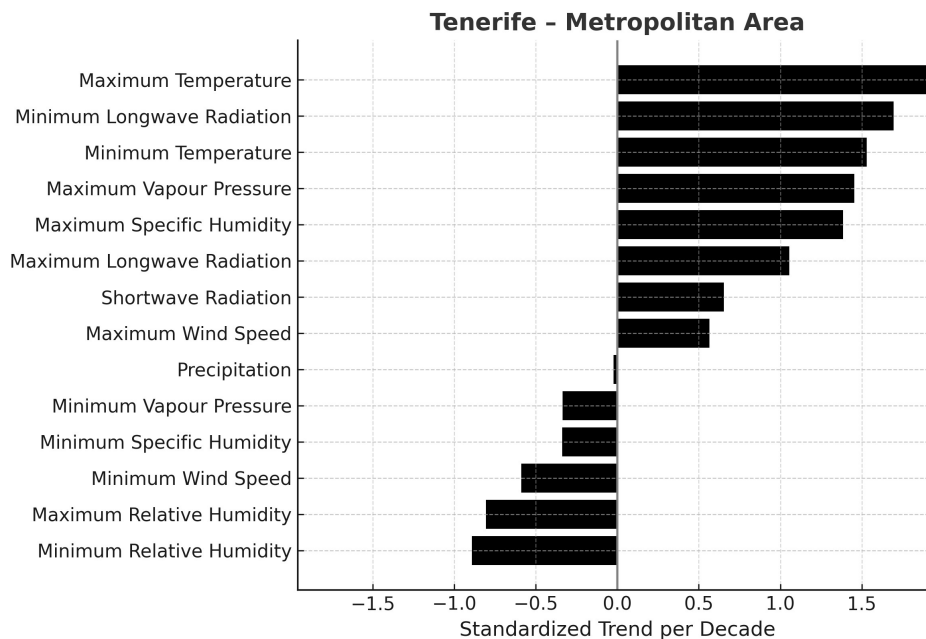


Figure 31: Tenerife Metropolitan Area – Normalized Trends

Normalized results again highlight strong warming. The maximum temperature shows a large positive change (~ 1.92), and minimum temperature is similarly prominent (~ 1.53). Minimum longwave radiation exhibits a major increase (~ 1.70) with maximum longwave radiation also rising (~ 1.05), confirming sustained enhancement of the surface energy balance. On the moisture front, maximum vapour pressure (~ 1.45) and maximum specific humidity (~ 1.39) both increase, indicating more absolute moisture during humid periods. However, minimum relative humidity declines sharply (~ -0.89) and is joined by a notable

reduction in maximum relative humidity (~ -0.81), pointing to a pervasive relative drying that affects both daytime minima and nighttime maxima. Additional negative signals in minimum vapour pressure (~ -0.34) and minimum specific humidity (~ -0.34) reinforce drier conditions during the least humid hours. Precipitation remains negligible in relative terms (~ -0.024). Wind changes are secondary; minimum wind speed decreases (~ -0.59), suggesting slightly calmer lows but with far smaller impact than the warming–drying signal. Overall, the metropolitan interior is hotter with stronger relative drying, especially visible in both daytime and nighttime humidity metrics.

Temperature and Radiation:

The interior of the Tenerife Metropolitan Area has undergone the most pronounced warming of all the island’s subregions. The daily maximum temperatures increased by roughly $0.7\text{--}0.8\text{ }^\circ\text{C}$ per decade ($p < 0.05$), yielding a total rise of about $2.2\text{ }^\circ\text{C}$ from 1995 to recent years. Daily minimum temperatures also rose ($\sim 0.2\text{ }^\circ\text{C}$ per decade, $p < 0.05$), indicating warmer nights, though the daytime warming signal is much larger. The strong heating is mirrored by a significant increase in longwave infrared radiation downwards: on the order of $\sim 2\text{ W/m}^2$ per decade ($p < 0.05$) additional longwave flux is now reaching the surface at night. This is consistent with both global warming and possible urban heat island effects as the metropolitan area includes urbanized zones that can emit more thermal radiation at night. Changes in shortwave radiation are again minor, a slight positive trend ($\sim 0.1\text{ W/m}^2$ per decade, $p < 0.05$) in shortwave radiation was observed, suggesting essentially stable or only marginally clearer sky conditions over time. In terms of normalized trends, the metropolitan interior’s warming stands out as a dominant change (maximum temperature has a normalized trend ~ 1.9 , the highest). The rise in nighttime longwave energy (normalized ~ 1.7) is also a key signal.

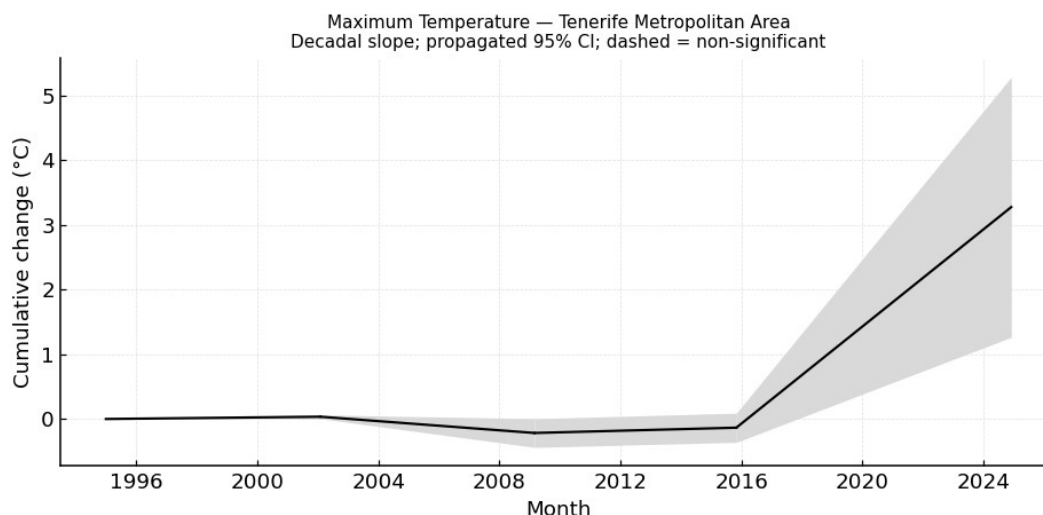


Figure 32: Maximum Temperature Trend – Tenerife Metropolitan Area

Humidity and Moisture:

The interior metropolitan atmosphere has a complex moisture trend, absolute moisture has increased, but relative humidity has decreased, especially in daytime, more so than in other regions. On the absolute side, vapour pressure during the most humid period of the day increased by about 0.65 hPa total ($p < 0.05$) from 1995 to 2024, reflecting a higher water vapour load in the air. The specific humidity at daily maximum shows a modest upward trend (~ 0.0004 kg/kg, $p < 0.05$). These suggest that, as the air has warmed, it holds more moisture in an absolute sense. However, the relative humidity trends reveal a drying effect. The minimum relative humidity fell by approximately 3–4% over the period ($p < 0.05$), which corresponds to around 1.1–1.3% lower relative humidity per decade. This is a notable drop, larger than in the other interior subregions, indicating that the hottest parts of the day are becoming considerably drier relative to the past. Unlike the North, the maximum daily relative humidity in the metropolitan area also shows a slight decrease (~ 1 –2%) over 30 years ($p < 0.05$). This suggests that even the overnight or early-morning humidity has declined a bit, possibly due to urban-related warming, night temperatures stay higher, preventing relative humidity from reaching past levels. The net effect is that this region is relatively drier at all times of day now, despite having more water vapour in absolute terms, a scenario consistent with warming air capacity outpacing moisture gains. The drop in relative humidity registers as a sizable normalized change (~ -0.9), second in magnitude only to temperature-related trends for this region. Meanwhile, the increase in absolute humidity is moderate (normalized ~ 1.3 –1.45), indicating a clear but not extreme rise compared to other changes.

Precipitation:

The metropolitan region of Tenerife does not receive as much rainfall as the northern slopes, and the long-term trend suggests a very slight decrease in precipitation. The data indicate a decline on the order of 1 mm per decade or less in annual rainfall ($p < 0.05$, though the trend is extremely small). Over nearly three decades, this adds up to perhaps 20–30 mm less total rain per decade now than in the mid-1990s, a change that is almost negligible relative to interannual variability. Consistently, the normalized trend for precipitation is effectively zero (-0.02), reinforcing that rainfall has remained virtually steady without any substantial directional change.

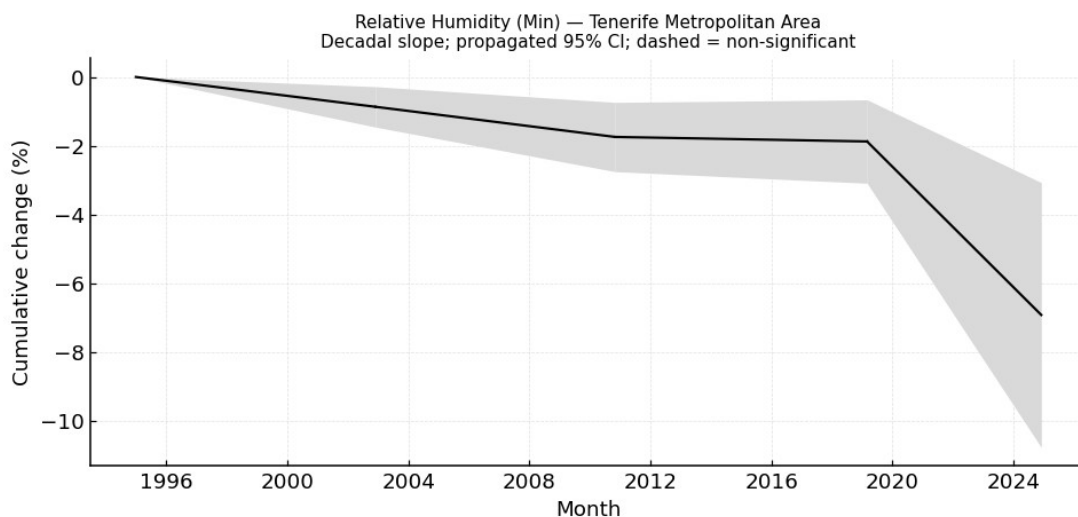


Figure 33: Minimum Relative Humidity Trend – Tenerife Metropolitan Area

Wind:

This area of Tenerife show minimal changes in wind behavior. The peak daily wind speeds have a small upward trend (~ 0.3 m/s total since 1995, $p < 0.05$), indicating a slight increase in the strength of the strongest winds, likely sea-breeze or downslope wind events affecting the inland area. This translates to roughly $+0.1$ m/s per decade, which is a subtle change that would likely not be noticeable without long-term analysis. Lowest daily wind speeds did not change appreciably. Such a decrease in minimum wind might reflect slightly calmer nights, perhaps due to reduced radiative cooling and weaker nocturnal drainage flows in a warmer environment, but the magnitude is very small.

3.1.5 La Gomera

Comparison of the trend between climate variables:

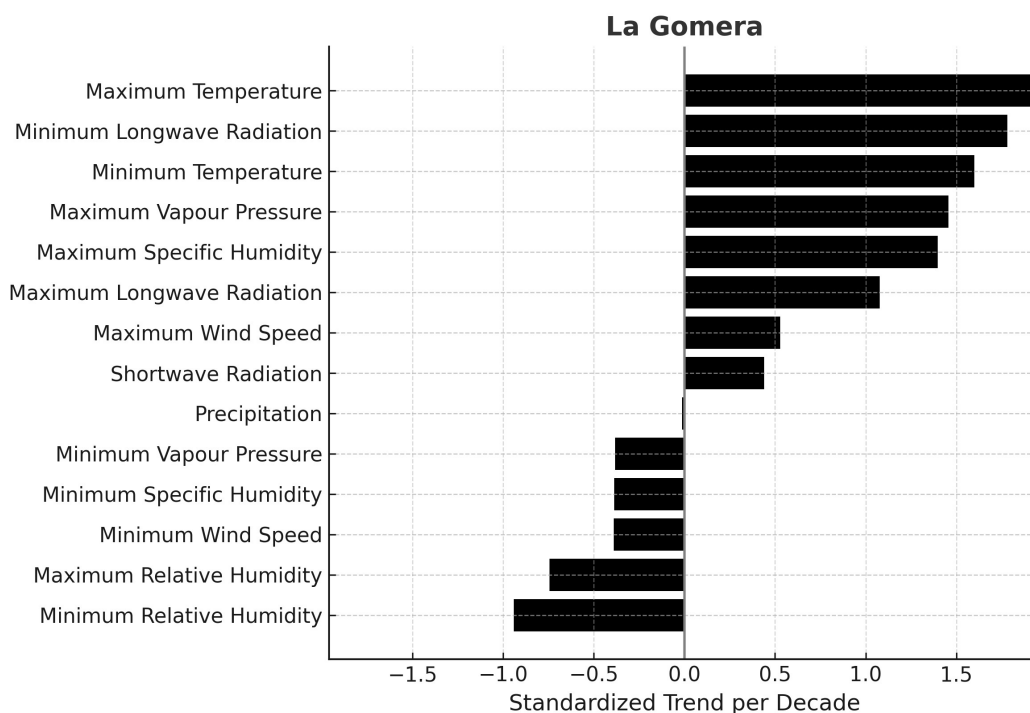


Figure 34: La Gomera – Normalized Trends

La Gomera's interior climate trends show strong warming coupled with notable drying in relative terms. Maximum temperature has a very high positive normalized trend (~ 1.93), with minimum temperature also large (~ 1.60). Nighttime longwave radiation increased (~ 1.78) alongside daytime longwave (~ 1.00).

Absolute humidity has risen: maximum vapour pressure (~ 1.46) and maximum specific humidity (~ 1.40) are both significantly positive. Relative humidity trends indicate a drying pattern: minimum relative humidity declines (~ -0.94), and maximum relative humidity also shows a drop (~ -0.74). Negative trends in minimum vapour pressure (~ -0.38) and specific humidity (~ -0.39) reflect drier air at its driest.

Precipitation trend is negligible (~ -0.027 normalized). Wind changes are small with minimum wind speed down slightly (~ -0.39) and maximum wind speed up slightly (~ 0.53). All told, La Gomera has become considerably warmer and relatively drier, both during the day and to a lesser extent at night.

Temperature and Radiation:

The rugged island of La Gomera has experienced substantial warming akin to its neighbors. The data indicate daily high temperatures have risen by around $0.7\text{ }^{\circ}\text{C}$ per decade ($p < 0.05$), giving roughly $+2.16\text{ }^{\circ}\text{C}$ total from 1995 to present. Nightly lows are up by about $0.21\text{ }^{\circ}\text{C}$ per decade ($p < 0.05$), so nights are warmer by around $+0.62\text{ }^{\circ}\text{C}$ over the period. This pervasive warming aligns with the Canary-wide trend. In response, the energy balance shows more longwave radiation being emitted downward: minimum longwave radiation increased by perhaps $\sim 1.4\text{ W/m}^2$ per decade ($p < 0.05$) and maximum longwave radiation by $\sim 1.0\text{ W/m}^2$ per decade ($p < 0.05$), consistent with higher atmospheric and surface temperatures. There's little change in incoming shortwave radiation, if anything a slight increase ($\sim 0.1\text{--}0.2\text{ W/m}^2$ per decade, $p < 0.05$) may suggest slightly less cloud cover on average, but La Gomera was fairly sunny to begin with, and it remains so. The warming is the most salient feature (maximum temperature normalized ~ 1.93). Given La Gomera's small size and ocean moderation, it's notable that the warming signal is virtually as strong as on larger islands, indicating a regional climate signal overriding local factors.

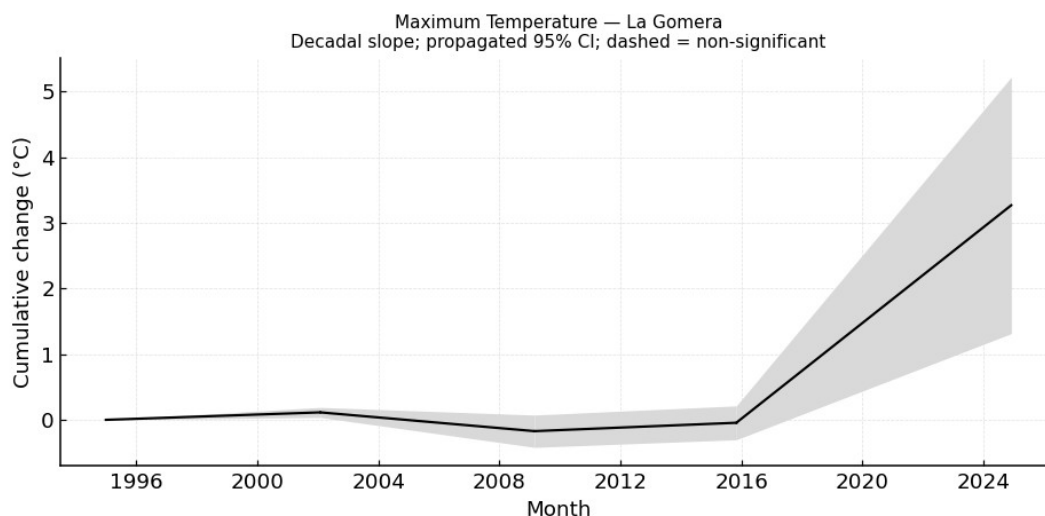


Figure 35: Maximum Temperature Trend - La Gomera

Humidity and Moisture:

La Gomera's atmosphere holds more moisture now in absolute terms, but relative humidity has decreased, particularly during the warmest times of day. The maximum vapour pressure has increased by $\sim 0.67\text{ hPa}$ ($p < 0.05$) since 1995 and maximum specific humidity by $\sim 0.0004\text{ kg/kg}$ ($p < 0.05$). These numbers show that on a humid day, there is more water vapour in the air than there used to be. However, because air temperatures are higher, the relative humidity at the driest time has fallen. The minimum relative humidity in La Gomera

dropped by roughly 3–4% over the 30-decade period ($p < 0.05$), about a 1.2–1.3% per decade decline. That indicates significantly drier feeling air during the hot part of the day. Additionally, the maximum relative humidity shows a small but noticeable decline of roughly 1% ($p < 0.05$) over the period. This suggests that nighttime or early-morning humidity, while still high (often in the 90%+), is slightly less often hitting extreme saturation now, likely due to warmer nights. Essentially, La Gomera’s relative humidity profile has shifted downward across the board: daytime lows are lower, and even nighttime highs are a bit lower, though the latter change is modest. Absolute humidity is up, but not enough to compensate for temperature in terms of relative humidity. The normalized trend for minimum relative humidity (~ -0.94) is significant, and for maximum relative humidity (~ -0.74) also relatively large for that metric, reflecting a general drying in relative terms.

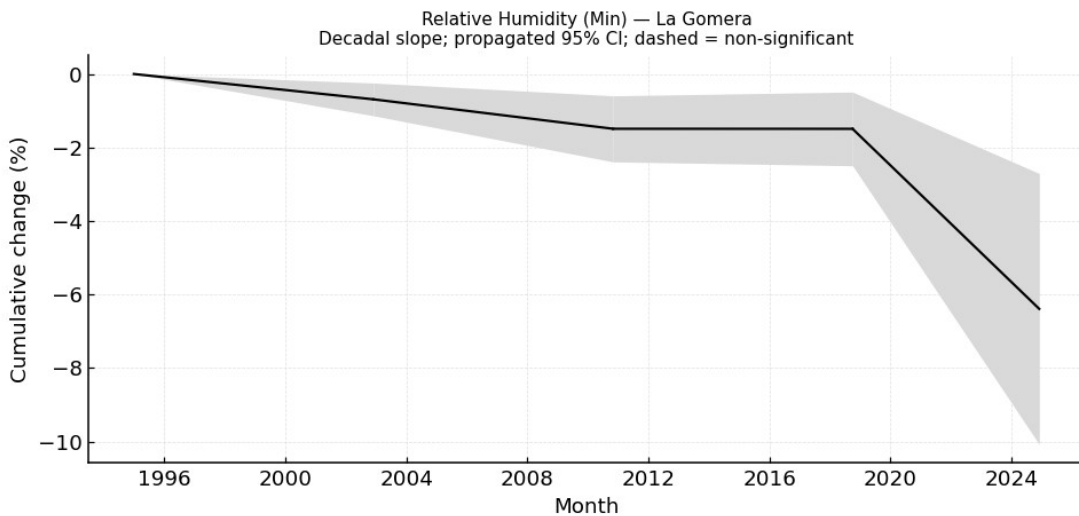


Figure 36: Minimum Relative Humidity Trend – La Gomera

Precipitation:

La Gomera’s annual precipitation is moderate, ~ 200 mm/year, mostly on the northern slope with much less in the south, sustained by trade-wind moisture and winter rains. The long-term precipitation trend for La Gomera shows no significant change. If any linear trend exists, it’s extremely small ($p < 0.05$ for a slight negative), on the order of a few millimeters decrease per decade over decades, which translates to maybe 10–20 mm total less rain now than in the mid-1990s. Such a change is negligible relative to natural variability, which can see differences of that magnitude from one decade to the next easily. Accordingly, normalized precipitation trend (~ -0.027) is basically flat. Therefore, while temperatures and relative humidity have changed, the actual rainfall input to La Gomera’s ecosystems appears to be unchanged. The island’s dense forests and terraces likely still receive similar rain amounts as before, it’s the evaporation and dryness of air that have increased due to warmth, not a reduction in rainfall.

Wind:

Wind patterns on La Gomera have altered only slightly over the 30-decade span. The fastest winds each day are up by ~ 0.25 m/s in total ($p < 0.05$), which is about $+0.08$ m/s per decade, effectively a very small increase. The calmest daily winds have decreased by ~ 0.09 m/s ($p < 0.05$). In plain terms, this means windy days might be imperceptibly windier and calm nights perhaps a touch calmer, but these changes are marginal. La Gomera's complex terrain will continue to dominate local wind patterns, with significant spatial variability around the island, and nothing in the data suggests a major shift in those patterns.

AET, PET, and SPEI (In Development)

3.1.6 Lanzarote

Comparison of the trend between climate variables:

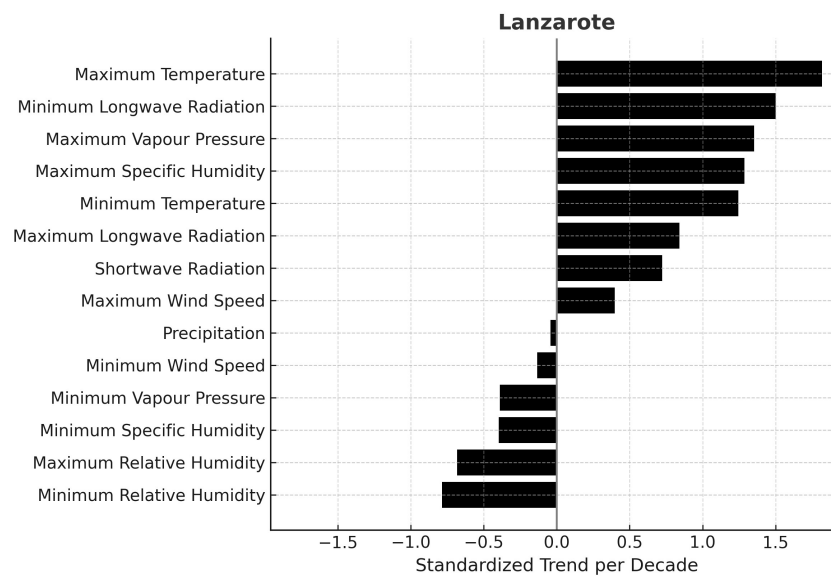


Figure 37: Lanzarote – Normalized Trends

Lanzarote's interior climate trends are characterized by strong warming and a drying in relative humidity. Maximum temperature has a very high normalized trend (~ 1.82), and minimum temperature, while positive, is a bit lower (~ 1.10) reflecting smaller night-time changes. Nighttime longwave radiation increased (~ 1.37), and maximum longwave radiation is up (~ 0.68). Absolute humidity has risen: maximum vapour pressure (~ 1.45) and maximum specific humidity (~ 1.40) both show large positive changes. Relative humidity trends indicate pronounced drying at minimum humidity (~ -0.80) and a noticeable decline at maximum relative humidity (~ -0.68) as well. Minimum vapour pressure (~ -0.38) and specific humidity (~ -0.39) trends are moderately negative, consistent with very dry conditions at the driest times. Precipitation's trend is effectively flat (~ -0.043 normalized, essentially no change in an already minimal rainfall regime). Wind changes are slight: minimum wind down

a bit (~ -0.13) and maximum wind up a bit (~ 0.40). Overall, Lanzarote has become much hotter and relatively drier, though as an already arid island, the relative changes occur on a background of low moisture.

Temperature and Radiation:

Lanzarote, being low-lying and exposed, has warmed significantly in the last few decades. Daily high temperatures have increased by approximately 0.7°C per decade ($p < 0.05$), totaling around $+2.1^\circ\text{C}$ from 1995 to 2024. This is a substantial warming, bringing already hot summer peaks to new highs. Interestingly, the daily low temperatures have risen a bit less than in other islands, about 0.15°C per decade ($p < 0.05$), which accumulates to roughly $+0.45^\circ\text{C}$ over 30 years. This suggests that nighttime warming on Lanzarote is somewhat muted compared to the daytime warming. Likely factors could be the island's flat terrain and persistent trade winds, which allow effective night cooling to continue. In line with the warming, downward longwave radiation trends upward: nighttime longwave radiation increased roughly $\sim 1.0\text{ W/m}^2$ per decade ($p < 0.05$), a bit less than other islands due to the smaller night warming, and daytime longwave radiation by about $\sim 0.8\text{ W/m}^2$ per decade ($p < 0.05$). Shortwave radiation shows perhaps a slight rise ($\sim 0.28\text{ W/m}^2$ per decade, $p < 0.05$), possibly due to even fewer clouds. Lanzarote's skies are typically clear, and they remain so.

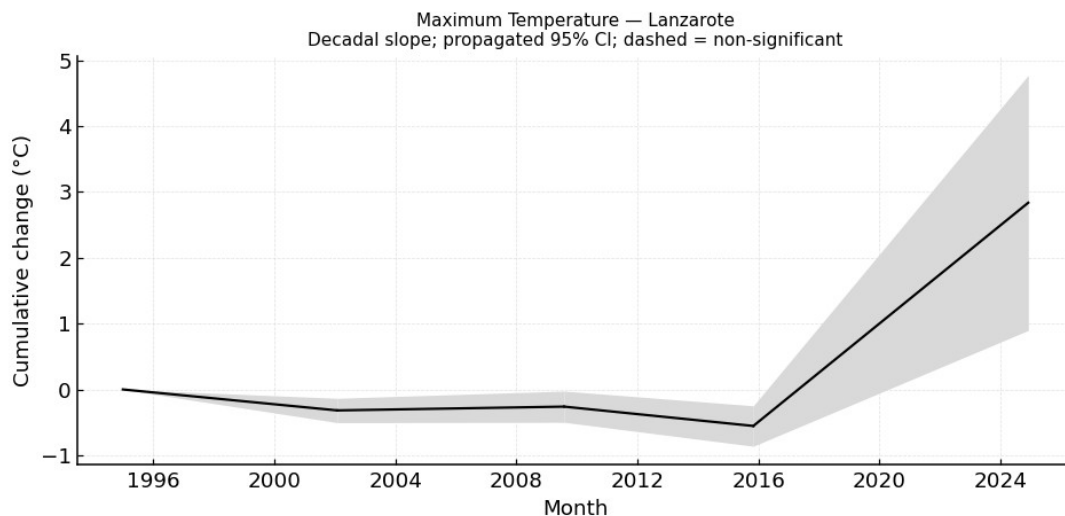


Figure 38: Maximum Temperature Trend - Lanzarote

Humidity and Moisture:

In Lanzarote's arid climate, absolute humidity has increased slightly, but relative humidity has decreased significantly as the island warms. The maximum vapour pressure is up by $\sim 0.65\text{ hPa}$ ($p < 0.05$), and maximum specific humidity by $\sim 0.0004\text{ kg/kg}$ ($p < 0.05$). Those numbers may sound small, but in percentage terms they represent a notable increase in absolute moisture for a desert-like environment – the air can carry a bit more moisture now thanks to higher temperatures and evaporation from the surrounding ocean. However, relative humidity has dropped because the warming expands the air's capacity for

moisture even more. The minimum relative humidity (which in Lanzarote on a hot afternoon can be extremely low) fell by roughly 3–4% ($p < 0.05$) over the 30-year period. So, if for instance, typical summer afternoon relative humidity was ~20%, it might now be ~16–17%. That makes already dry conditions feel even drier. The maximum daily relative humidity (often at night or early morning before sunrise) also declined slightly, by on the order of 1% ($p < 0.05$). Nights in Lanzarote, which often saw humidity recover to maybe 80–90% with dew in some areas, now might top out at a slightly lower value because the nights are a bit warmer. Still, relative humidity at night remains fairly high (the island often cools enough to reach dew point in localized spots). In summary, Lanzarote’s climate has shifted to an even drier regime in relative terms: daytime dryness is more extreme, and nighttime humidity doesn’t quite reach past levels (though it’s still much higher than daytime relative humidity). Absolute humidity went up, but it was starting from a low base; relative humidity went down because the temperature effect dominates. These trends correspond to normalized changes of ~ -0.80 (minimum relative humidity) and ~ -0.68 (maximum relative humidity), indicating a substantial drying signal for the island.

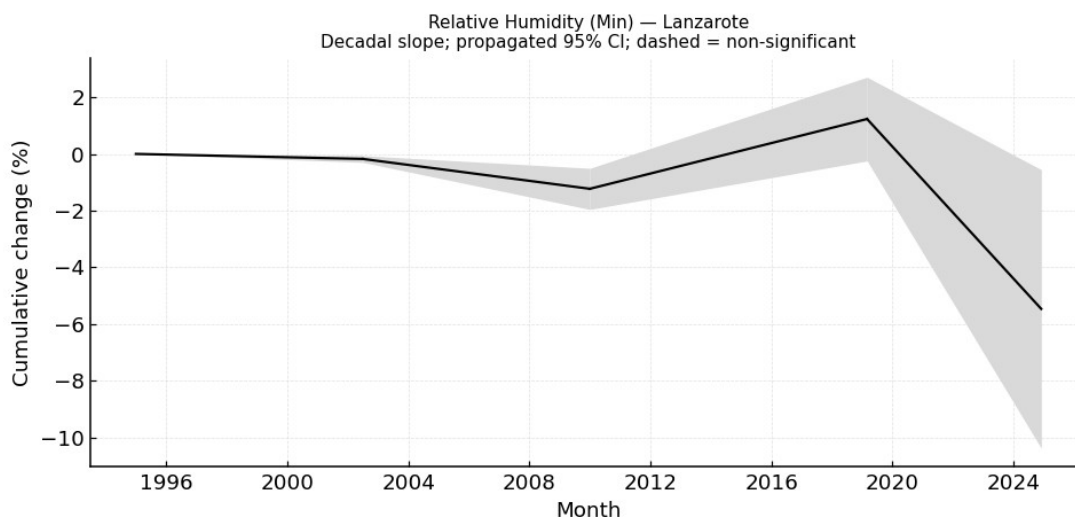


Figure 39: Minimum Relative Humidity Trend - Lanzarote

Precipitation:

Lanzarote is one of the driest places in the Canary Islands, averaging on the order of 100 mm of rain per decade or less in many areas. This rainfall is highly erratic and often comes from the odd winter shower or decaying frontal system. The long-term data indicate no statistically significant trend in this scant precipitation. Essentially, Lanzarote was dry in the 1990s and remains just as dry today ($p < 0.05$ for a minuscule negative trend). Over 30 years, any linear change is on the order of a few millimetres, utterly inconsequential relative to variability. The normalized precipitation trend (~ -0.043) underscores that there’s been no real change. In practical terms, drought frequency or average annual rainfall in Lanzarote has not shifted. The island’s groundwater and soil moisture will deplete faster under higher heat, but they are not being replenished any less by rain than before. Thus, Lanzarote’s aridity has intensified in a relative sense, but the climate has not become any drier in an absolute sense of rainfall received.

Wind:

Winds on Lanzarote are heavily influenced by the trade winds and local convection, and the long-term changes in wind metrics are slight. The strongest daily winds have a mild upward trend (~ 0.20 m/s total since 1995, $p < 0.05$), equating to ~ 0.07 m/s per decade. This could reflect a barely detectable increase in the frequency or strength of windy days, but it's a very small signal. The calmest daily winds have changed by about -0.05 m/s ($p < 0.05$), essentially no change at all.

3.1.7 Fuerteventura

Comparison of the trend between climate variables:

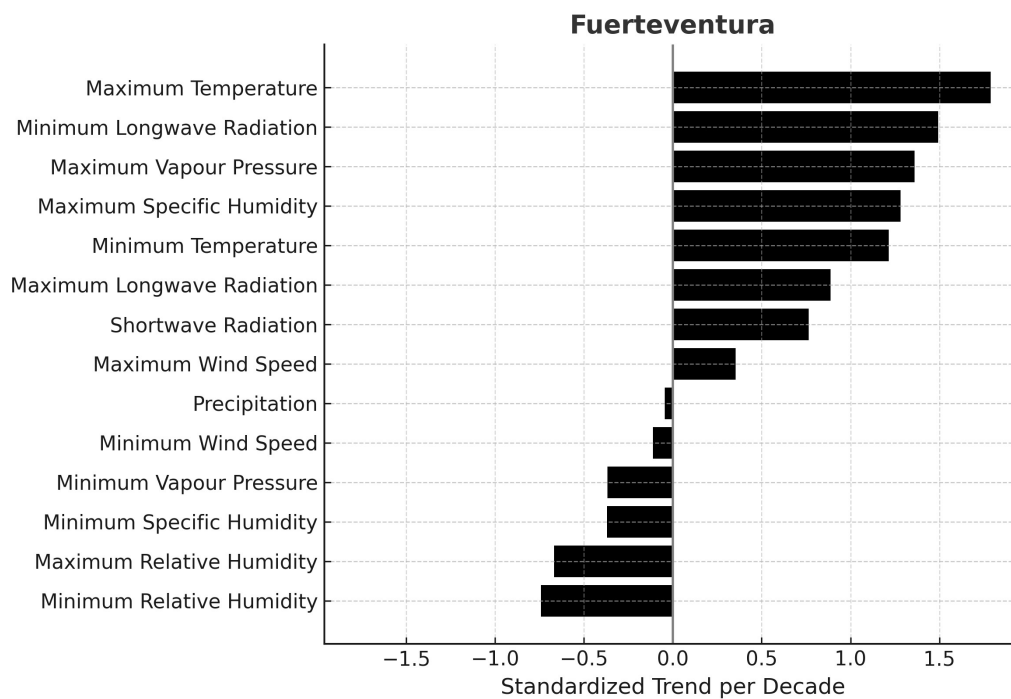


Figure 40: Fuerteventura – Normalized Trends

Fuerteventura's interior climate trends, like Lanzarote's, show a strong warming and drying pattern. Maximum temperature has a high normalized increase (~ 1.79), and minimum temperature is positive but smaller (~ 1.10). Nighttime longwave radiation is up (~ 1.32), with maximum longwave also increased (~ 0.66). Absolute moisture has risen: maximum vapour pressure (~ 1.43) and maximum specific humidity (~ 1.33) both show large positive shifts. Relative humidity trends are downward: minimum relative humidity drops (~ -0.85), and maximum relative humidity also edges down (~ -0.67). Minimum vapour pressure (~ -0.38) and specific humidity (~ -0.37) trends point to very dry low-humidity periods. Precipitation trend is essentially flat (~ -0.044 normalized). Wind changes are minor: minimum wind down slightly (~ -0.11) and maximum wind up slightly (~ 0.35). Overall, Fuerteventura has become significantly hotter and relatively drier, reinforcing its desert climate characteristics.

Temperature and Radiation:

Fuerteventura has warmed markedly over the past years, closely paralleling Lanzarote's trend. The island's daily high temperatures have risen by about 0.7 °C per decade ($p < 0.05$), amounting to roughly +2.1 °C in 30 years. Daily low temperatures are up about 0.15 °C per decade ($p < 0.05$), around +0.45 °C total – again a somewhat smaller night-time warming, likely due to similar reasons as Lanzarote (flat terrain, efficient nighttime cooling). These changes are quite significant in a place that already experiences hot conditions, new record highs have likely been set in recent years. Correspondingly, nighttime longwave radiation increased on the order of ~1.0 W/m² per decade ($p < 0.05$) and daytime longwave by ~0.8 W/m² per decade ($p < 0.05$), reflecting the warmer air and surface. Shortwave radiation shows a small rise (~0.27 W/m² per decade, $p < 0.05$), which could indicate even fewer clouds on average. The warming is the primary climate change factor (maximum temperature normalized ~1.79).

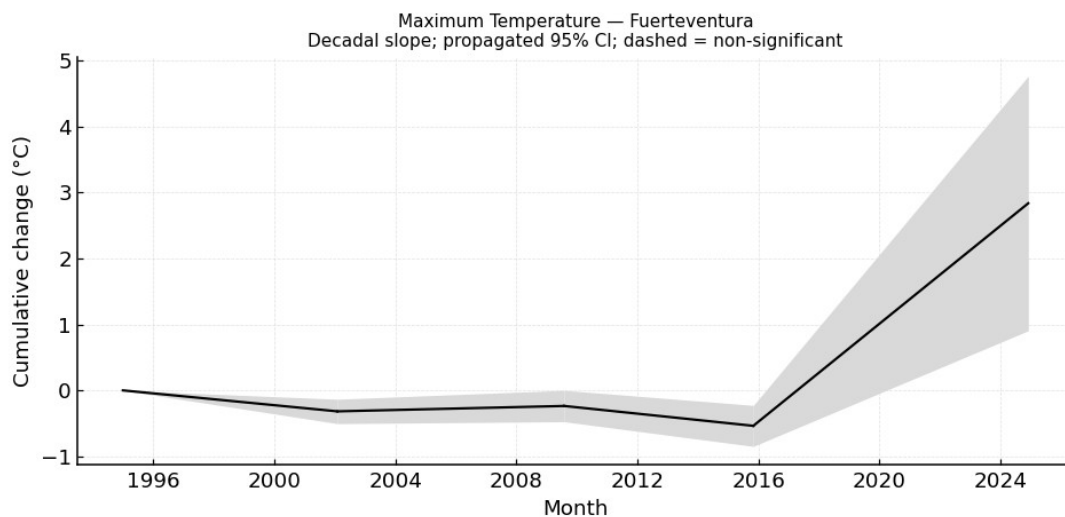


Figure 41: Maximum Temperature Trend – Fuerteventura

Humidity and Moisture:

Fuerteventura's atmosphere now carries slightly more moisture in absolute terms, but the relative humidity has decreased with rising temperatures. The maximum vapour pressure increased by ~0.65 hPa ($p < 0.05$) since 1995, and maximum specific humidity by ~0.0004 kg/kg ($p < 0.05$). This implies an uptick in absolute moisture content during humid periods, fed by the warm surrounding ocean. Nevertheless, relative humidity at the driest time of day has fallen significantly. The minimum relative humidity dropped by roughly 3% ($p < 0.05$) over 30 years (~1% per decade). In practical terms, already parched afternoons are even drier. The maximum relative humidity has also decreased slightly, by roughly 1% or so ($p < 0.05$). Fuerteventura's nights, which can see humidity rise with cooling, are a bit warmer now, so they don't reach quite as high relative humidity as before. But they still can get

relatively humid, often above 80% in predawn hours in low-lying areas, just a tad less often touching saturation. So, the overall pattern is consistent with a warming desert climate that is more moisture in the air in an absolute sense, but proportionally less relative humidity because the capacity of the air has grown more. The normalized drops in relative humidity (~ -0.85 for minimum relative humidity, ~ -0.67 for maximum relative humidity) signify that this drying is a key part of Fuerteventura's climate change signal.

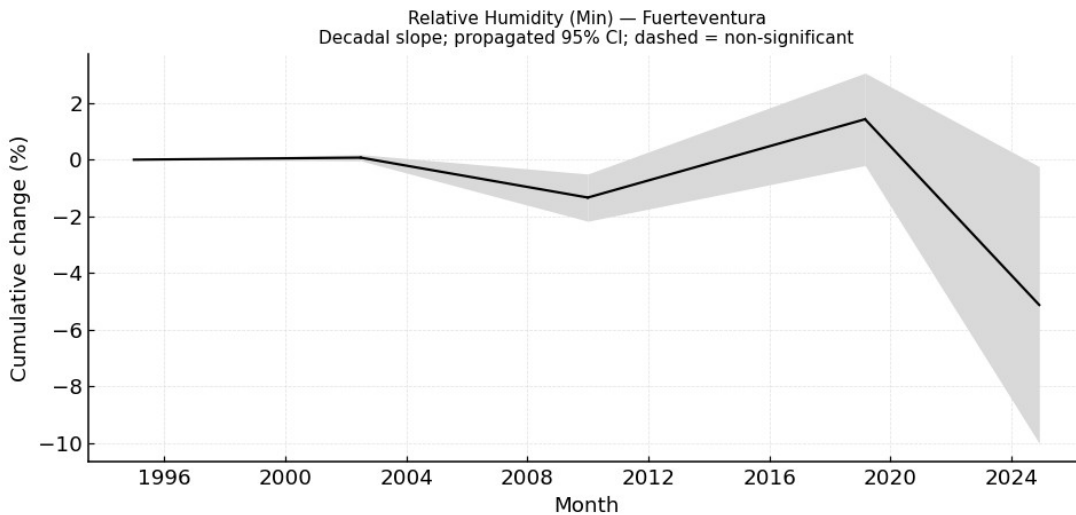


Figure 42: Minimum Relative Humidity - Fuerteventura

Precipitation:

Fuerteventura is extremely arid, averaging on the order of 100 mm of rain per year or less, and similar to Lanzarote. There is no evidence of a significant trend in this meager precipitation. Any linear change from 1995 to 2024 is vanishingly small ($p < 0.05$ for a negligible negative slope). The island continues to have very infrequent rainfall, with large variability driven by occasional storms or the lack thereof. The normalized precipitation trend (~ -0.044) basically indicates stability, no meaningful change in how much rain falls annually.

Wind:

The wind climate of Fuerteventura shows only trivial changes. The maximum wind speeds have a slight upward trend (~ 0.18 m/s total over 30 years, $p < 0.05$), or about $+0.06$ m/s per decade. This tiny increase suggests virtually no perceivable change. The minimum wind speeds have changed by about -0.04 m/s ($p < 0.05$), which is essentially no change at all, calm conditions in Fuerteventura, which are not very common given its exposure, are just as calm.

3.2 Azores

3.2.1 Azores – Western Group

Comparison of the trend between climate variables:

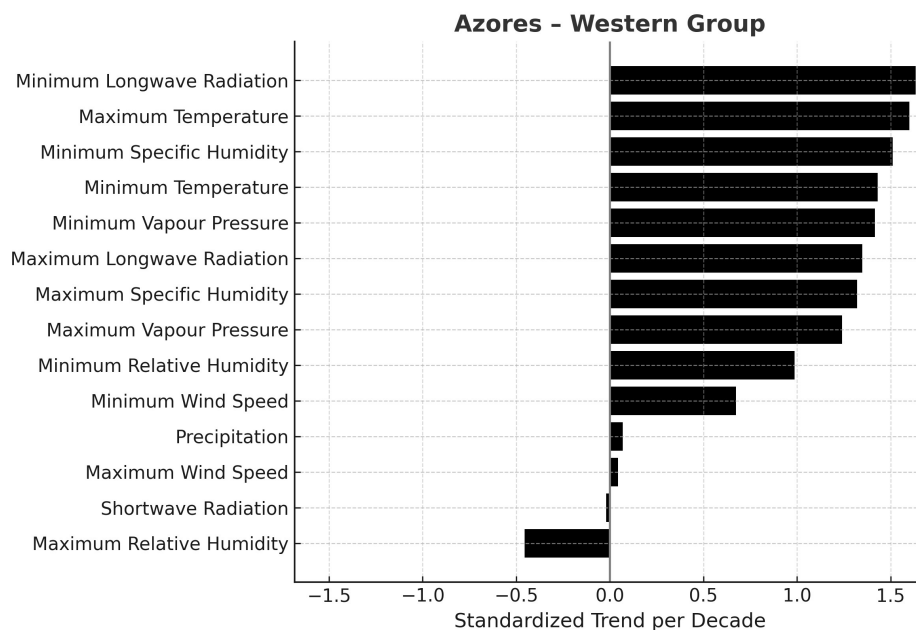


Figure 43: Western Group of Azores – Normalized Trends

The Western Azores show coherent warming and moistening trends. Overall, the variables with the largest relative changes are night-time longwave radiation, maximum temperature, specific humidity (especially minimum), and vapour pressure (normalized trend ~1.3–1.6). Variables like precipitation, wind, and shortwave radiation have very small normalized trends (≤ 0.07).

Temperature and Radiation:

Across the Western Group, both daytime and nighttime air temperatures exhibit statistically significant positive trends. Maximum temperature increases by approximately $+0.65$ °C per decade and minimum temperature by $+0.74$ °C per decade ($p < 0.05$). The slightly greater rise in minimum temperature results in a progressive reduction of the diurnal temperature range.

Longwave radiation fluxes also display pronounced upward trends, with outgoing daytime flux increasing by approximately $+1.55$ W/m² per decade and nighttime flux by $+2.46$ W/m² per decade. These increases are consistent with enhanced thermal emission from a warming surface–atmosphere system. In contrast, shortwave radiation remains effectively

stable, showing a negligible weighted trend of -0.37 W/m^2 per decade, indicating little or no long-term change in incident solar energy.

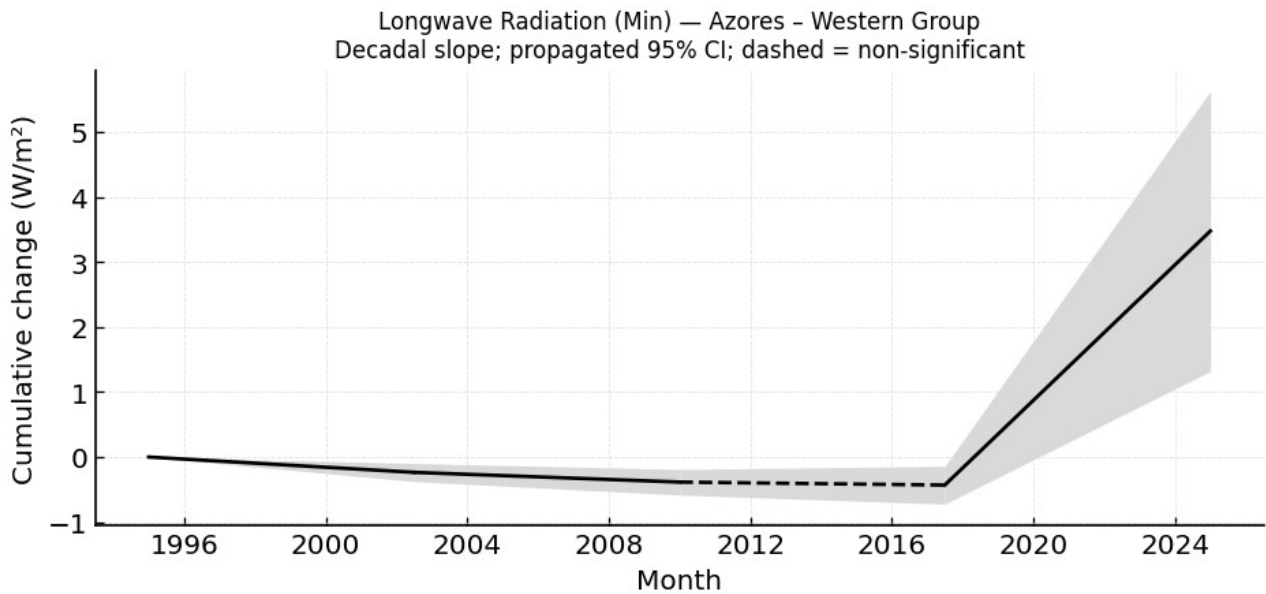


Figure 44: Minimum Longwave Radiation – Azores Western Group

Humidity and Moisture:

Atmospheric moisture content exhibits clear upward trends. Maximum specific humidity increases by approximately $+0.00039 \text{ kg/kg}$ per decade and $+0.000384 \text{ kg/kg}$ per decade the minimum values, implying a substantial rise in absolute humidity. Vapour pressure similarly increases by approximately $+56\text{--}57 \text{ Pa}$ per decade ($p < 0.05$).

Relative humidity trends are heterogeneous, nighttime relative humidity rises by about $+1.54 \%$ per decade ($p < 0.05$), whereas daytime values remain nearly constant (-0.08% per decade). Collectively, these results indicate an increasingly humid nocturnal atmosphere, while daytime relative humidity remains stable. The concurrent rise in specific humidity with relatively unchanged relative humidity suggests an overall warmer and moister atmosphere, consistent with the enhanced moisture-holding capacity of warmer air. Normalized slopes ($\sim 1.3\text{--}1.5$) further indicate that humidity-related variables exhibit among the strongest changes observed.

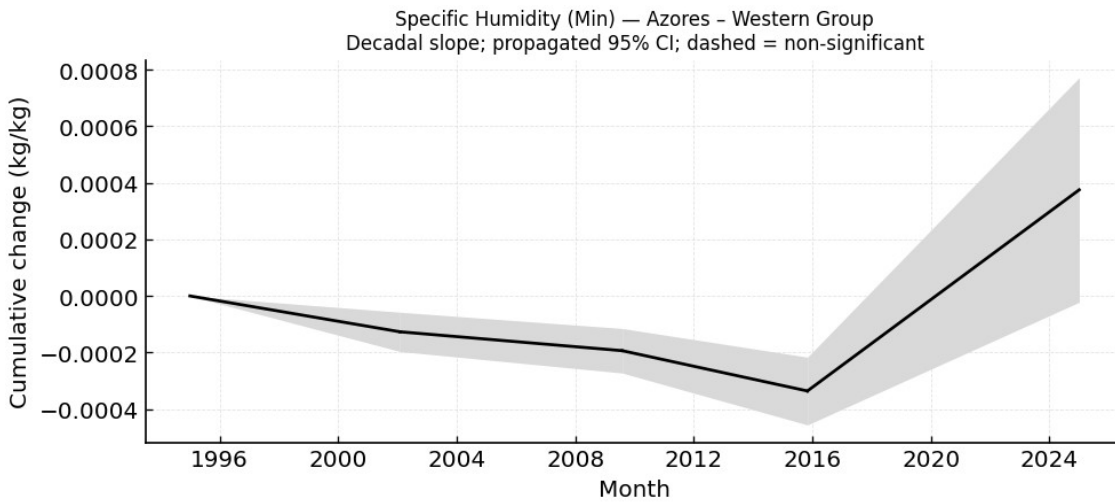


Figure 45: Minimum Specific Humidity – Azores Western Group

Precipitation:

Precipitation displays a modest positive trend of approximately +15 mm per decade ($p < 0.05$). However, when normalized to interannual variability, this represents a very small relative change (~ 0.07). Consequently, annual rainfall in the Western Azores has increased only marginally. The overall climate thus appears slightly wetter but not substantially altered in terms of aridity.

Wind:

Trends in wind speed are minor, averaging approximately +0.07 m/s per decade for both daily maxima and minima ($p < 0.05$). Given the low normalized values (< 0.1), these changes are negligible in practical terms. Wind regimes in the Western Group can therefore be regarded as essentially stable.

3.2.2 Azores – Central Group

Comparison of the trend between climate variables:

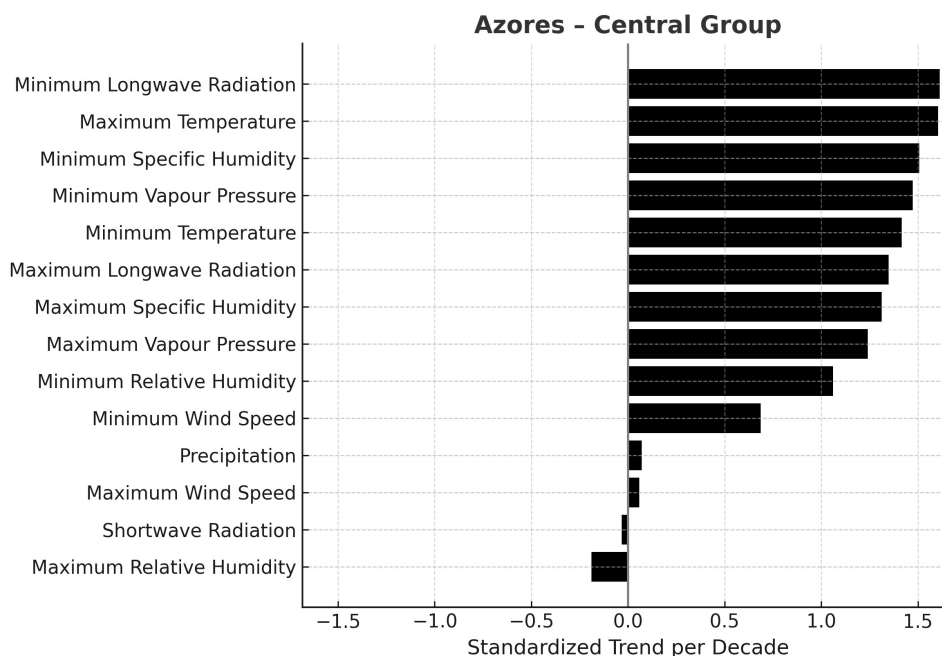


Figure 46: Central Group of Azores – Normalized Trends

The Central Group exhibits patterns comparable to those observed in the Western Group. The strongest normalized trends again occur for nighttime longwave radiation, daytime temperature, and humidity parameters, while precipitation and wind show minimal change. All reported trends are statistically significant ($p < 0.05$).

Temperature and radiation:

Temperatures are rising in the Central Group: maximum temperature trend ~ 0.64 °C/decade, minimum temperature ~ 0.73 °C/decade (both $p < 0.05$). Again, night-time lows rise slightly faster, narrowing the diurnal range. Longwave radiation increases by about $+1.63$ W/m² per decade at its maximum and $+2.56$ W/m² per decade at its minimum. Maximum shortwave radiation shows a negligible negative trend (~ -0.54 W/m²/dec, normalized near zero). In sum, the group is warming significantly, with corresponding rises in outgoing longwave energy, while solar flux is essentially unchanged.

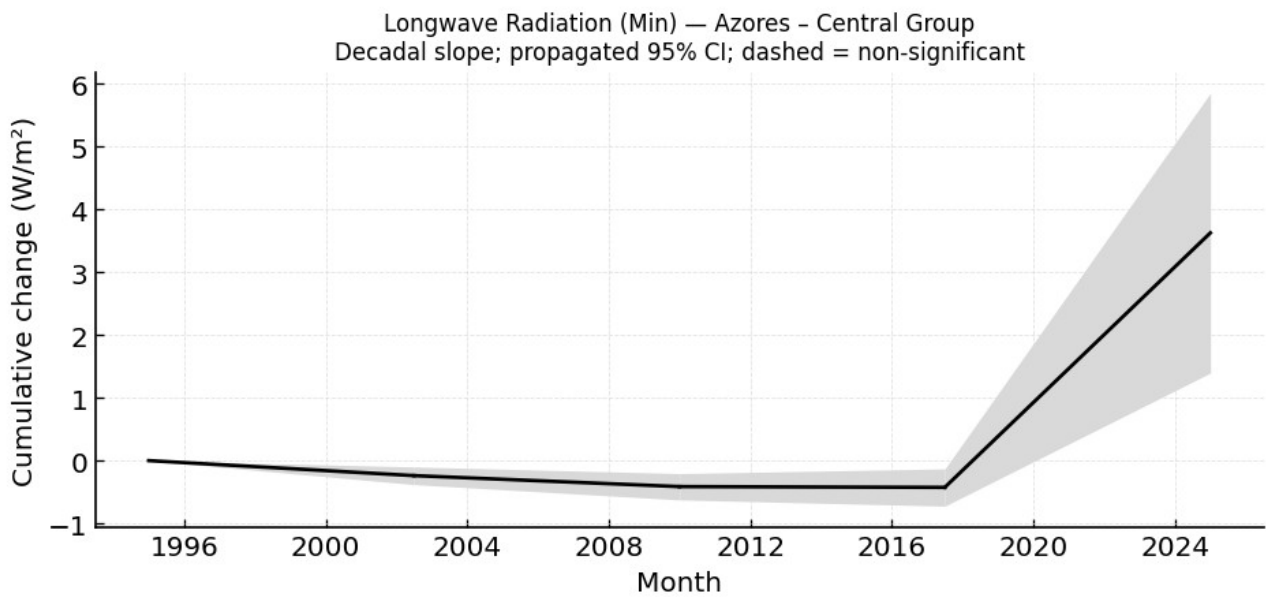


Figure 47: Minimum Longwave Radiation – Azores Central Group

Humidity and moisture:

Absolute humidity is increasing notably. Relative humidity minimum rises $\sim 1.59\%$ /decade ($p < 0.05$) while relative humidity maximum is unchanged ($\sim -0.03\%$). Specific humidity increases $\sim 0.000373\text{--}0.000386$ kg/kg per decade ($p < 0.05$), and vapour pressure increases $\sim 56\text{--}57$ Pa/decade. These indicate more water vapour in the atmosphere, especially at night. The normalized trends ($\sim 1.3\text{--}1.5$ for these variables) show moisture is increasing strongly relative to its variability. The pattern is the same as in the Western Group, nights become more humid, days essentially the same, consistent with warmer air holding extra moisture.

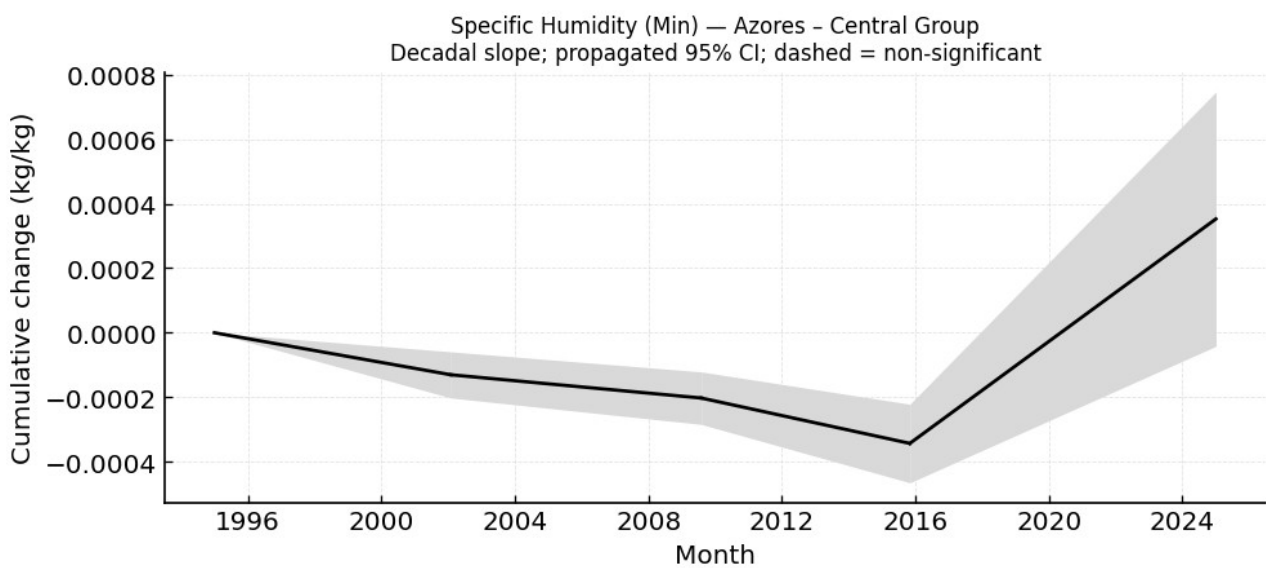


Figure 48: Minimum Specific Humidity – Azores Central Group

Precipitation:

A small increase of +15.78 mm per decade ($p < 0.05$, normalized ~ 0.07). This is statistically significant but very minor in magnitude. As in the Western Group, the modest rise in rainfall means the climate is not becoming notably drier. Rather, it is staying roughly neutral in aridity.

Wind:

Weak upward trends of about +0.091 m/s per decade for daily maximum and +0.075 m/s per decade for daily minimum ($p < 0.05$). These values are extremely small relative to typical wind speeds, as seen with the normalized trends (~ 0.06 – 0.69). In practice, wind strength has remained essentially steady in the Central Group.

3.2.3 Azores - Eastern Group

Comparison of the trend between climate variables:

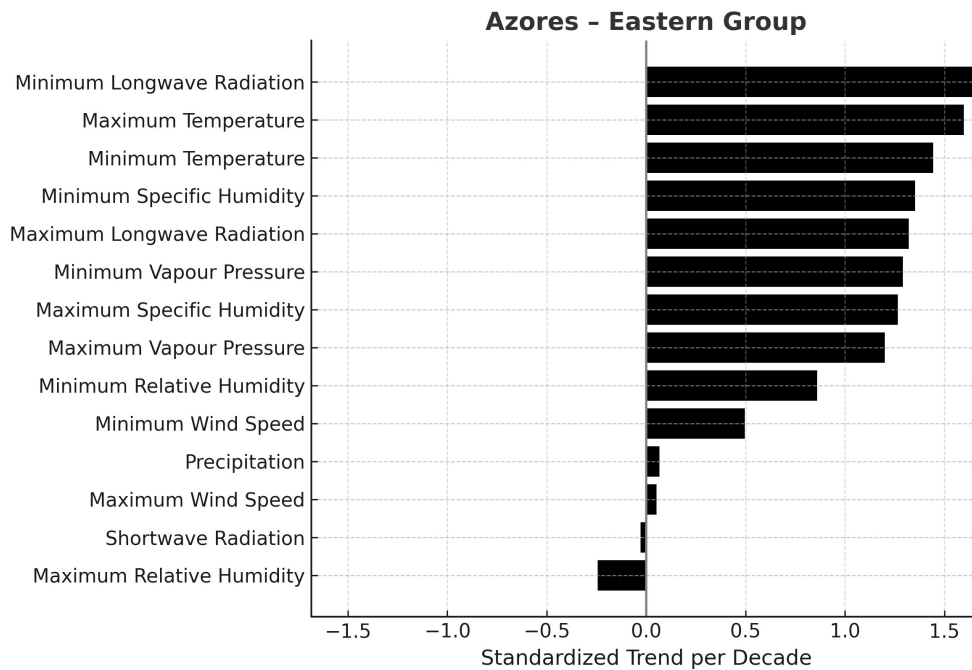


Figure 49: Eastern Group of Azores – Normalized Trends

The Eastern Azores show the same general pattern observed across the archipelago. The strongest normalized trends correspond to nighttime longwave radiation (~ 1.68), daytime temperature (~ 1.60), and atmospheric moisture variables (~ 1.20 – 1.35), while changes in precipitation and wind are minimal. All weighted trends are statistically significant ($p < 0.05$). In summary, the Eastern Group is warming, nights even more, and getting slightly

moister, just like the other groups. The increase in temperature and moisture mirrors regional trends, while precipitation rises remain very small.

Temperature and radiation:

Again, both temperatures rise significantly: +0.642 °C/dec for maximum and +0.750 °C/dec for minimum ($p < 0.05$). Night warming exceeds day warming, so diurnal range narrows as elsewhere. Daytime longwave up +1.54 W/m²/dec; nighttime longwave +2.49 W/m²/dec ($p < 0.05$ for both). Shortwave flux slightly declines (~-0.45 W/m²/dec, negligible in normalized terms). The result is a pronounced warming signal in both air temperature and outgoing longwave flux, with little change to incoming solar radiation.

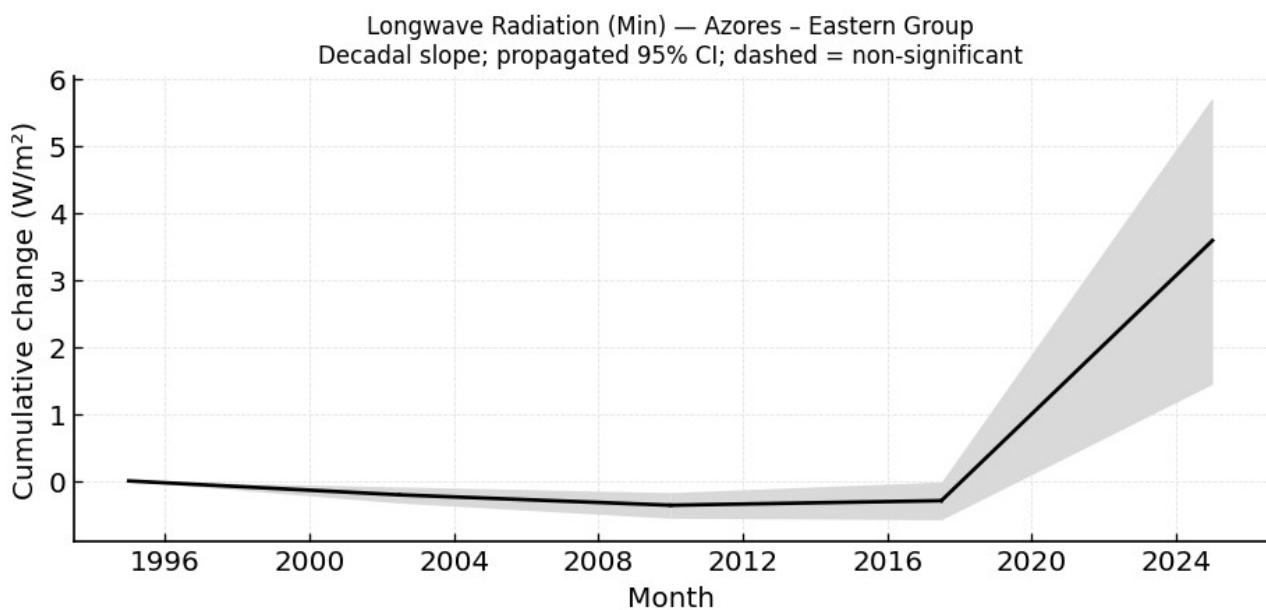


Figure 50: Minimum Longwave Radiation – Azores Eastern Group

Humidity and moisture:

Moisture content increases at nighttime with relative humidity +1.23%/dec ($p < 0.05$) and remains stable at daytime (~0.045%/decade). Maximum specific humidity up +0.000378 kg/kg and the minimum values +0.000348 kg/kg per decade. Vapour pressure maximum +55.63 Pa and minimum +52.91 Pa per decade. These trends (normalized ~1.2–1.4) indicate more water vapour in the air, especially at night. The pattern is consistent: warmer temperatures allow higher absolute humidity, yielding increased vapour pressure even with little change in relative humidity during the day.

Precipitation:

Slight positive trend of +14.38 mm/decade ($p < 0.05$), normalized ~ 0.067 . This rise is comparable to the other groups and extremely small relative to normal variation. Thus, eastern islands have had a tiny increase in rainfall, but essentially no major shift in aridity.

Wind:

Minimal increases of +0.080 m/s per decade in maximum values and +0.051 m/s per decade in minimum (both $p < 0.05$). Such small changes (normalized ≤ 0.10) imply that wind regimes remain effectively unchanged in the Eastern Group.

3.3 Madeira

3.3.1 Madeira Island

Madeira – South Coast

Comparison of the trend between climate variables:

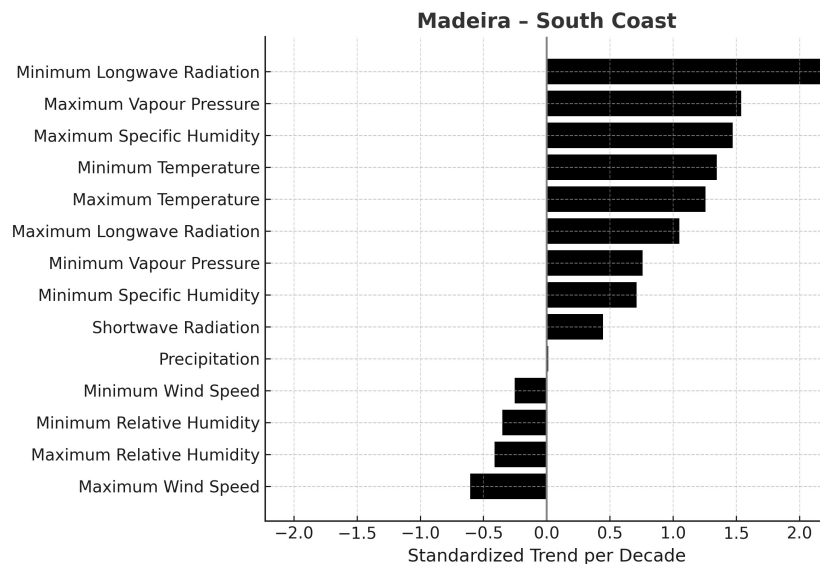


Figure 51: South Coast of Madeira – Normalized Trends

On the South Coast, the strongest upward trends are in minimum longwave radiation and atmospheric moisture. In particular, minimum daily longwave radiation shows the largest positive normalized change, followed by increases in vapour pressure and specific humidity, and by warming in temperature. Both minimum and maximum temperature rise strongly (normalized trends ~ 1.35 and 1.26 , respectively) and daily maximum longwave radiation also increases. In contrast, wind speed and relative humidity show modest

declining trends. Precipitation has a near-zero normalized trend, indicating almost no relative change. (All trends above are statistically significant at $p < 0.05$.)

Temperature and Radiation:

Temperatures are rising markedly with maximum temperatures increase by roughly $+1.05\text{ }^{\circ}\text{C}$ per decade, and minimum temperatures by about $+0.63\text{ }^{\circ}\text{C}$ per decade (both $p < 0.05$). This warming is very large compared to natural variability. Radiation trends align with this warming: daily longwave radiation has risen on average. For example, minimum longwave radiation increased by roughly $+1.94\text{ W/m}^2$ per decade, and maximum longwave by $+1.22\text{ W/m}^2$ per decade. Shortwave radiation also shows a modest rise (~ 0.54 units per decade), consistent with clearer skies or more sunshine. In other words, the South Coast is becoming warmer and slightly more insolation-rich over time.

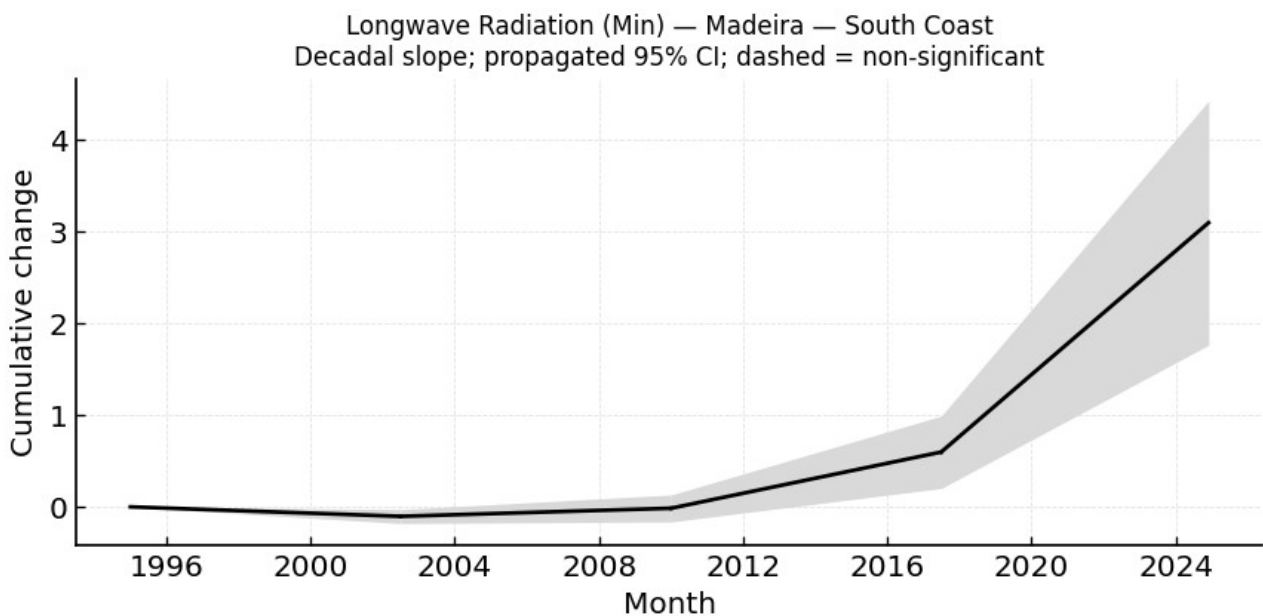


Figure 52: Minimum Longwave Radiation Trend – Madeira South Coast

Humidity and Moisture:

Despite the warming, the air is becoming moister in absolute terms. Specific is increasing: in absolute terms, daily maximum specific humidity rises by about 0.00047 kg/kg per decade ($\sim 0.47\text{ g/kg}$) and daily minimum by $\sim 0.00013\text{ kg/kg}$ per decade. Vapour shows a comparable rise of roughly $+0.73\text{ hPa}$ per decade for daily maximum and $+0.21\text{ hPa}$ per decade for daily minimum. These increases are statistically significant ($p < 0.05$). Relative humidity is trending downward, however the maximum relative humidity declines by $\sim 1.6\%$ points per decade, and daytime (minimum) relative humidity falls by about 1.9% per decade (both $p < 0.05$). This means the air is warmer and holding more moisture, but also drier relative to its saturation level. (Baseline values: typical relative humidity on the South Coast ranges from $\sim 98\%$ at night to $\sim 43\%$ in the heat of day; specific humidity ~ 0.012 to 0.005 kg/kg ; vapour pressure ~ 18.4 to 8.3 hPa .)

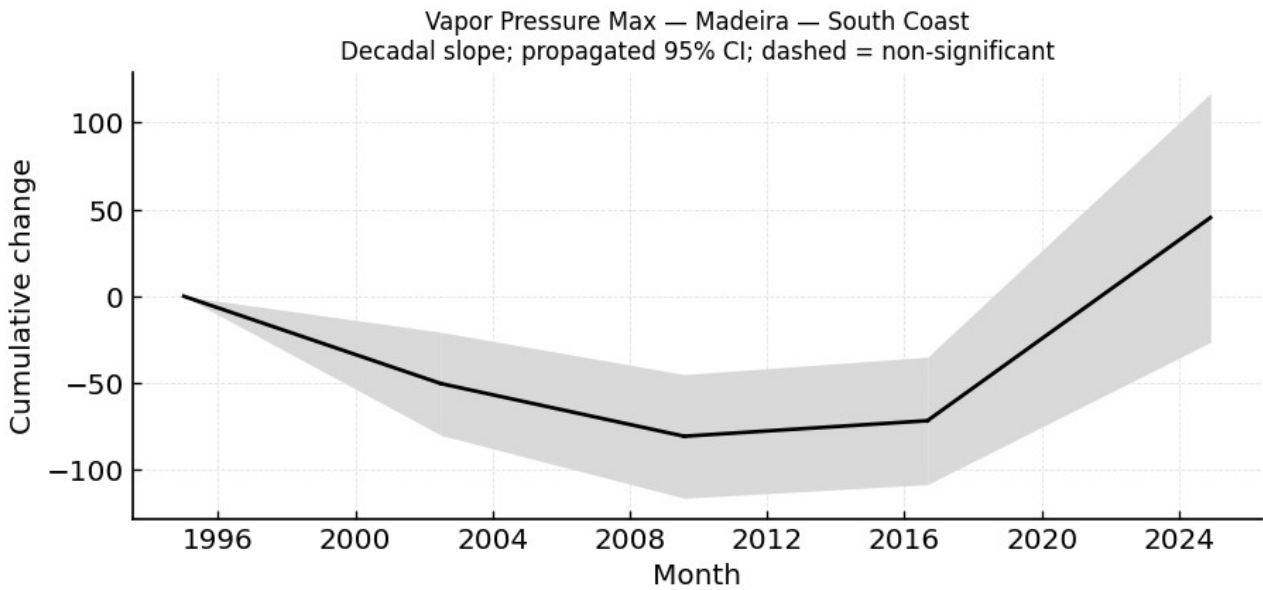


Figure 53: Maximum Vapour Pressure Trend – Madeira South Coast

Precipitation:

Annual precipitation on the South Coast averages about 645 mm. Trend analysis shows a small increase in precipitation: roughly +2.1 mm per decade ($p < 0.05$). In practical terms this is only ~0.3% increase per decade, so rainfall is essentially steady. Because of its small magnitude, the normalized trend is near zero.

Wind:

Typical winds are moderate with monthly-mean daily maximum wind ~11.7 m/s and minimum of ~0.39 m/s. Trends indicate slightly weaker winds of maximum wind speeds are decreasing by about -0.46 m/s per decade ($p < 0.05$), while minimum wind speeds are essentially unchanged (~-0.03 m/s per decade).

Madeira – North Coast

Comparison of the trend between climate variables:

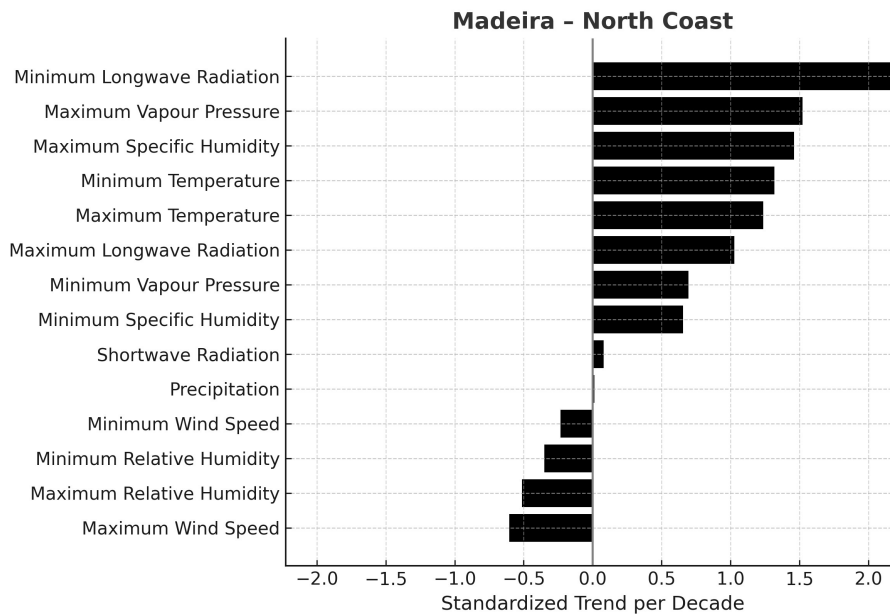


Figure 54: North Coast of Madeira – Normalized Trends

The North Coast shows a very similar pattern to the South Coast. The largest normalized increases are in nighttime longwave radiation and moisture variables. Minimum longwave radiation tops the list (normalized ~2.23), followed by rises in vapour pressure and specific humidity (normalized ~1.52–1.46), and strong warming in temperature (minimum and maximum temperature normalized ~1.32 and 1.24). Shortwave radiation has a smaller positive trend (normalized ~0.08). Declines are seen in wind speed and relative humidity: maximum wind speed (normalized ~-0.60) and relative humidity (normalized -0.51 for nighttime relative humidity) are decreasing, though these trends are much smaller in magnitude. Precipitation again has negligible normalized change (~0.013). All major trends except one are statistically significant; notably, the decrease in minimum vapour pressure here was not significant ($p \sim 0.055$).

Temperature and Radiation:

The North Coast climate is very similar to the South, warming is comparably large. It was found +1.05 °C/decade in maximum temperature and +0.63 °C/decade in minimum temperature (both $p < 0.05$). Longwave radiation is increasing: nighttime (minimum) longwave radiation ~1.95 W/m² per decade, daytime (maximum) +1.03 W/m² per decade. Shortwave radiation has a tiny rise (~0.08 units/decade, not as pronounced). In practical terms, the North Coast is warming at roughly the same pace as the South Coast, with more outgoing longwave flux as a result.

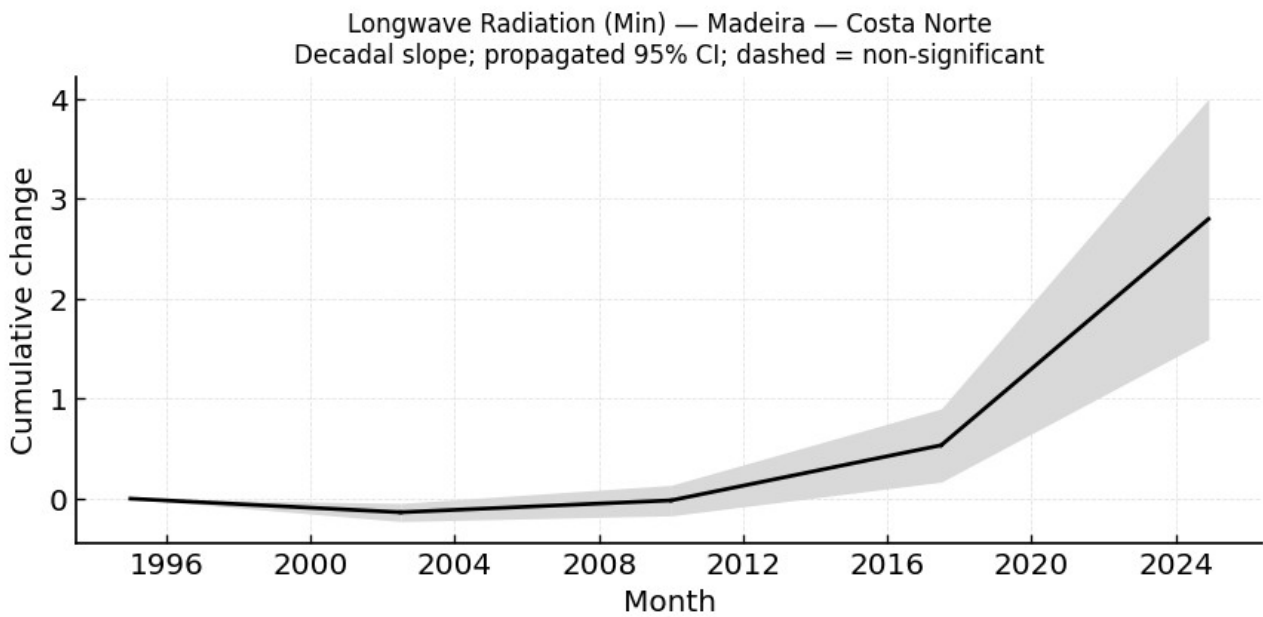


Figure 55: Minimum Longwave Radiation Trend – North Coast of Madeira

Humidity and Moisture:

Absolute humidity is rising on the North Coast. Specific humidity increases by about +0.00046 kg/kg per decade the maximum and +0.00011 kg/kg the minimum. Maximum vapour pressure rises are about +0.72 hPa/decade and +0.18 hPa/decade the minimum. In contrast, relative humidity shows modest declines with nighttime relative humidity drops roughly -1.9% per decade, daytime relative humidity -3.5% per decade (both $p < 0.05$).

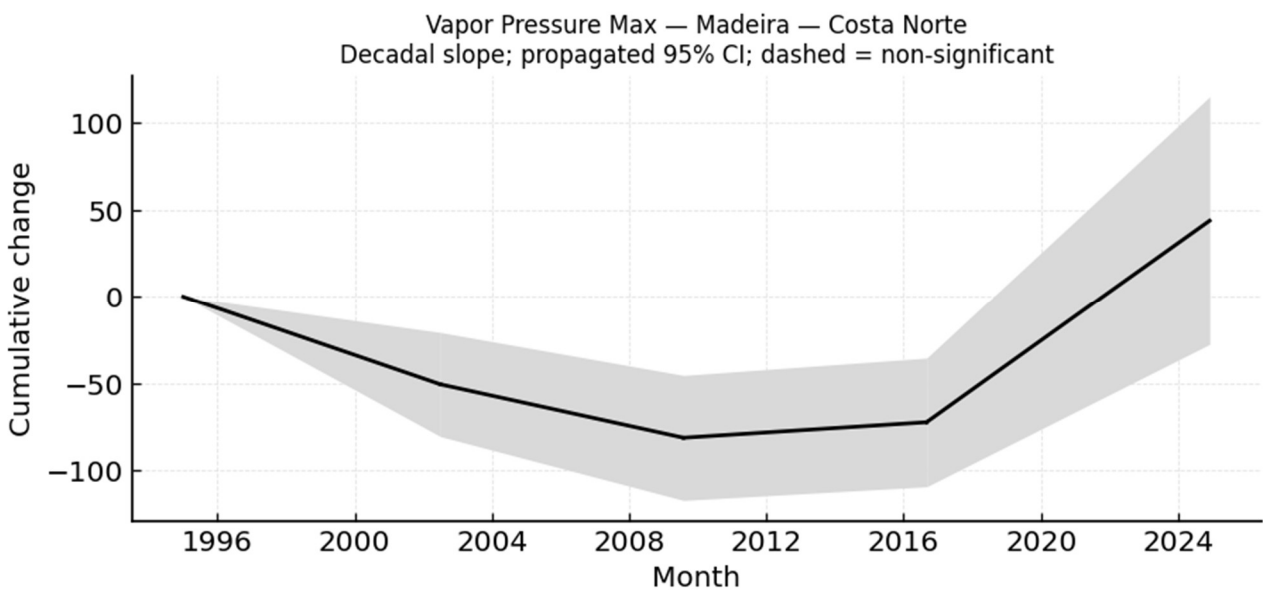


Figure 56: Maximum Vapour Pressure Trend – North Coast of Madeira

Precipitation:

North Coast mean annual rainfall is ~645 mm. The trend is a slight increase of about +2.10 mm per decade ($p < 0.05$). Again, this is a tiny fraction of the mean, on the order of +0.3% per decade. Consequently, the normalized trend is nearly zero. In practical terms, rainfall is effectively steady, with only a very small upward drift.

Wind:

Mean maximum wind on the North Coast is ~11.6 m/s and trends show a modest slowdown with maximum wind declines by ~-0.47 m/s per decade ($p < 0.05$). Minimum wind is virtually unchanged (~-0.03 m/s per decade). Overall, the strongest winds are weakening slightly, similar to the South Coast.

Madeira – Mountain Regions

Comparison of the trend between climate variables:

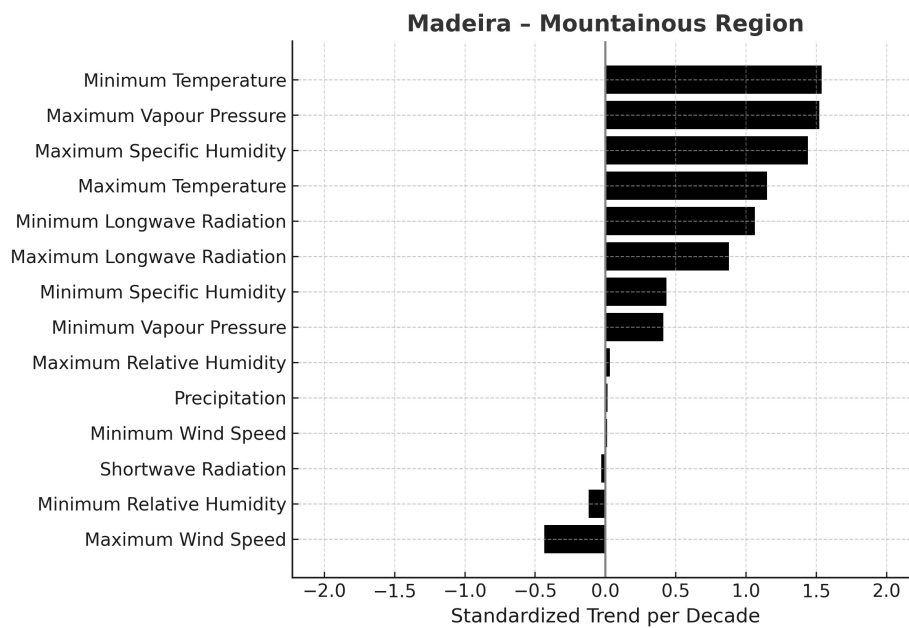


Figure 57: Mountainous Region of Madeira – Normalized Trends

In the mountainous interior, temperature trends dominate. The largest normalized trend is in minimum temperature (~1.54), followed closely by maximum vapour pressure and specific humidity (~1.52 and 1.44), then maximum temperature (1.15) and night-time longwave (1.06). Daytime longwave radiation has a smaller rise (0.88). The strongest negative trend is a decrease in maximum wind speed (~-0.44). Other declines are minor (nighttime relative humidity ~-0.12; shortwave nearly zero). Precipitation again shows an almost zero normalized trend (~0.015). All these trends are statistically significant ($p < 0.05$). In short, this region is transitioning towards a warmer, more humid, but not wetter climate, with weaker winds and an amplified nighttime heat retention effect.

Temperature and Radiation:

The highlands are cooler are mean annual maximum $\sim 18.8^{\circ}\text{C}$ and minimum $\sim 6.8^{\circ}\text{C}$. Nevertheless, they are warming strongly. Minimum temperature is increasing $\sim 0.70^{\circ}\text{C}$ per decade and maximum $\sim 1.11^{\circ}\text{C}$ per decade ($p < 0.05$). Thus, mountain warming is comparable or even slightly higher than on the coasts (especially the larger increase in nightly minima). Longwave radiation increases are present but smaller: nighttime longwave rises $\sim 1.06 \text{ W/m}^2$ per decade, daytime $+0.88 \text{ W/m}^2$. Shortwave radiation shows effectively no trend (small negative ~ -0.03 units/decade). In summary, mountain temperatures are rising by roughly a tenth of a degree per year, significantly altering the climate at higher elevations.

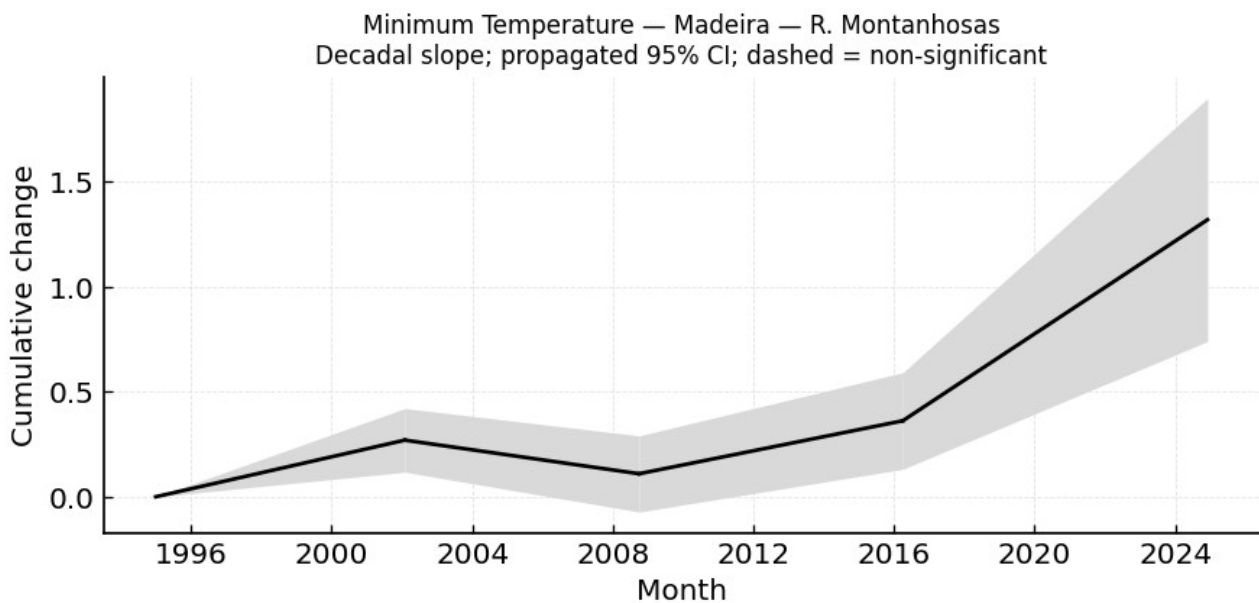


Figure 58: Minimum Temperature Trend - Mountainous Region of Madeira

Humidity and Moisture:

Absolute humidity is rising but from a much drier baseline. Maximum specific humidity increases $\sim 0.00040 \text{ kg/kg}$ per decade and maximum vapour pressure $+0.72 \text{ hPa/decade}$. Daily minimum specific humidity and vapour pressure also rise modestly. Relative humidity trends are weak, nighttime relative humidity is nearly flat ($+0.3$ points/decade, $p \sim 0.14$ not significant), and daytime relative humidity shows a slight decline (-1.2 points/decade, $p < 0.05$). Baseline conditions of relative humidity nearly 99% at night but only $\sim 14\%$ in afternoon. Thus, even though the air is very dry in the mountains (especially daytime), it is becoming slightly moister in absolute terms with higher vapour pressure, but relative humidity is mostly unchanged.

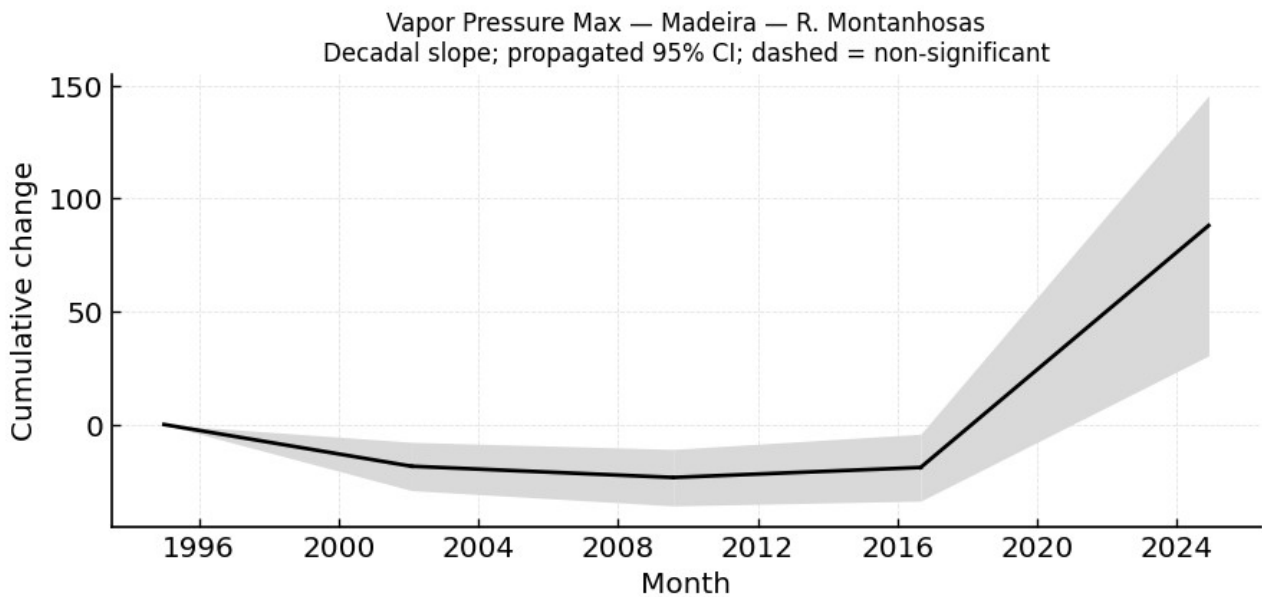


Figure 59: Maximum Vapour Pressure Trend - Mountainous Region of Madeira

Precipitation:

The mountains receive the heaviest rainfall (~1014 mm/year). Precipitation is increasing slightly with about +4.15 mm per decade ($p < 0.05$). This is about a +0.4% per decade rise. The normalized trend is near zero. Practically, rainfall in the mountains has remained essentially constant, perhaps with a barely perceptible increase.

Wind:

Winds are strongest here with maximums of ~16.5 m/s. Maximum wind speed shows a slight decline (~-0.52 m/s per decade, $p < 0.05$) and minimum wind is flat. Thus, mountain winds are weakening by a few percent per decade, though variability is high.

3.3.2 Porto Santo

Comparison of the trend between climate variables:

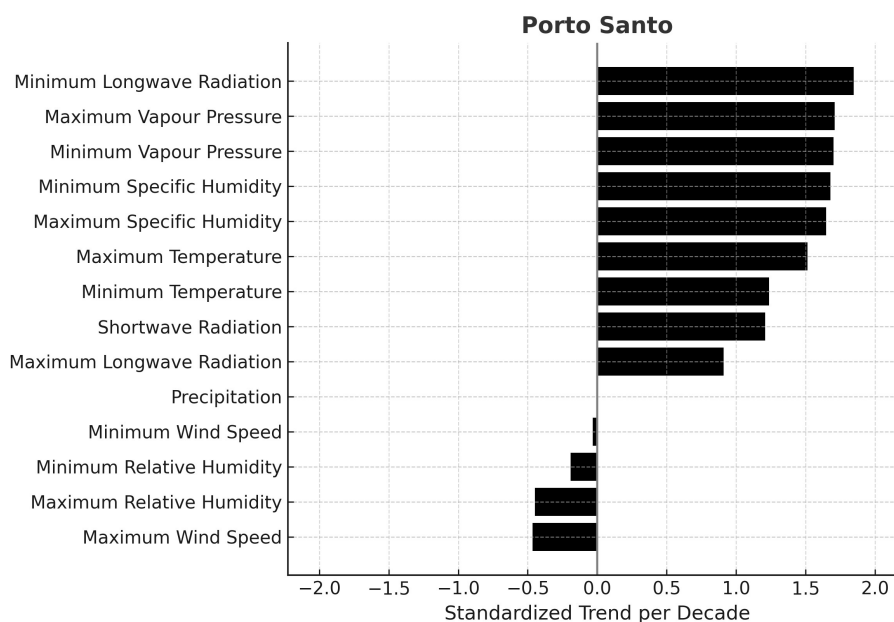


Figure 60: Porto Santo – Normalized Trends

The climate trends observed on Porto Santo closely resemble those identified for Madeira. The largest normalized increases occur in nighttime longwave radiation (approximately 1.85) and in the atmospheric moisture variables, namely vapour pressure and specific humidity (ranging from about 1.70 to 1.68). Temperature follows, with maximum temperature showing a normalized increase of around 1.51 and minimum temperature of approximately 1.24. Shortwave radiation also rises (normalized value 1.21), while daytime longwave radiation presents a moderate increase (0.91). Declines are evident in wind and humidity indicators: maximum wind speed decreases (-0.47) and relative humidity declines both at night (-0.45) and during the day (-0.19). The precipitation trend is nearly zero (-0.006 normalized). All major trends described here are statistically significant ($p < 0.05$). The combination points to a more energy-loaded and humid but comparatively drier atmosphere, consistent with the broader warming pattern across Madeira's region.

Temperature and Radiation:

Porto Santo records the warmest mean temperatures within the archipelago, with an average annual maximum of approximately 20.2 °C and a minimum near 14.4 °C. The island is also experiencing a progressive warming trend, though the rate of change is slightly lower than that observed on Madeira. The maximum temperature has increased by roughly +0.76 °C per decade, while the minimum temperature has risen by about +0.63 °C per decade (both statistically significant at $p < 0.05$). Nighttime longwave radiation has increased by approximately +1.85 W/m² per decade, and daytime longwave radiation by about +0.91 W/m² per decade. Shortwave radiation has also increased, by roughly +1.21 W/m² per decade. In summary, Porto Santo is undergoing a consistent warming trend, with

daytime temperatures that were already higher continuing to rise by nearly three-quarters of a degree per decade.

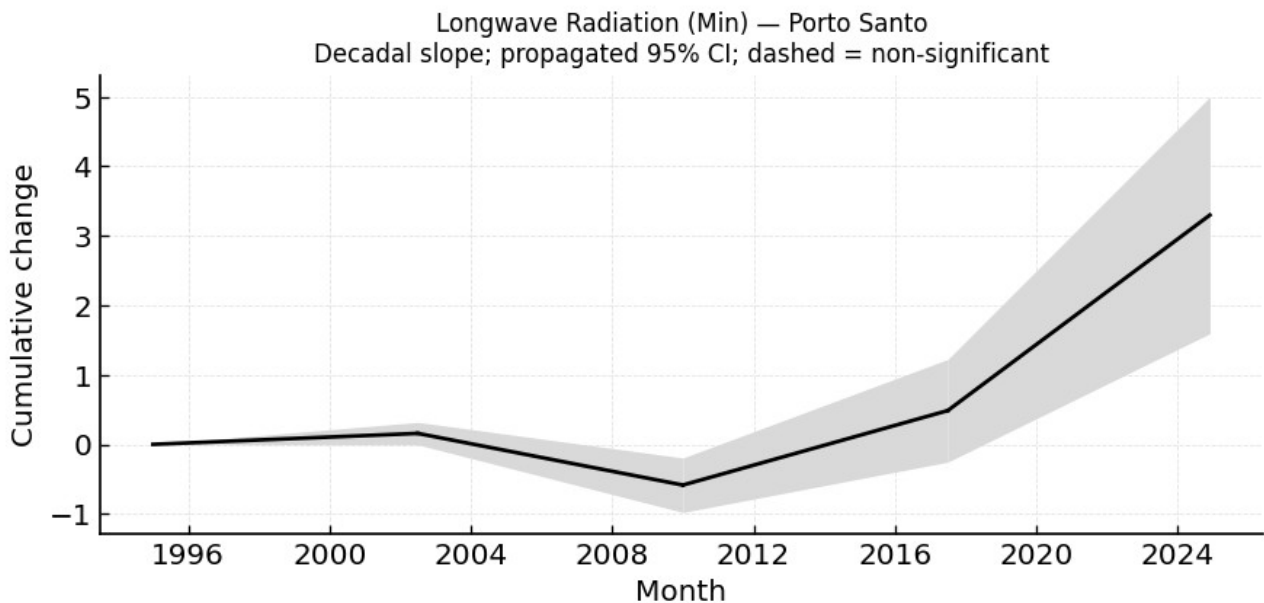


Figure 61: Minimum Longwave Radiation Trend – Porto Santo

Humidity and Moisture:

Humidity-related trends are particularly pronounced on Porto Santo. The specific humidity during the most humid periods of the day has increased by approximately +0.00062 kg/kg per decade, while vapour pressure has risen by about +0.77 hPa per decade. Even the minimum (typically nighttime) values of these variables have increased substantially. However, relative humidity has declined: nighttime relative humidity has decreased by around 1.8 percentage points per decade, and daytime relative humidity by roughly 1.1 percentage points per decade (both significant at $p < 0.05$). Baseline values indicate that relative humidity averages around 97 % at night and 52 % during the day; vapour pressure ranges from approximately 20.5 hPa to 10.3 hPa; and specific humidity varies between about 0.0127 kg/kg and 0.0064 kg/kg. As in other parts of the archipelago, the atmosphere over Porto Santo is becoming warmer and relatively drier, even as it holds more absolute moisture.

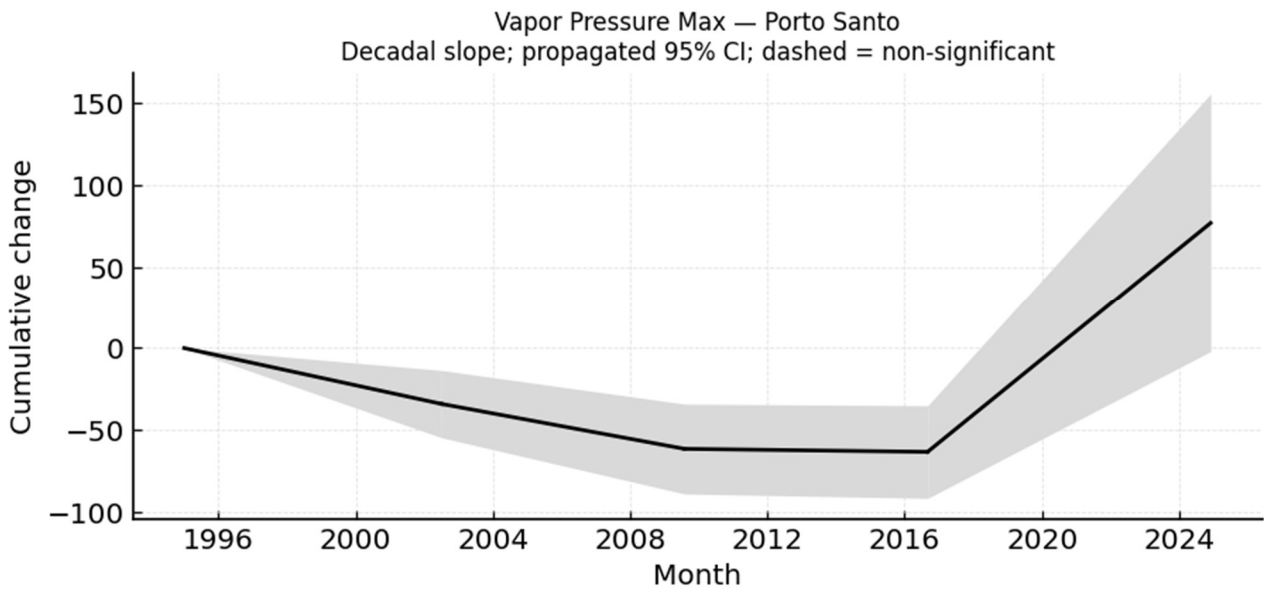


Figure 62: Maximum Vapour Pressure Trend – Porto Santo

Precipitation:

Porto Santo is characteristically dry, with mean annual precipitation around 330 mm. The data show a slight decrease in rainfall, approximately -0.47 mm per decade ($p < 0.05$). This represents a negligible change, equivalent to about -0.14% per decade. In practical terms, precipitation on the island remains stable or only very slightly declining.

Wind:

Porto Santo is exposed to relatively strong winds, with maximum values near 15.4 m/s and minimum values around 0.71 m/s. The maximum wind speed has decreased by approximately -0.33 m/s per decade ($p < 0.05$), a somewhat smaller decline than that observed on Madeira. Minimum wind speed shows no significant trend (around -0.008 m/s per decade). Overall, similar to Madeira, Porto Santo's strongest winds are weakening modestly over time.

3.4 Cape Verde

3.4.1 Santiago

Comparison of the trend between climate variables:

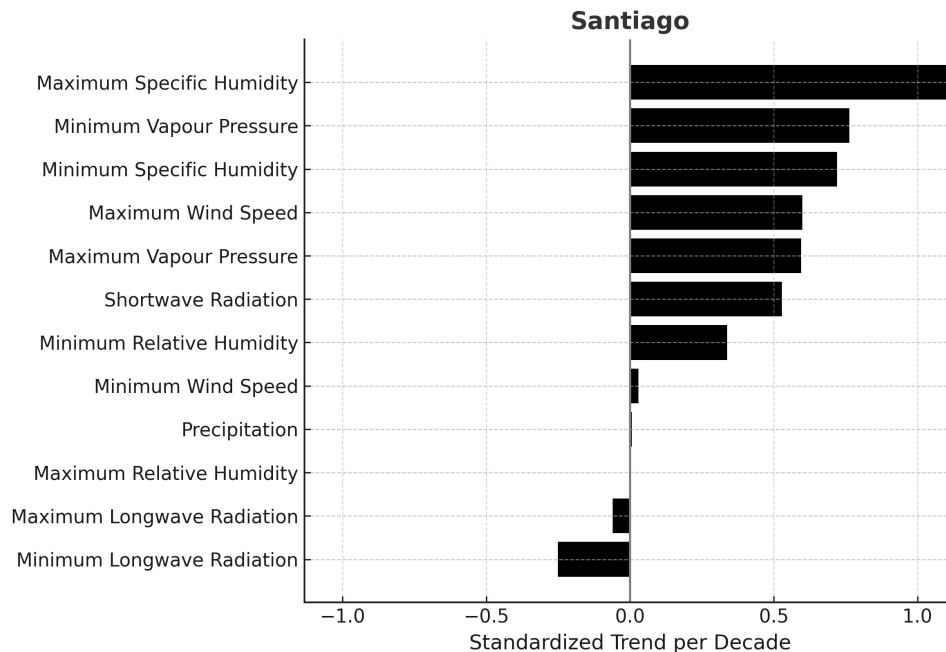


Figure 63: Santiago – Normalized Trends

In Santiago, the strongest normalized trends are in atmospheric moisture and solar radiation. Specific humidity (moisture content) shows the largest normalized increase (~1.13), followed by increases in specific-humidity minimum (~0.72) and vapour pressure (normalized ~0.76 for minima, ~0.59 for maxima). Shortwave radiation also increases substantially (normalized ~0.53). In contrast, daytime and nighttime longwave radiation both decline (normalized ~-0.06 and ~-0.25, respectively). Relative-humidity has essentially no trend at the daily maximum, and precipitation's normalized trend is near zero (~0.006). Nearly all these trends are statistically significant ($p < 0.05$), indicating that these changes are robust.

Radiation:

Santiago's incoming solar radiation is rising markedly: the weighted shortwave-flux trend is about +1.16 (normalized ~0.53) per decade ($p < 0.001$). This suggests more solar energy reaching the surface, possibly due to clearer skies or fewer clouds. Daytime (downward) longwave radiation shows a slight decline (slope ~-0.036, normalized ~-0.06, $p < 0.001$), and nighttime longwave radiation declines more strongly (slope ~-0.252, normalized ~-0.25, $p < 0.001$). Thus, the island is receiving more sunlight while emitting less infrared at night. The net radiative effect is increased surface heating by day, partly offset by enhanced

cooling at night. All radiation trends are highly significant, reflecting a clear shift towards higher net radiative input in Santiago.

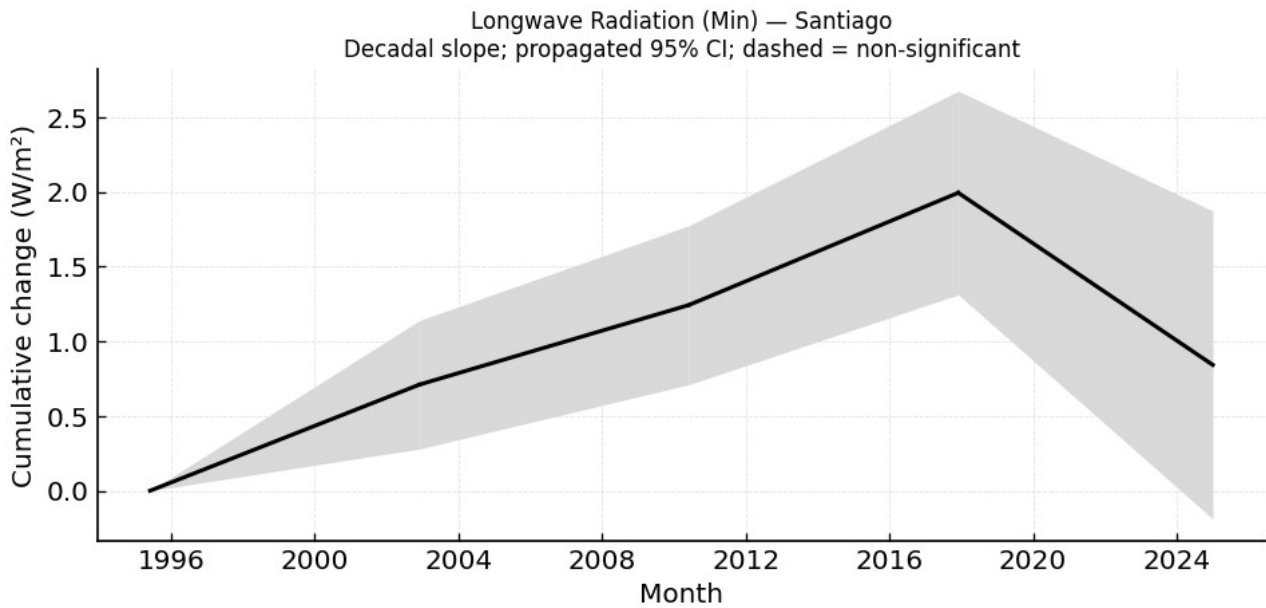


Figure 64: Minimum Longwave Radiation Trend - Santiago

Humidity and Moisture:

Santiago is very dry (average daytime relative humidity minimum ~22%). Trends indicate rising humidity. The daily maximum relative humidity stays at ~100%, but the daily minimum relative humidity is increasing (slope ~0.928 per decade, normalized ~0.34, $p < 0.001$), meaning the driest times are becoming less dry. Absolute humidity also rises: specific humidity increases (normalized slope >1.12 for the daily max, ~0.72 for the minimum) and vapour pressure increases (normalized ~0.75 for minima, ~0.59 for maxima). These upward trends ($p < 0.001$) show that the air is holding more water vapour overall. In summary, the atmosphere over Santiago is becoming moister even though relative dryness is high. This could slightly ease drought stress in an otherwise arid environment.

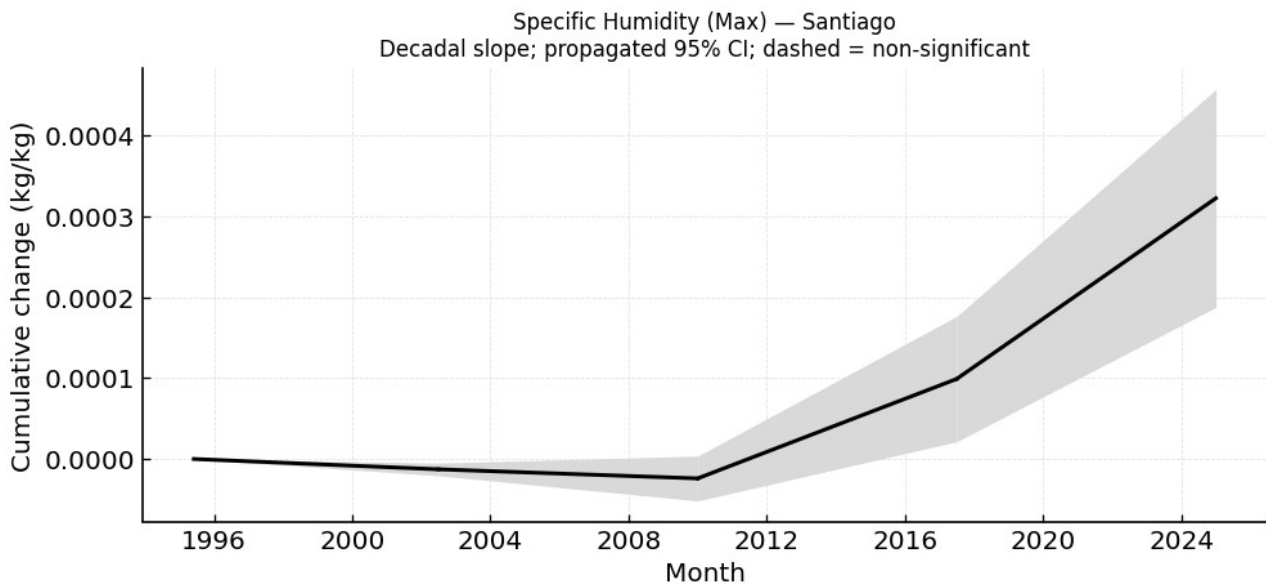


Figure 65: Maximum Specific Humidity Trend - Santiago

Precipitation:

Santiago’s annual precipitation is very low (~150 mm/year, mostly in Aug–Oct). The trend is +0.434 mm/decade ($p < 0.05$), but its normalized magnitude is negligible (~0.006). In practical terms, rainfall is essentially stable, the tiny increase is far smaller than year-to-decade variability. Therefore, there is no appreciable long-term change in Santiago’s already scarce rainfall.

Wind:

Maximum wind speed in Santiago is increasing (slope ~1.07m/s per decade, normalized ~0.60, $p < 0.05$) while minimum wind speed is essentially flat (slope ~0.001, normalized ~0.03). The rise in peak winds implies more intense windy episodes. Since Santiago is already a windy island, this trend indicates slightly heightened windiness. All wind trends are statistically significant, confirming a modest strengthening of wind extremes.

3.4.2 Boa Vista

Comparison of the trend between climate variables:

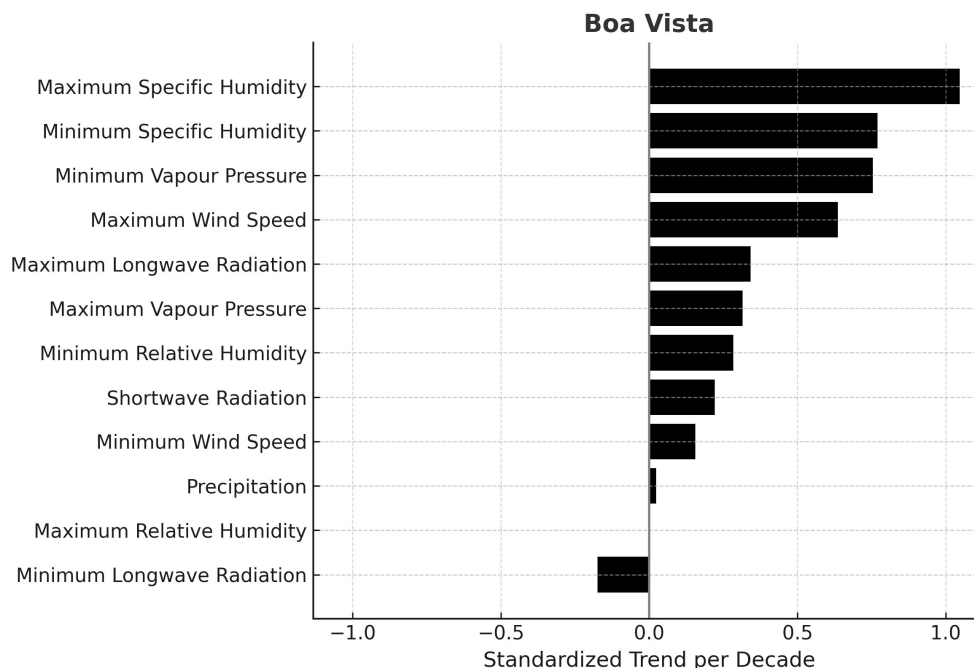


Figure 66: Boa Vista – Normalized Trends

Boa Vista shows the largest normalized increases in moisture and wind. Specific humidity (max) increases strongly (normalized ~ 1.05) and its daily minimum also rises (~ 0.77). Vapour pressure increases (minimum normalized ~ 0.75), and maximum wind speed rises (normalized ~ 0.64). Daytime longwave radiation also trends upward (normalized ~ 0.34), while nighttime longwave declines (normalized ~ -0.17). Shortwave radiation increases moderately (normalized ~ 0.22). Precipitation's normalized change is almost zero (~ 0.023), indicating effectively no trend. Relative-humidity extremes show no change at the high end and a significant rise in the daily minimum (normalized ~ 0.28 , $p < 0.05$). Nearly all trends (except relative humidity maximum) are significant ($p < 0.05$).

Radiation:

In Boa Vista, shortwave radiation is rising (slope ~ 0.805 per decade, normalized ~ 0.222 , $p < 0.001$), so the island is receiving more sunlight. Daytime longwave radiation is also increasing (slope ~ 0.194 , normalized ~ 0.342 , $p < 0.001$), whereas nighttime longwave radiation is decreasing (slope ~ -0.156 , normalized ~ -0.174 , $p < 0.001$). This combination implies warmer days radiating more IR and cooler nights radiating less. The increased solar flux suggests clearer skies or stronger insolation. All radiation trends are significant, highlighting a shift towards greater daytime heating and altered thermal balance.

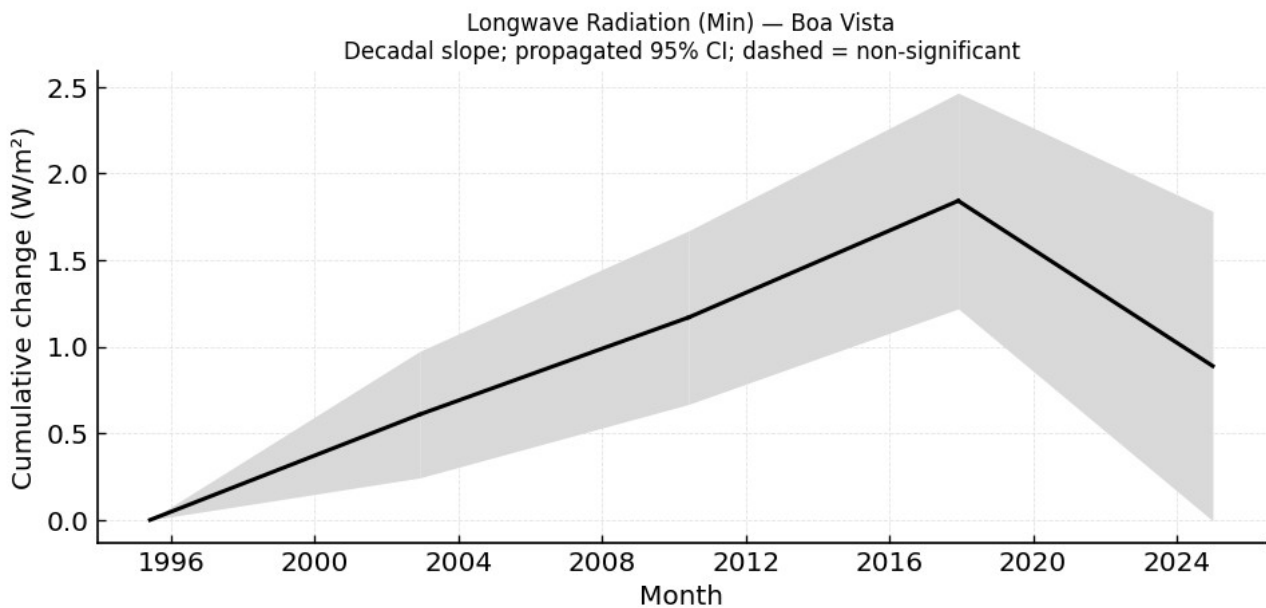


Figure 67: Minimum Longwave Radiation Trend – Boa Vista

Humidity and Moisture:

Boa Vista’s monthly maximum relative humidity stays at 100%, and daily minimum relative humidity increases (slope ~ 0.811 per decade, normalized ~ 0.284 , $p < 0.01$). Thus even the driest hours are becoming more humid. Specific humidity and vapour pressure both rise substantially (normalized ~ 1.047 for specific humidity maximum, ~ 0.75 for vapor-pressure min), indicating a wetter atmosphere. These significant increases ($p < 0.001$) show that the island’s air is holding more moisture over time. Though Boa Vista is arid (annual rain $\sim 100\text{--}125$ mm), these trends suggest a net gain in moisture.

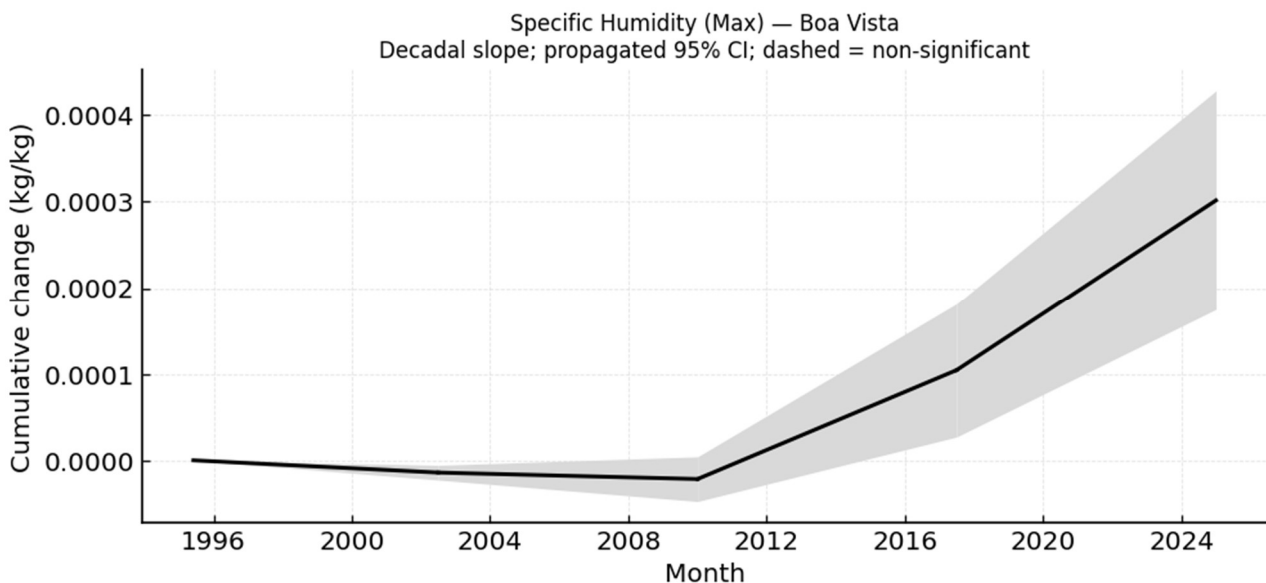


Figure 68: Maximum Specific Humidity Trend – Boa Vista

Precipitation:

Boa Vista's annual rainfall is very low on the order of 100 mm or less. The trend is +1.409 mm/decade ($p < 0.001$) with a normalized magnitude ~ 0.023 , which is almost negligible. In other words, total precipitation is essentially unchanged; the small positive slope is too minor relative to variability to alter the climate. Rainfall remains effectively stable.

Wind:

Maximum wind speed is increasing markedly (slope ~ 1.131 per decade, normalized ~ 0.637 , $p < 0.001$), while minimum wind speed shows a very slight rise (slope ~ 0.0068 , normalized ~ 0.156 , $p < 0.001$). The stronger increase in peak winds indicates that gusty wind conditions are intensifying. Boa Vista's trade winds are already strong and getting stronger, which could impact coastal erosion or dust transport. These wind trends are significant, confirming more extreme wind behavior.

3.4.3 Brava

Comparison of the trend between climate variables:

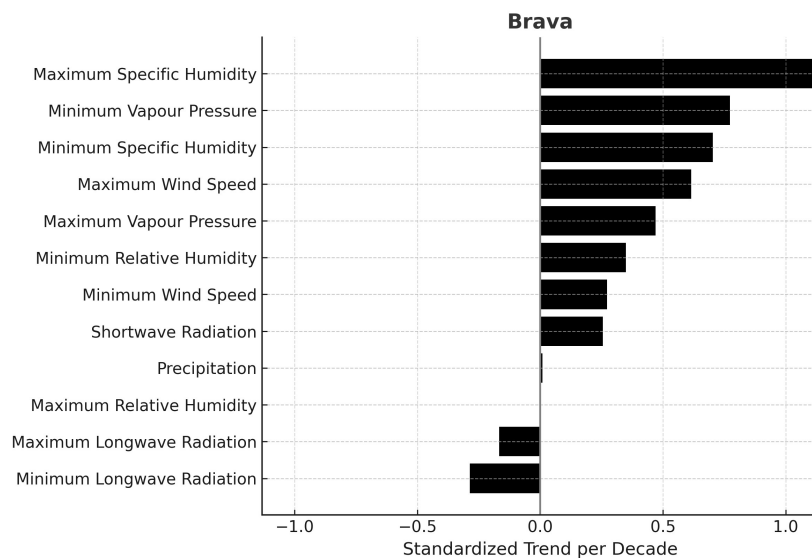


Figure 69: Brava – Normalized Trends

Brava exhibits strong normalized increases in moisture and wind. Specific humidity (max) rises steeply (normalized ~ 1.13) and its minimum also increases (normalized ~ 0.70). Vapour pressure increases (minimum normalized ~ 0.77 , max ~ 0.47), and maximum wind speed increases (normalized ~ 0.61). Shortwave radiation increases (normalized ~ 0.26). Both daytime and nighttime longwave radiation decline (normalized ~ -0.17 and ~ -0.29).

Precipitation's normalized trend (~ 0.010) is essentially zero. Almost all trends (except relative humidity maximum) are highly significant ($p < 0.05$).

Radiation:

Shortwave radiation in Brava is increasing (slope ~ 1.198 per decade, normalized ~ 0.256 , $p < 0.001$), signaling more solar heating. Daytime longwave radiation is decreasing (slope ~ -0.116 , normalized ~ -0.166 , $p < 0.001$) and nighttime longwave decreases more (slope ~ -0.356 , normalized ~ -0.286 , $p < 0.001$). Thus, Brava receives more sunlight while emitting less infrared, a pattern that implies net warming by increased incoming radiation and cooler nights. All these trends are significant, indicating a clear shift in Brava's radiative balance.

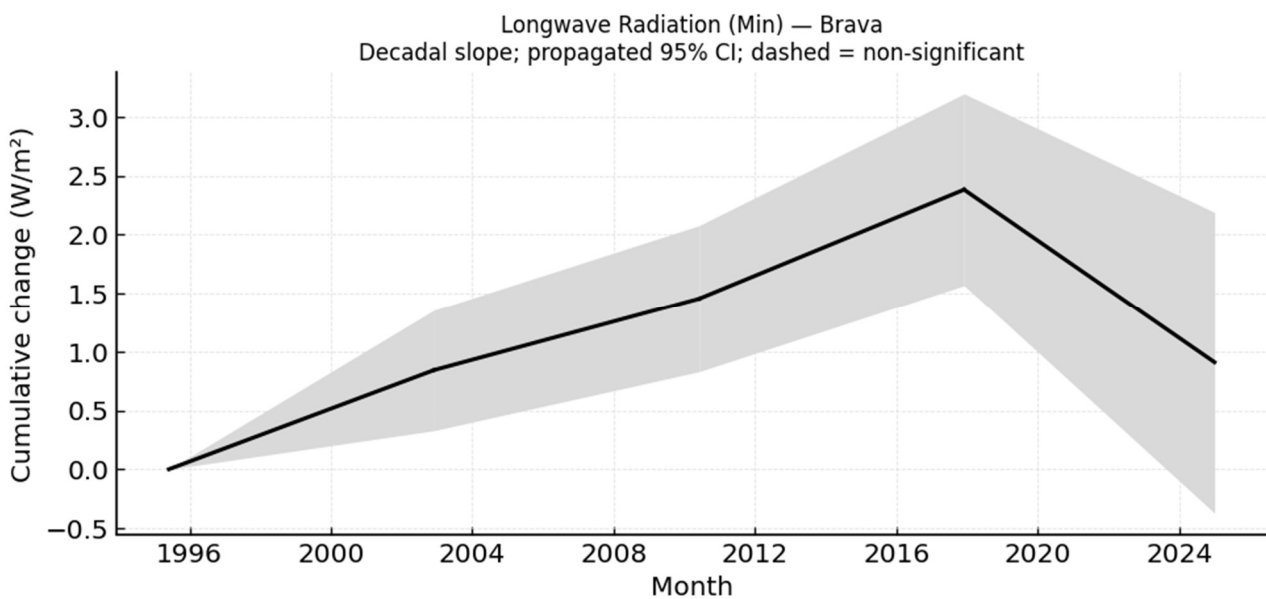


Figure 70: Minimum Longwave Radiation Trend - Brava

Humidity and Moisture:

On Brava, daily maximum relative humidity remains at 100%, while daily minimum relative humidity is rising (slope ~ 0.944 per decade, normalized ~ 0.349 , $p < 0.001$). This means the island's driest periods are becoming wetter. Specific humidity and vapour pressure also increase markedly (normalized ~ 1.127 for specific-humidity max, ~ 0.772 for vapor-pressure min). These increases are significant ($p < 0.05$), showing a substantial rise in atmospheric moisture. In practical terms, Brava's air is becoming less arid over time.

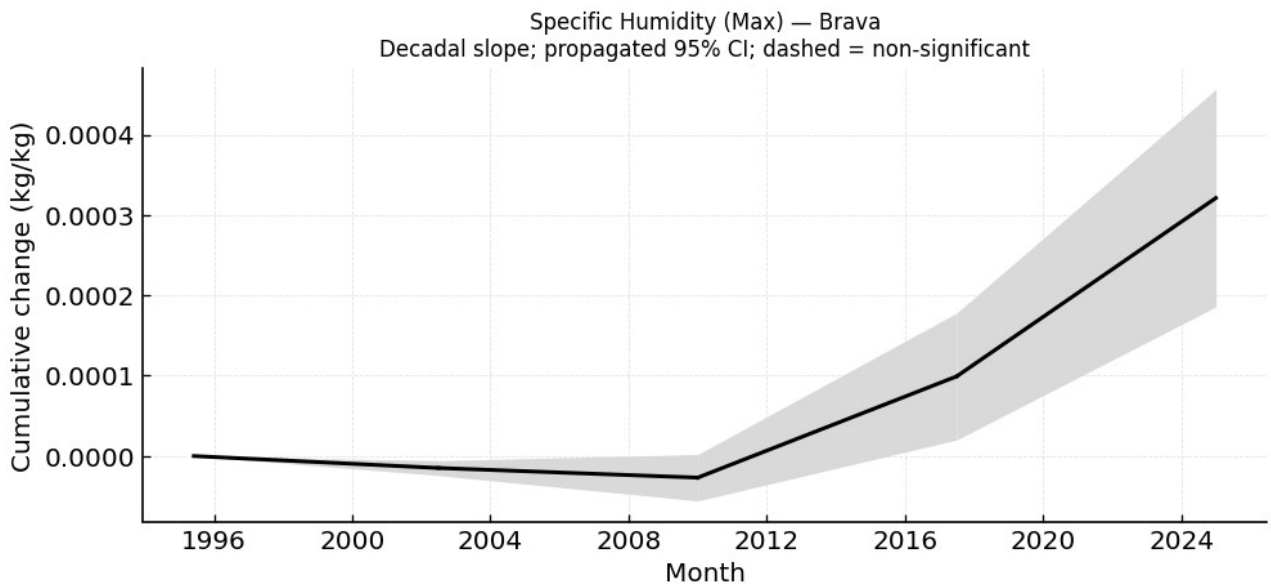


Figure 71: Maximum Specific Humidity Trend - Brava

Precipitation:

Brava's total rainfall is limited (roughly a few hundred mm/decade). The trend is +0.706 mm/decade ($p < 0.001$), with normalized slope ~ 0.0098 . This increase is negligible compared to natural fluctuations. Consequently, Brava's precipitation regime remains essentially unchanged, with no meaningful long-term trend.

Wind:

Maximum wind speed on Brava increases (slope ~ 1.112 m/s per decade, normalized ~ 0.615 , $p < 0.001$) and minimum wind also increases slightly (slope ~ 0.0097 m/s, normalized ~ 0.272 , $p < 0.001$). The larger rise in peak winds indicates more intense windy episodes. Brava's trade winds are intensifying, which could affect coastal erosion. All wind trends are significant, confirming this robust increase in windiness.

3.4.4 Fogo

Comparison of the trend between climate variables:

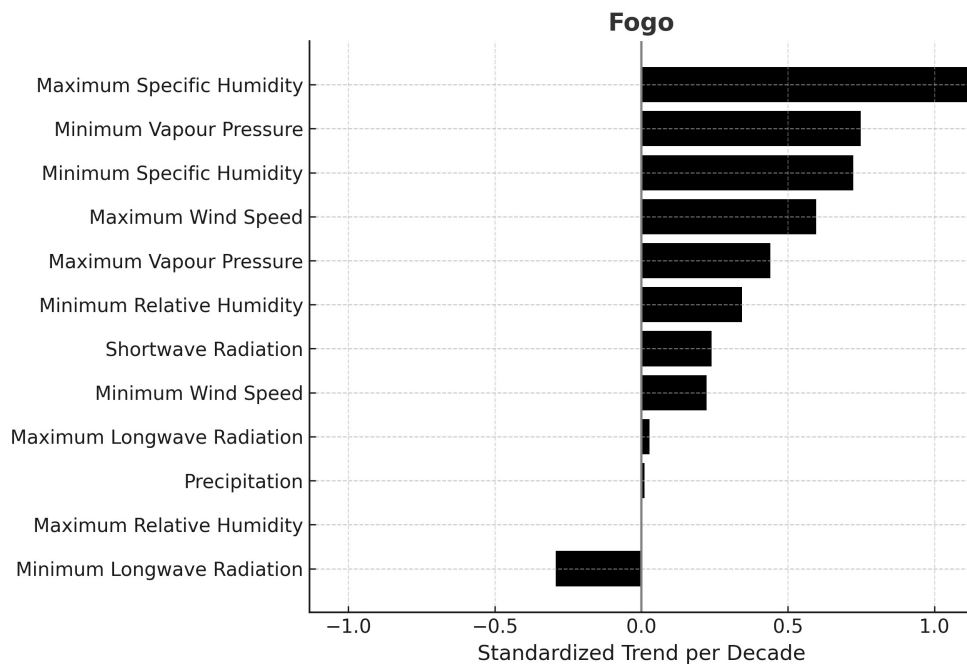


Figure 72: Fogo - Normalized Trends

Fogo's strongest trends are in moisture and wind. Maximum specific humidity increases significantly (normalized ~ 1.13) and specific-humidity minimum also rises (normalized ~ 0.72). Vapour pressure increases (minimum normalized ~ 0.75) and maximum wind speed increases (normalized ~ 0.60). Shortwave radiation increases moderately (normalized ~ 0.24). Daytime longwave radiation shows almost flat trend (normalized ~ 0.03), while nighttime longwave declines strongly (normalized ~ -0.29). Precipitation's normalized change is ~ 0.011 , i.e. effectively zero. All trends except relative humidity maximum are highly significant ($p < 0.05$).

Radiation:

In Fogo, shortwave radiation is rising (slope ~ 0.869 per decade, normalized ~ 0.239 , $p < 0.001$), indicating more solar input. Daytime longwave radiation rises negligibly (slope ~ 0.021 , normalized ~ 0.029 , $p < 0.001$), but nighttime longwave decreases substantially (slope ~ -0.387 , normalized ~ -0.293 , $p < 0.001$). This pattern implies increased daytime heating and enhanced nocturnal cooling. Fogo thus experiences a net increase in incoming energy. All radiation trends are significant.

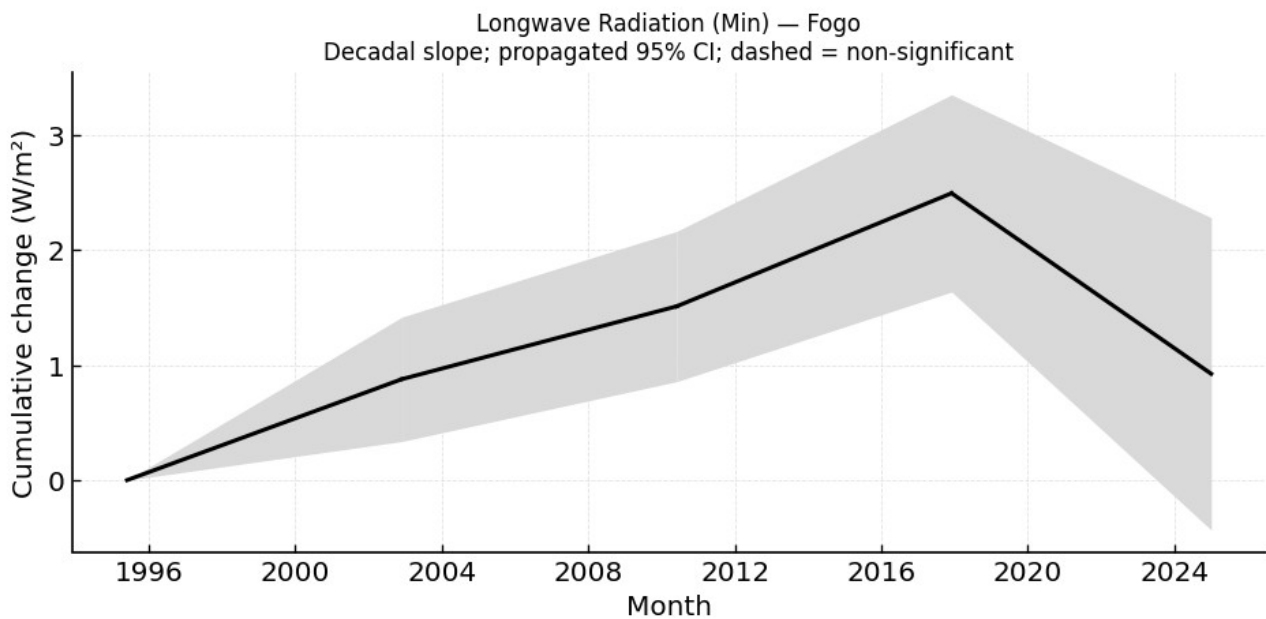


Figure 73: Minimum Longwave Radiation Trend - Fogo

Humidity and Moisture:

Fogo remains dry, but trends show rising humidity. Daily maximum relative humidity stays at 100%, and daily minimum relative humidity increases (slope ~ 0.888 per decade, normalized ~ 0.344 , $p < 0.001$). Specific humidity and vapour pressure both rise significantly (normalized ~ 1.131 for maximum specific humidity, ~ 0.749 for minimum vapour pressure). These indicate that Fogo's air is becoming more humid despite its aridity. The rising moisture content ($p < 0.001$) may slightly mitigate extreme dryness.

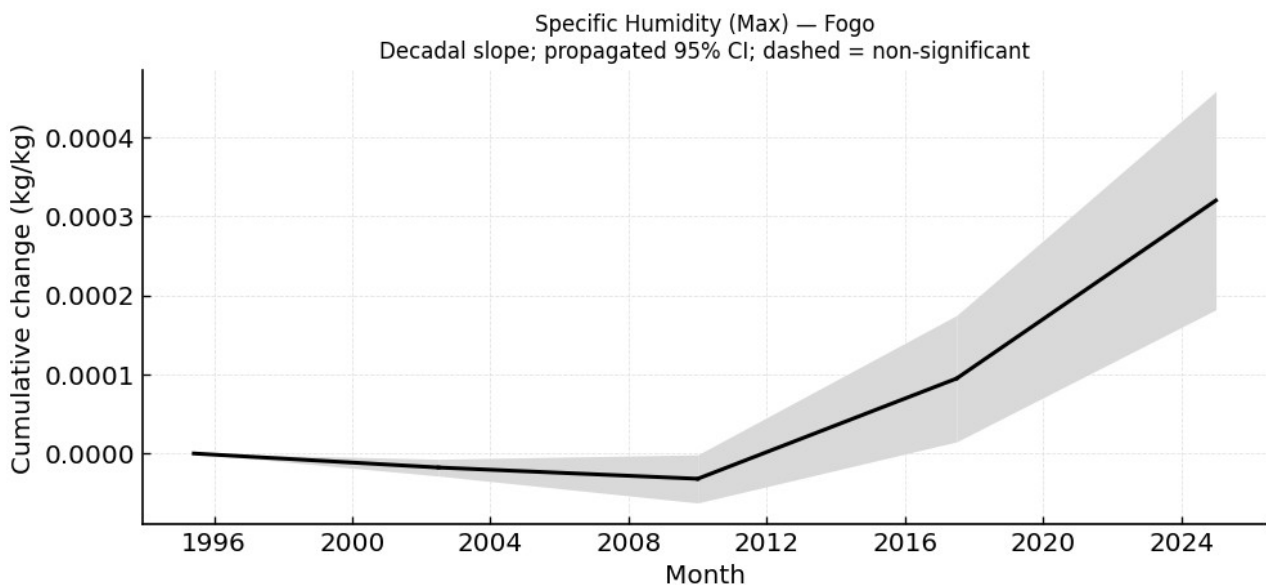


Figure 74: Maximum Specific Humidity Trend - Fogo

Precipitation:

Fogo's annual rainfall is on the order of a few hundred mm. The trend is +1.091 mm/decade ($p < 0.001$), but normalized magnitude ~ 0.011 is negligible. Thus precipitation shows no meaningful change; any increase is too small to affect the overall rainfall pattern.

Wind:

Maximum wind speed increases (slope ~ 1.082 per decade, normalized ~ 0.596 , $p < 0.001$) while minimum wind also rises slightly (slope ~ 0.0090 , normalized ~ 0.223 , $p < 0.001$). The stronger rise in peak winds indicates that high winds are intensifying. Fogo's wind regime thus shows increasing gustiness. Both wind trends are significant.

3.4.5 Maio

Comparison of the trend between climate variables:

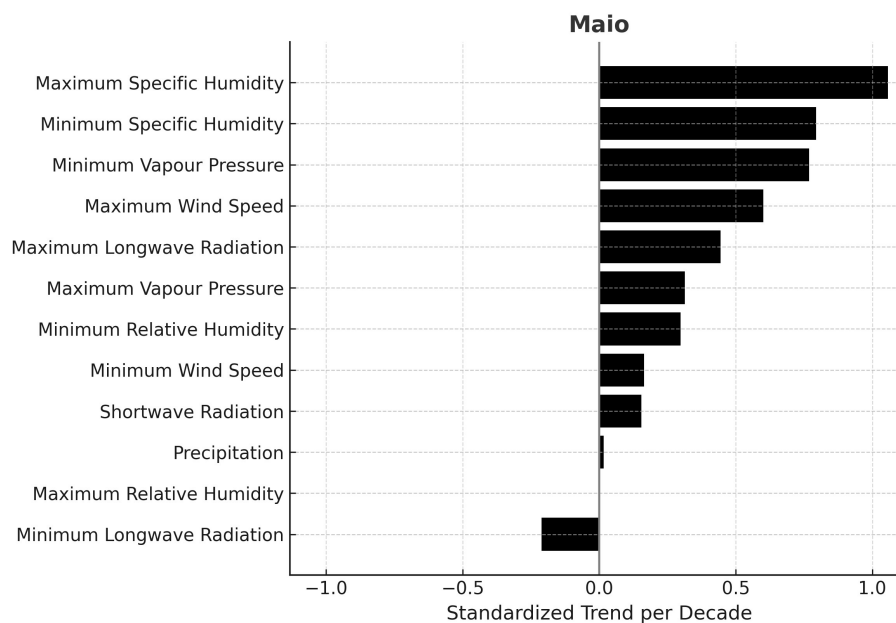


Figure 75: Maio – Normalized Trends

Maio's trends again highlight moisture and wind. Specific humidity (max) increases markedly (normalized ~ 1.06) and its minimum also rises (normalized ~ 0.79). Vapour pressure increases (minimum normalized ~ 0.77) and maximum wind speed rises (normalized ~ 0.60). Unlike most other islands, daytime longwave radiation rises (normalized ~ 0.45), while nighttime longwave still decreases (normalized ~ -0.21). Shortwave radiation increases modestly (normalized ~ 0.155). The daily minimum relative humidity trend (normalized

~0.298) is marginal ($p \approx 0.011$). Precipitation's normalized trend (~0.017) is virtually zero. All major trends (except relative humidity extremes) are statistically significant.

Radiation:

Maio's solar radiation is rising (slope ~1.178 per decade, normalized ~0.155, $p < 0.001$). Daytime longwave radiation also rises (slope ~0.267, normalized ~0.445, $p < 0.001$), which is different from the other islands' decline. Nighttime longwave radiation decreases (slope ~-0.194, normalized ~-0.212, $p < 0.001$). Together, these imply overall warming (more incoming and more outgoing IR). All radiation trends are significant, suggesting Maio is experiencing increased heating.

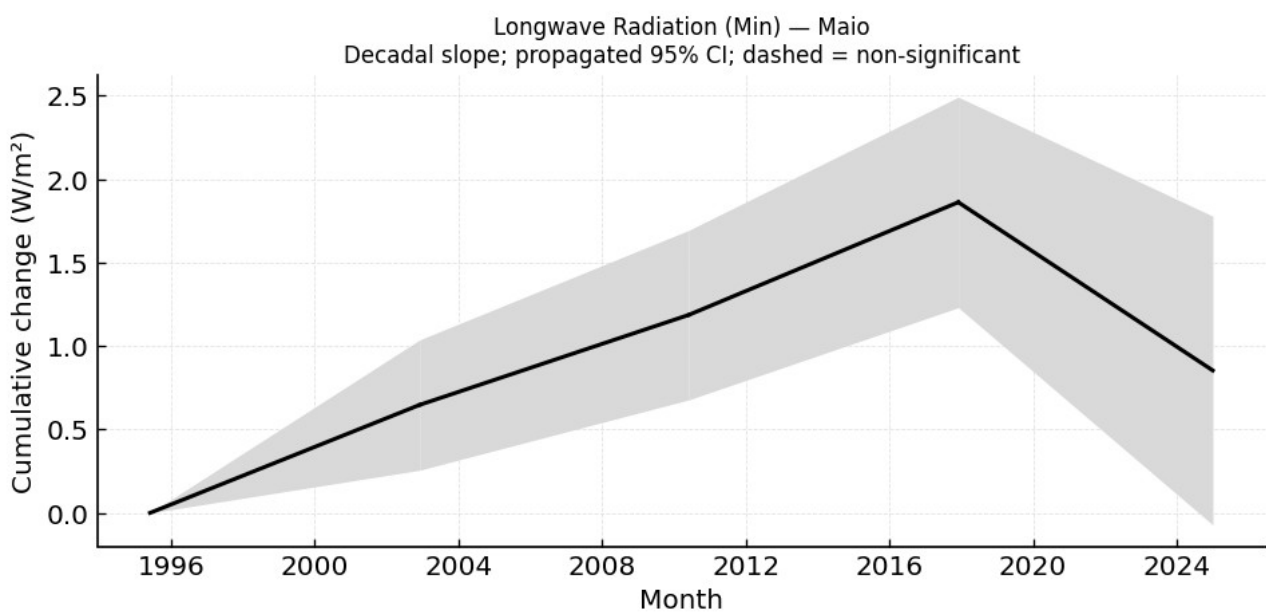


Figure 76: Minimum Longwave Radiation Trend - Maio

Humidity and Moisture:

Maio is arid, but moisture is increasing. Maximum relative humidity remains 100%. Minimum relative humidity rises (slope ~0.849 per decade, normalized ~0.298, $p \approx 0.011$), a weaker signal but still positive. Specific humidity and vapour pressure rise strongly (normalized ~1.057 for spec-humax, ~0.768 for vap-pres-min, $p < 0.001$). These indicate the air is holding more moisture. Despite marginal relative humidity changes, the absolute humidity increase is clear, pointing to slightly wetter conditions.

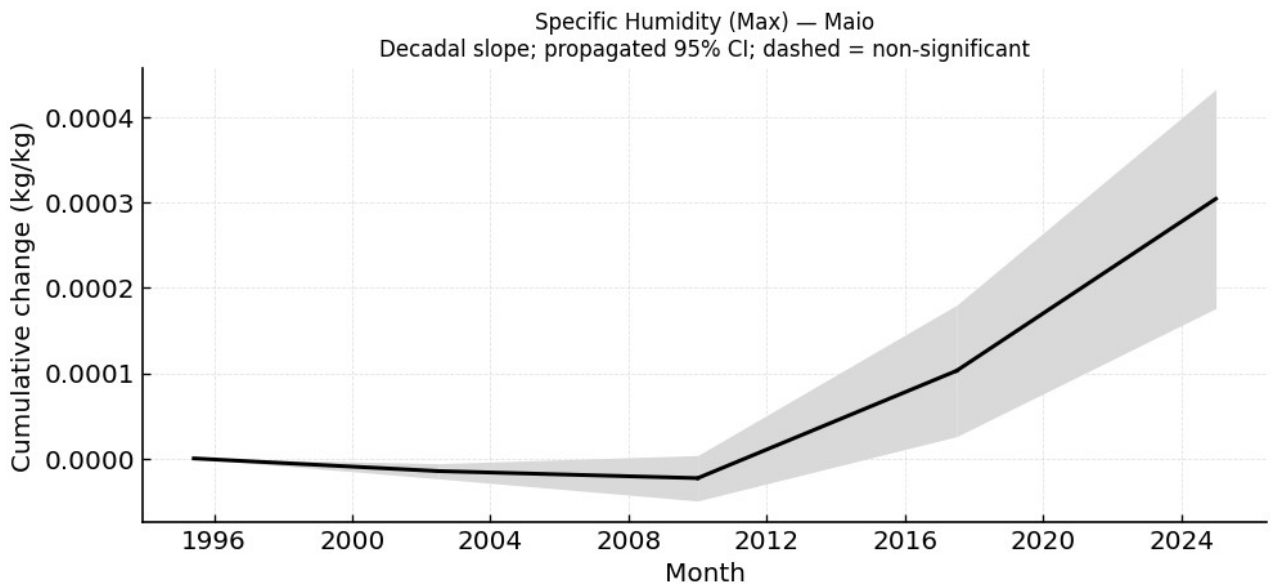


Figure 77: Maximum Specific Humidity Trend - Maio

Precipitation:

Maio’s annual rainfall is very low (on the order of ~100 mm/decade). The trend is +1.066 mm/decade ($p < 0.001$), with a negligible normalized effect (~0.017). In practice, precipitation is stable, showing only a very small upward drift. No appreciable change in total rainfall is evident.

Wind:

Maximum wind speed increases (slope ~1.071 per decade, normalized ~0.602, $p < 0.001$), and minimum wind speed also rises slightly (slope ~0.0070, normalized ~0.164, $p < 0.001$). The stronger rise in peak winds suggests more intense wind events. Maio’s windy conditions are intensifying at the extremes. These wind trends are significant.

3.4.6 Sal

Comparison of the trend between climate variables:

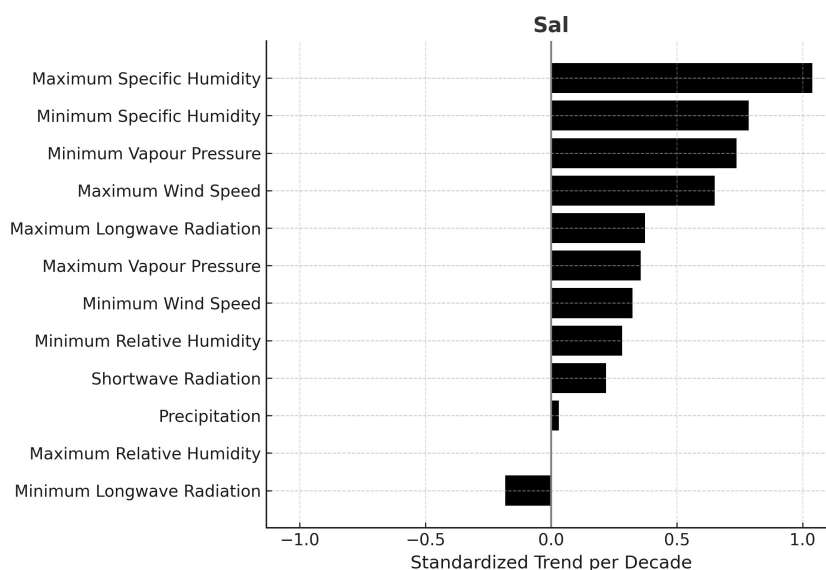


Figure 78: Sal – Normalized Trends

Sal exhibits very strong moisture and wind increases. Specific humidity (max) rises (normalized ~ 1.04) and its minimum increases (normalized ~ 0.79). Vapour pressure rises (minimum normalized ~ 0.74), and maximum wind increases (normalized ~ 0.65 , the largest among variables). Daytime longwave radiation increases (normalized ~ 0.37), unlike on many other islands, while nighttime longwave decreases slightly (normalized ~ -0.18). Shortwave radiation increases moderately (normalized ~ 0.22). The relative humidity minimum trend (normalized ~ 0.28) is weak ($p \approx 0.073$). Precipitation's normalized trend (~ 0.031) is very small. All major trends (except relative humidity extremes) are significant ($p < 0.05$).

Radiation:

In Sal, incoming solar radiation increases (slope ~ 0.839 per decade, normalized ~ 0.219 , $p < 0.001$). Daytime longwave radiation also increases (slope ~ 0.240 , normalized ~ 0.373 , $p < 0.001$), unlike the declines seen elsewhere. Nighttime longwave radiation decreases slightly (slope ~ -0.186 , normalized ~ -0.183 , $p < 0.001$). The combined effect is increased energy input. These significant trends suggest net warming on Sal.

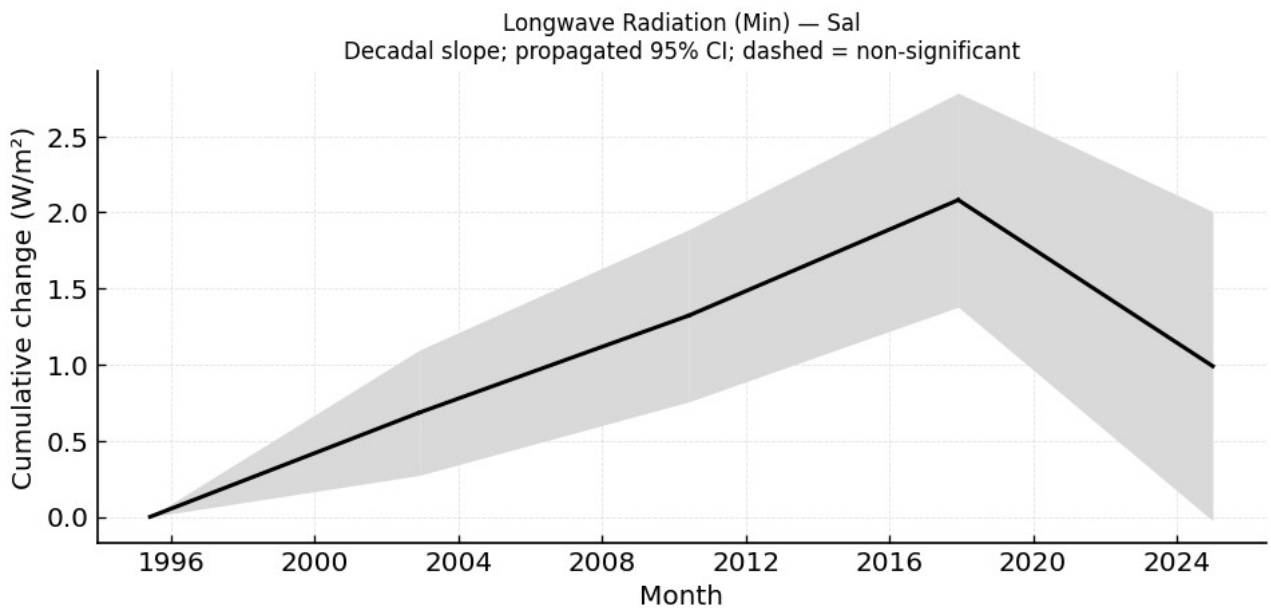


Figure 79: Minimum Longwave Radiation Trend - Sal

Humidity and Moisture:

Sal's daily maximum relative humidity stays at 100%. Daily minimum relative humidity shows a slight upward trend (slope ~ 0.808 per decade, normalized ~ 0.282) but it is not statistically significant ($p \approx 0.073$). However, absolute moisture content rises: specific humidity (normalized ~ 1.039) and vapour pressure (normalized ~ 0.74 for minima) increase significantly ($p < 0.001$). These indicate the air over Sal is becoming more humid, even if relative-humidity changes are modest.

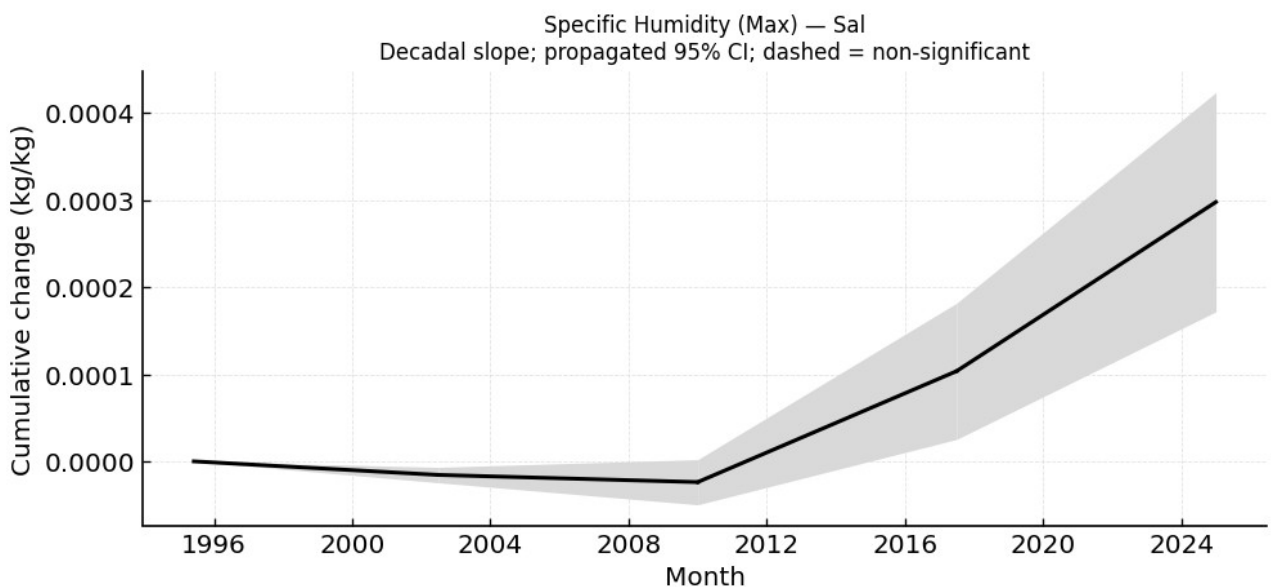


Figure 80: Maximum Specific Humidity Trend - Sal

Precipitation:

Sal's annual rainfall is low (~150 mm/decade). The trend is +1.813 mm/decade ($p < 0.001$) with normalized magnitude ~0.031. This change is very small relative to variability. Thus, Sal's rainfall pattern remains essentially unchanged.

Wind:

Maximum wind speed increases substantially (slope ~1.158 per decade, normalized ~0.650, $p < 0.001$). Minimum wind speed also rises slightly (slope ~0.014, normalized ~0.324, $p < 0.001$), but to a lesser degree. The strong increase in peak winds indicates even windier conditions. All wind trends are significant.

3.4.7 Santo Antão

Comparison of the trend between climate variables:

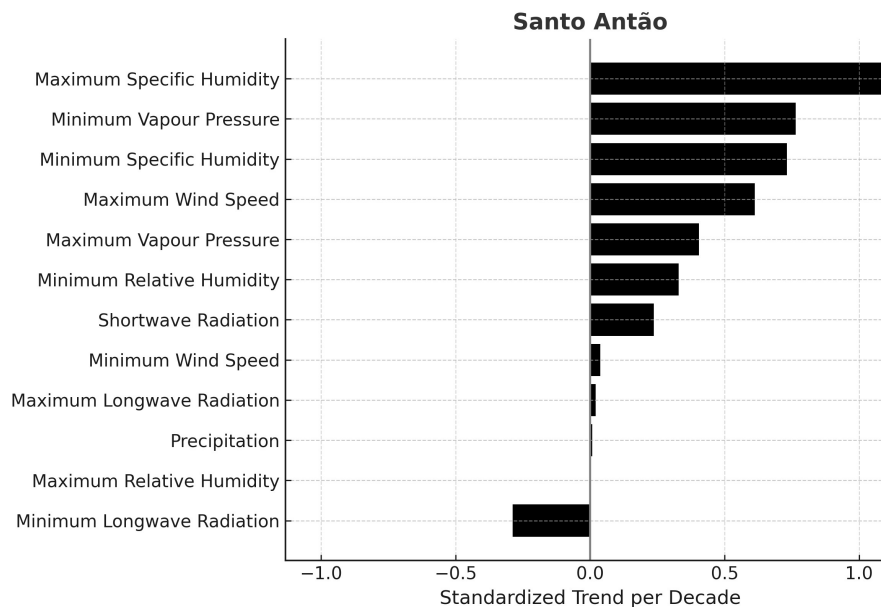


Figure 81: Santo Antão - Normalized Trends

Santo Antão's highest normalized trends are in moisture (specific humidity ~1.11, vapour pressure minimum ~0.76) and wind (maximum ~0.61). Shortwave radiation increases (normalized ~0.236). Daytime longwave is nearly flat (normalized ~0.021) and nighttime longwave decreases (normalized ~-0.287). Minimum relative humidity increases (normalized ~0.329). Precipitation's normalized change (~0.008) is negligible. All trends (except relative humidity max) are statistically significant.

Radiation:

On Santo Antão, shortwave radiation rises (slope ~ 0.871 per decade, normalized ~ 0.236 , $p < 0.001$). Daytime longwave radiation is essentially unchanged (slope ~ 0.015 , normalized ~ 0.021 , $p < 0.001$), while nighttime longwave decreases (slope ~ -0.355 , normalized ~ -0.287 , $p < 0.001$). This pattern suggests more solar heating and cooler nights. Net incoming energy thus increases. These radiation trends are significant.

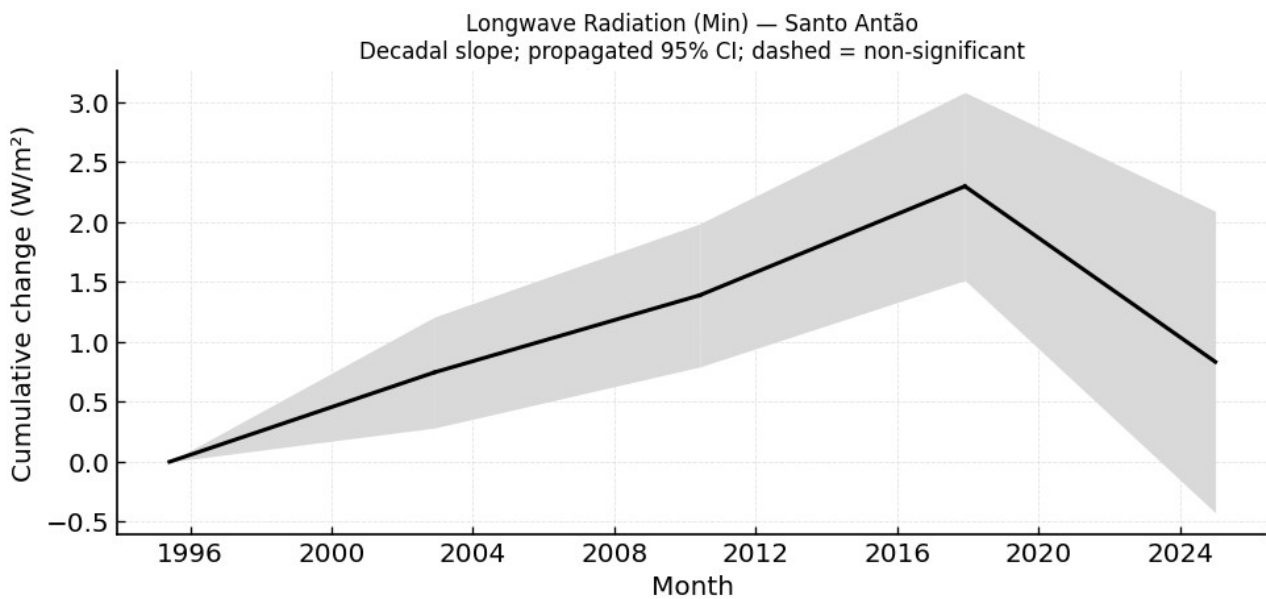


Figure 82: Minimum Longwave Radiation Trend – Santo Antão

Humidity and Moisture:

Daily maximum relative humidity remains 100%; daily minimum relative humidity increases (slope ~ 0.874 per decade, normalized ~ 0.329 , $p < 0.001$). Specific humidity and vapour pressure rise markedly (spec-humax normalized ~ 1.112 , vap-pres-min normalized ~ 0.765 , $p < 0.001$). These significant changes mean Santo Antão's air is becoming more humid, reducing extreme dryness during the day.

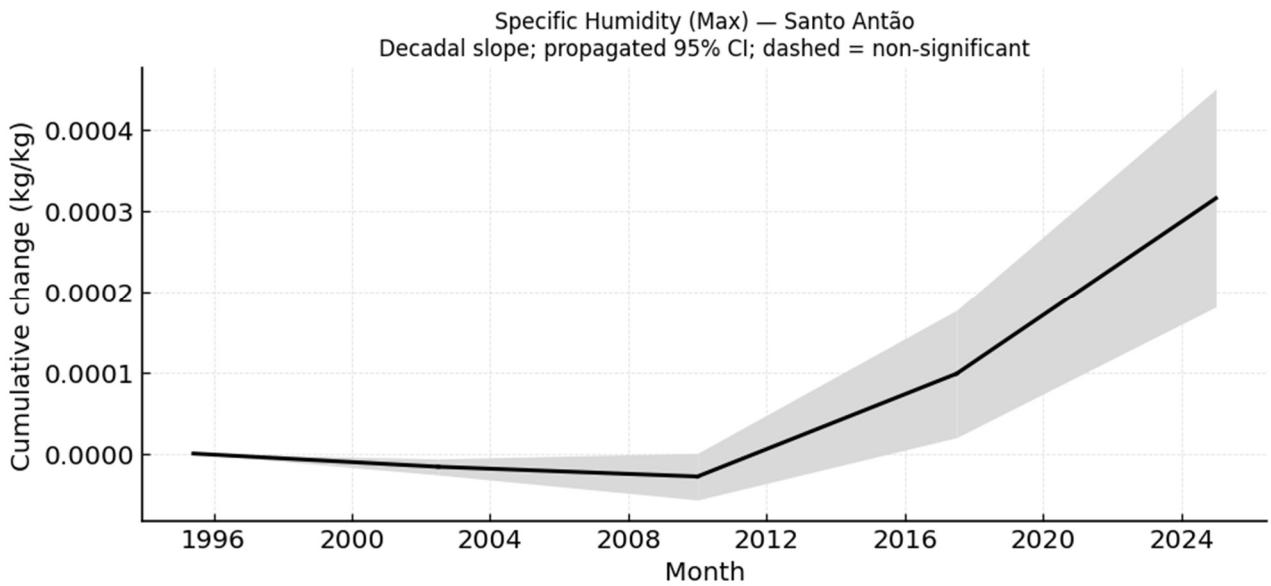


Figure 83: Maximum Specific Humidity Trend – Santo Antão

Precipitation:

Santo Antão’s annual precipitation (under ~200 mm) shows a small increase (+0.605 mm/decade, $p < 0.001$) with negligible normalized magnitude (~0.0076). In practice, rainfall is essentially steady over time. No appreciable long-term change is apparent.

Wind:

Maximum wind speed increases (slope ~1.112 per decade, normalized ~0.613, $p < 0.001$); minimum wind speed is nearly flat (slope ~0.0015, normalized ~0.038, $p < 0.001$). The rise in peak winds indicates stronger gusts. Both wind trends are significant.

3.4.8 São Nicolau

Comparison of the trend between climate variables:

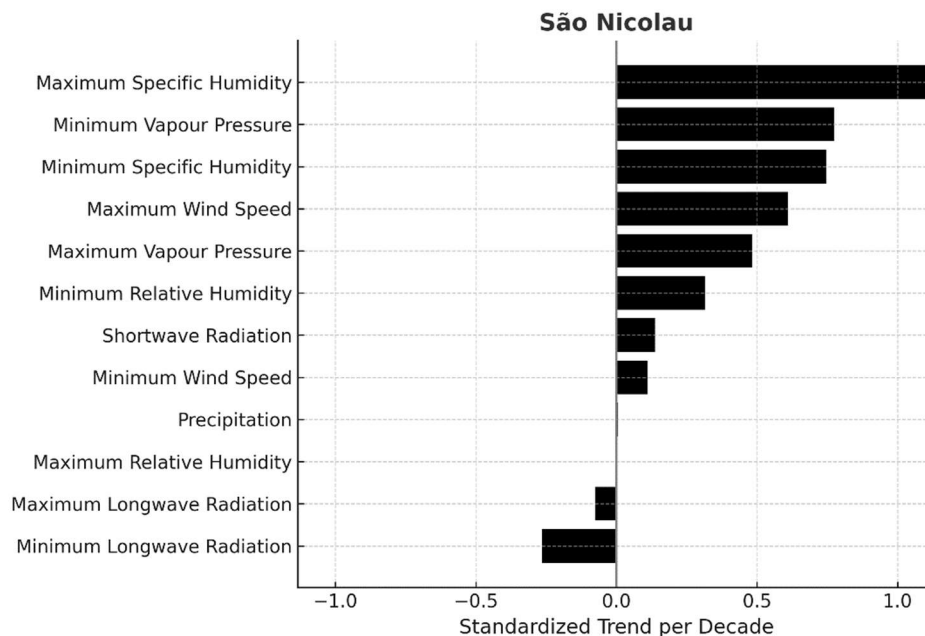


Figure 84: São Nicolau – Normalized Trends

São Nicolau shows its largest normalized trends in moisture and wind. Maximum specific humidity rises significantly (normalized ~ 1.13) and its minimum increases (normalized ~ 0.75). Vapour pressure rises (minimum normalized ~ 0.77 , max ~ 0.48), and maximum wind increases (normalized ~ 0.61). Shortwave radiation increases (normalized ~ 0.137). Both daytime and nighttime longwave radiation decrease (normalized ~ -0.076 and ~ -0.266). Minimum relative humidity increases (normalized ~ 0.316). Precipitation's normalized trend (~ 0.0055) is effectively zero. All trends except relative humidity max are significant.

Radiation:

São Nicolau's incoming solar radiation increases (slope ~ 0.962 per decade, normalized ~ 0.137 , $p < 0.001$). Daytime longwave radiation decreases slightly (slope ~ -0.052 , normalized ~ -0.076 , $p < 0.001$), and nighttime longwave decreases more strongly (slope ~ -0.312 , normalized ~ -0.266 , $p < 0.001$). Thus, solar heating increases while infrared emission drops, yielding a net warming effect. These significant trends indicate a shift towards higher daytime heating and cooler nights.

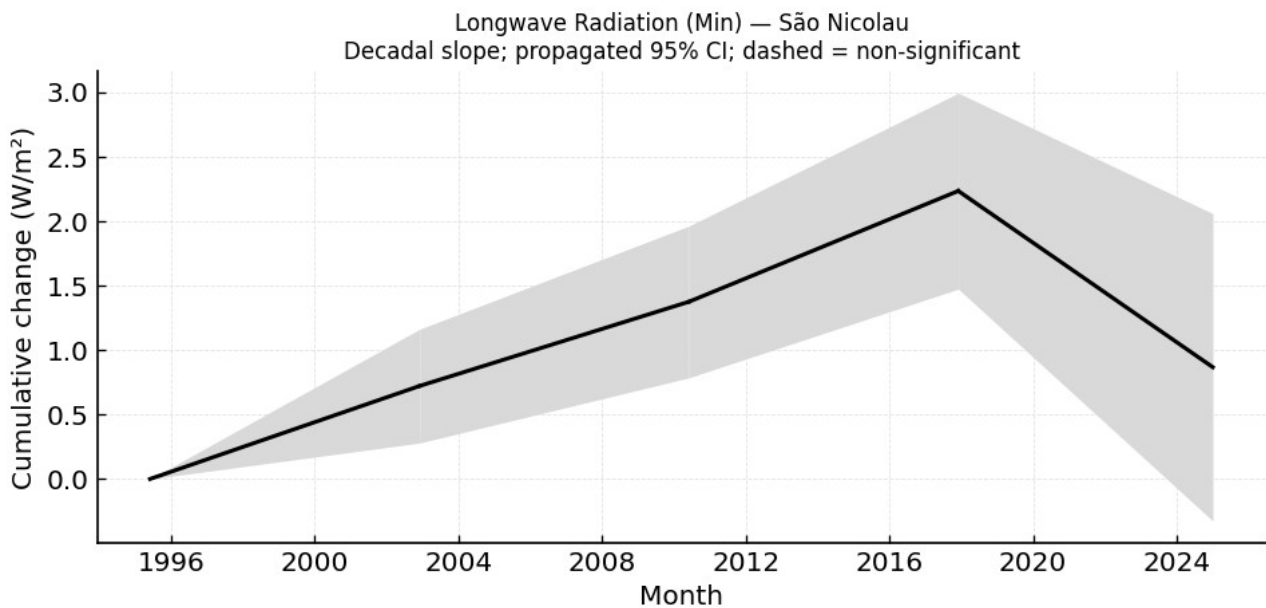


Figure 85: Minimum Longwave Radiation Trend – São Nicolau

Humidity and Moisture:

Daily minimum relative humidity increases (slope ~ 0.876 per decade, normalized ~ 0.316 , $p < 0.001$), with maximum relative humidity at 100%. Specific humidity and vapour pressure also rise significantly (normalized ~ 1.133 and ~ 0.774 , respectively). These trends indicate more atmospheric moisture. Even though relative humidity is saturated at night, the overall moisture content of the air is clearly increasing.

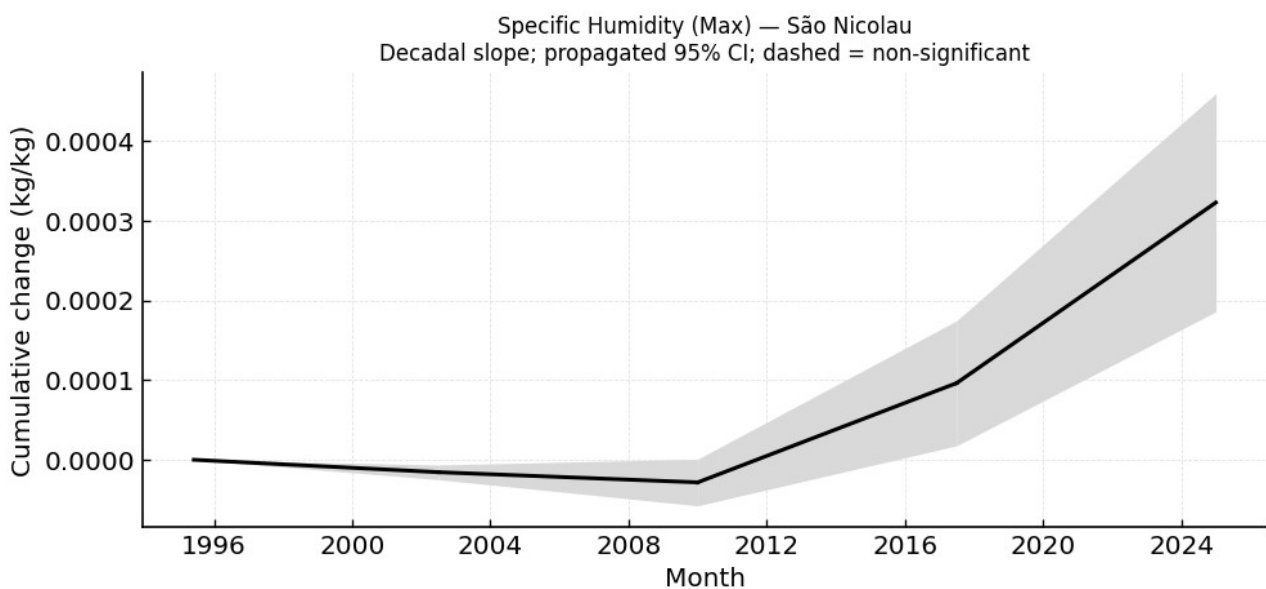


Figure 86: Maximum Specific Humidity Trend – São Nicolau

Precipitation:

São Nicolau's rainfall (~100–150 mm/decade) shows a small upward trend (+0.349 mm/decade, $p < 0.001$), with normalized magnitude ~0.0055. This change is negligible in practice. Precipitation patterns are essentially unchanged over time, with the tiny increase far outweighed by natural variability.

Wind:

Maximum wind speed increases (slope ~1.104 per decade, normalized ~0.611, $p < 0.001$), and minimum wind speed rises slightly (slope ~0.0048, normalized ~0.112, $p < 0.001$). The notable rise in peak wind indicates stronger wind events. These wind trends are significant.

3.4.9 São Vicente

Comparison of the trend between climate variables:

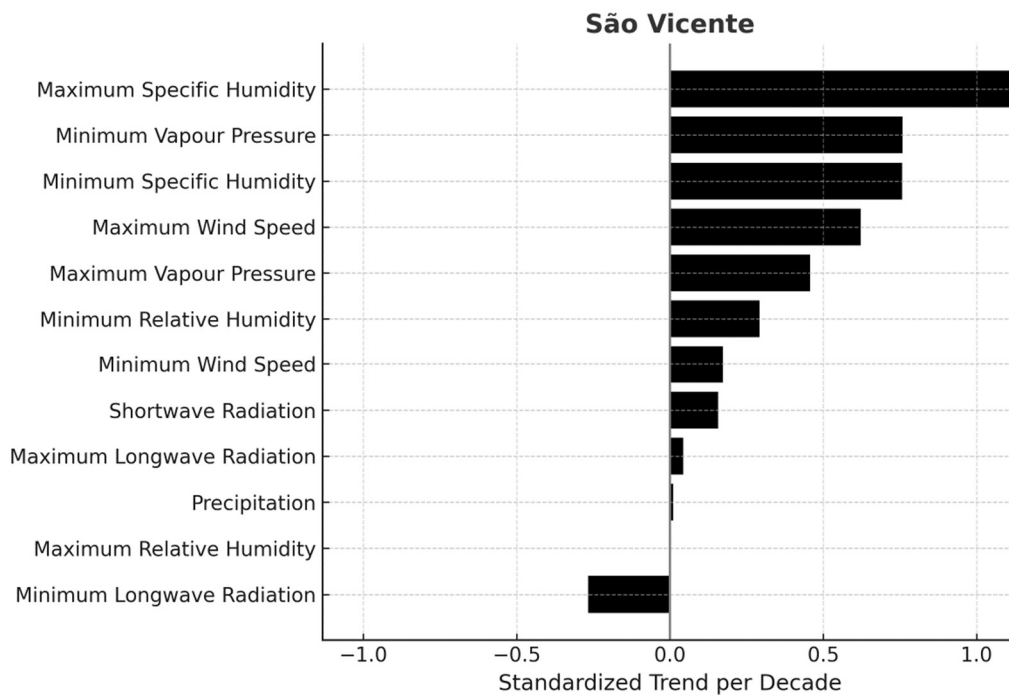


Figure 87: São Vicente – Normalized Trends

São Vicente's strongest trends are in moisture and wind. Specific humidity (max) rises (normalized ~1.12) and its minimum increases (normalized ~0.76). Vapour pressure increases (minimum normalized ~0.76, max ~0.46), and maximum wind increases (normalized ~0.62). Shortwave radiation increases (normalized ~0.157). Daytime longwave radiation increases slightly (normalized ~0.044), while nighttime longwave decreases (normalized ~-0.267).

Minimum relative humidity increases (normalized ~ 0.293). Precipitation's normalized trend (~ 0.0103) is negligible. All trends (except maximum relative humidity) are significant.

Radiation:

São Vicente's solar radiation is rising (slope ~ 0.714 per decade, normalized ~ 0.157 , $p < 0.001$). Daytime longwave radiation also rises (slope ~ 0.027 , normalized ~ 0.044 , $p < 0.001$), unlike most other islands. Nighttime longwave radiation falls (slope ~ -0.278 , normalized ~ -0.267 , $p < 0.001$). Thus, more sunlight is received while nights become cooler. These significant trends imply net warming by increased incoming radiation and enhanced nocturnal cooling.

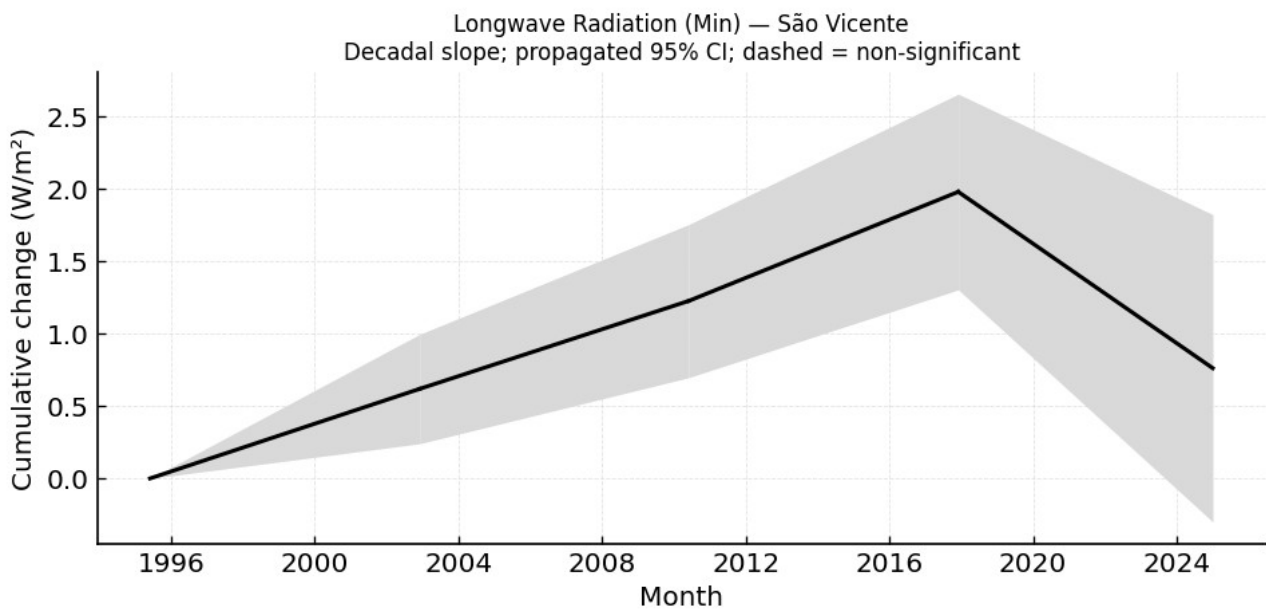


Figure 88: Minimum Longwave Radiation Trend – São Vicente

Humidity and Moisture:

Daily maximum relative humidity remains 100%; daily minimum relative humidity is rising (slope ~ 0.827 per decade, normalized ~ 0.293 , $p < 0.001$). Specific humidity and vapour pressure increase significantly (normalized ~ 1.120 for spec-humax, ~ 0.759 for vap-pres-min). These patterns mean the air is becoming more humid overall. The significant moisture increases point to reduced dryness on the island.

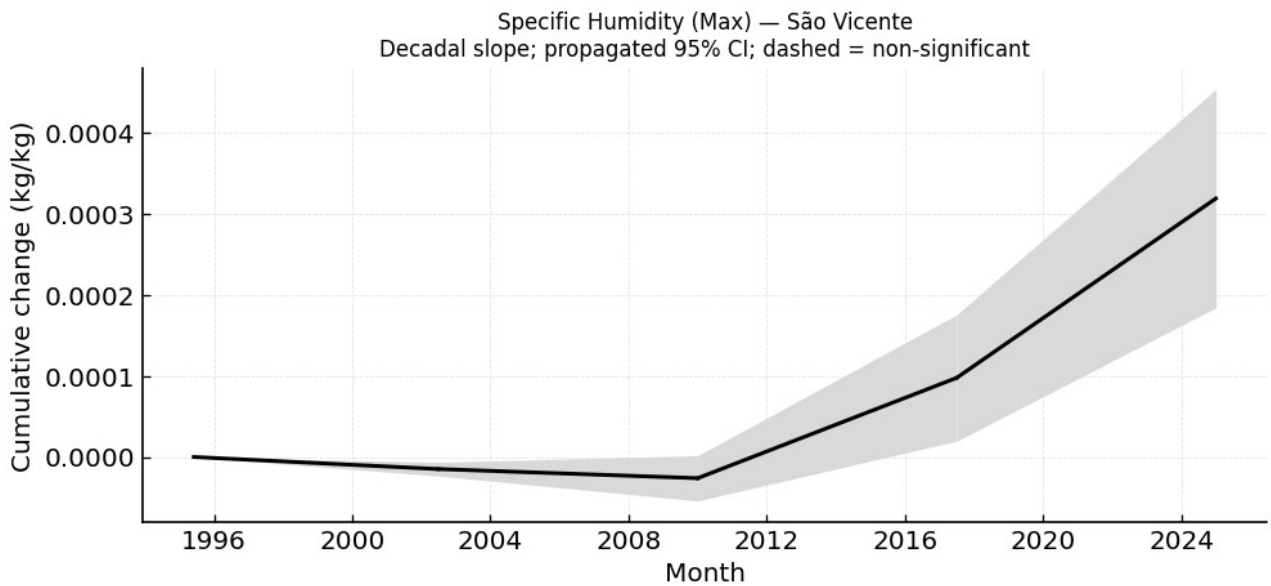


Figure 89: Maximum Specific Humidity Trend – São Vicente

Precipitation:

São Vicente has low rainfall (~150 mm/decade). The long-term trend is +0.609 mm/decade ($p < 0.001$) with normalized magnitude ~0.010. This change is negligible, so precipitation remains effectively unchanged.

Wind:

Maximum wind speed increases (slope ~1.120 per decade, normalized ~0.622, $p < 0.001$); minimum wind speed also rises slightly (slope ~0.007, normalized ~0.173, $p < 0.001$). The significant rise in peak winds indicates stronger gusts.

4. Conclusion

The analysis of historical climate data underscores that Macaronesia's islands are experiencing **unprecedented warming and drying**, with significant impacts on water resources and drought risk. The combined evidence, from temperature, humidity, and evapotranspiration trends, paints a clear picture: **water stress is intensifying**. Steep mountains that once captured moist trade winds now see slower fog drip and faster runoff: lowlands grow hotter with little extra rain. This necessitates a reorientation of local water policies.

Importantly, the project's high-resolution methodology proved its worth. By downscaling ERA5 and integrating PySEBAL outputs, GENESIS generated fine-grained climate signals where station networks are weak. This multi-indicator approach revealed how warming translates into higher PET and lower SPEI (drought index), enabling us to pinpoint when and where droughts became harsher. Such detail empowers regional authorities to target adaptation – for example, identifying specific subregions that need new water storage or forest restoration to mitigate local deficits.

In summary, the GENESIS D.1.1 results deliver a robust climate risk assessment for Macaronesia. The **growing heat and dryness** documented here demand immediate action – yet the project's innovative methods ensure that such action will be guided by precise, locally relevant data. Investing in resilient water infrastructure and ecosystems will be critical to safeguard Macaronesian communities and economies against the changing climate.

References

1. Bioclimatic indicators dataset for the orographically complex Canary Islands archipelago. Sosa-Guillén, P., González, A., Pérez, J.C. et al. 2024.
2. Groundwater vulnerability on small islands. *Nature Clim Change* 6, 1100–1103. Holding, S., Allen, D., Foster, S. et al. 2016.
3. Cropper, Thomas E. *Climate Change Across The Macaronesian Geographical Region, 1850 - 2100*. PhD thesis, University of Sheffield. 2015.
4. Ritter, A. and C.M. Regalado. Hydrological fluxes of a crest laurel subtropical forest in the Garajonay National Park. 2007.
5. Viera Ruiz, G., Oliva Cabrera, S., Pereira, P., Mota, A., Regalado, C., Ritter, A., Martel, G., González, F., Brandon, R., Domene, X., & Carabassa, V. *Action: A1. Acting zone status analysis. Protocol to improve the environmental quality and resistance to climate*. Life Nieblas. 2021.
6. Kebede, M. M., Kumar, M., Mekonnen, M. M., & Clement, T. P. *Enhancing Groundwater Recharge Through Nature-Based Solutions: Benefits and Barriers*. 2024.
7. ADAPTaRES: Uso Eficiente del Agua y su Reutilización para la Adaptación al Cambio Climático en la Macaronesia. [En línea] https://adaptares.com/wp-content/uploads/2019/01/Folleto-ADAPTaRES_ES_HQ.pdf .
8. (IEEP), Institute for European Environmental Policy. *IMPACTS OF CLIMATE CHANGE ON ALL EUROPEAN ISLANDS*. 2013.
9. Garachico, Life. *Coastal Flooding Adaptation to Climate Change through flexible strategies in Macaronesia urban areas*. 2021.
10. Correa, J., López-Díez, A., Dorta, P. et al. *Evolution of warm nights in the Canary Islands (1950–2023): evidence for climate change in the Southeastern North Atlantic*. 2025.
11. Mycoo, M., M. Wairiu, D. Campbell, V. Duvat, Y. Golbuu, S. Maharaj, J. Nalau, P. Nunn, J. Pinnegar, and O. Warrick. *Small Islands*. In: *Climate Change 2022: Impacts, Adaptation and Vulnerability. Contribution of Working Group II to the Sixth Assessment Report of the Intergovernmental Panel on Climate Change*. 2022.
12. Comission, European. *Forging a climate-resilient Europe - the new EU Strategy on Adaptation to Climate*. 2021.
13. —. *The European Ocean Pact*. 2025.
14. *Simple equations for temperature simulations on mid-latitude volcanic islands: a case study from Jeju*. Hagedorn, Benjamin & Mair, Alan & Tillery, Suzanne & El-Kadi, Aly & Ha, Kyoochul & Koh, Gi-Won. 2014.
15. Fernández-Palacios, José & Nogué, Sandra & Criado, Constantino & Connor, Simon & Góis-Marques, Carlos A. & Sequeira, Miguel & de Nascimento, Lea. *Climate change and human impact in Macaronesia*. 2016.
16. Cook, Jonathan. *3 Steps to Scaling Up Nature-Based Solutions for Climate Adaptation*. World Resources Institute. [En línea] <https://wri.org.cn/en/insights/3-steps-scaling-nature-based-solutions-climate-adaptation#:~:text=Adaptation%20wri,water%20supplies%2C%20reduce%20wildfire,2020>.

17. New Azores archipelago daily precipitation dataset and its links with large-scale modes of climate variability. Hernández, A., Kutiel, H., Trigo, R.M., Valente, M.A., Sigró, J., Cropper, T. and Santo, F.E. 2016.
18. Upper-ocean response to the passage of tropical cyclones in the Azores region. Lima, M. M., Gouveia, C. M., and Trigo, R. M. 2022.
19. Roy, J., P. Tschakert, H. Waisman, S. Abdul Halim, P. Antwi-Agyei, P. Dasgupta, B. Hayward, M. Kanninen, D. Liverman, C. Okereke, P.F. Pinho, K. Riahi, and A.G. Suarez Rodriguez. Sustainable Development, Poverty Eradication and Reducing Inequalities. 2018.
20. Serrano Notivoli, R., Luis, M. D., & Beguería, S. STEAD (Spanish TEMperature At Daily scale). 2018.
21. Muñoz-Sabater, J., Dutra, E., Agustí-Panareda, A., Albergel, C., Arduini, G., Balsamo, G., Boussetta, S., Choulga, M., Harrigan, S., Hersbach, H., Martens, B., Miralles, D. G., Piles, M., Rodríguez-Fernández, N. J., Zsoter, E., Buontempo, C., and Thépaut, Thépaut, ERA5-Land: a state-of-the-art global reanalysis dataset for land applications. 2021.
22. Hersbach H, Bell B, Berrisford P, et al. The ERA5 global reanalysis. 2020.
23. Jury, M. R., & Bernard, D. Nocturnal Rainfall East of the Antilles Islands. 2021.
24. Cantet, P., Déqué, M., Palany, P., & Maridet, J. L. The importance of using a high-resolution model to study the climate change on small islands: the Lesser Antilles case. 2014.
25. The digital climate atlas of the Canary Islands: A tool to improve knowledge of climate and temperature and precipitation trends in the Atlantic islands. Luque Söllheim, Á. L., Máyer Suárez, P., & García Hernández, F. 2024.
26. Downscaling climate change impacts, socio-economic implications and alternative adaptation pathways. al, : Leon et. 2021 : s.n.
27. The Adapt2Clima Project: Assessment Of Future Climate Impacts On Agricultural Areas Of Three Mediterranean Islands. BRILLI, Lorenzo, et al. 2018.
28. Downscaled climate data of Canary Island (Las Palmas).
29. Downscaled climate data of Canary Island (Santa Cruz de Tenerife).
30. Downscaled climate data of Azores.
31. Downscaled climate data of Cape Verde.
32. Downscaled climate data of Madeira.
33. Evapotranspiration estimation using Surface Energy Balance Model and medium resolution satellite data: An operational approach for continuous monitoring. Pareeth, S., Karimi, P. 2023.
34. A remote sensing surface energy balance algorithm for land (SEBAL). 1. Formulation. W.G.M. Bastiaanssen, M. Menenti, R.A. Feddes, A.A.M. Holtslag. 1998.
35. Landsat. Williams, Darrel L., Goward, Samuel y Arvidson, Terry. 2006.
36. NASA. README Document for NASA GLDAS Version 2 Data Products. [En línea] 2025. https://hydro1.gesdisc.eosdis.nasa.gov/data/GLDAS/GLDAS_NOAH025_3H.2.1/doc/README_GLDAS2.pdf.
37. Geographic Resources Analysis Support System (GRASS) Software, Version 8.4. Open Source Geospatial Foundation. Team, GRASS Development. 2024.

38. Copernicus Global Digital Elevation Model. Distributed by OpenTopography. Agency, European Space. 2024.
39. PySEBAL results for Gran Canaria and La Palma.
40. A Multiscalar Drought Index Sensitive to Global Warming: The Standardized Precipitation Evapotranspiration Index. Vicente-Serrano, Sergio & Beguería, Santiago & López-Moreno, J.I. 2010.
41. Standardized Precipitation Index: user guide. (WMO), World Meteorological Organization. 2012.
42. WaPOR (Water Productivity through Open access of Remotely sensed derived data). Food and Agriculture Organization. 2024.
43. Contribution of precipitation and reference evapotranspiration to drought indices under different climates. Sergio M. Vicente-Serrano, Gerard Van der Schrier, Santiago Beguería, Cesar Azorin-Molina, Juan-I. Lopez-Moreno. 2015.
44. WaPOR data of the Canary Islands.
45. WaPOR data of Madeira.
46. WaPOR data of Cape Verde.
47. STL: A Seasonal-Trend Decomposition Procedure Based on Loess. Cleveland, R. B. 1990.
48. Estimates of the Regression Coefficient Based on Kendall's Tau. Sen, P. K. 1968.
49. The Influence of Autocorrelation on the Ability to Detect Trend in Hydrological Series. Yue, S., et al. 2002.
50. The Jackknife and the Bootstrap for General Stationary Observations. Kunsch, Hans R. 1989.
51. Optimal Detection of Changepoints With a Linear Computational Cost. Killick, R., Fearnhead, P., & Eckley, I. A. 2012.
52. Precipitation error rates of downscaled data.
53. Climate data trends of the archipelagos of Macaronesia.
54. Estimate of the regression coefficient based on Kendall's tau. Sen, P. K. 1968.